

Development of Novel Air Electrode Materials for Fuel Cells

Solar Activated Fuel Cells

Bartłomiej Kolodziejczyk



UNIVERSITY OF ICELAND



University
of Akureyri



Development of Novel Air Electrode Materials for Fuel Cells

Solar Activated Fuel Cells

Bartłomiej Kolodziejczyk

A 30 ECTS credit units Master's thesis

Supervisors

Dr. Bjorn Winther-Jensen (Project advisor)

Prof. Douglas MacFarlane (Project advisor)

Dr. Thorsteinn Ingi Sigfusson (Academic advisor)

Dr. David Dvorak (Academic advisor)

A Master's thesis done at
RES | The School for Renewable Energy Science
in affiliation with
University of Iceland &
University of Akureyri

The Master Thesis was supported by a grant from Iceland, Liechtenstein and Norway through the EEA Financial Mechanism - Project PL0460.

Akureyri, February 2011

Development of Novel Air Electrode Materials for Fuel Cells

Solar Activated Fuel Cells

A 30 ECTS credit units Master's thesis

© Bartłomiej Kolodziejczyk, 2011

RES | The School for Renewable Energy Science

Solborg at Nordurslod

IS600 Akureyri, Iceland

Telephone + 354 464 0100

www.res.is

Printed in 09/02/2011

at Stell Printing in Akureyri, Iceland

ABSTRACT

Fuel cells convert chemical energy directly into electrical energy and heat with high efficiency and low emission of pollutants. However, before fuel cell technology can gain a significant share of the energy market, many important issues have to be solved. These issues include many different aspects, one of them is the development of alternative materials for fuel cells. Present fuel cell prototypes very often use materials selected when fuel cells gained interest, it was more than 25 years ago. Commercialization aspects, including cost and durability, have revealed inadequacies in some of these materials. This paper describes research and its results on development of new electrode materials for fuel cells. Main interest was concentrated on conducting polymer – PEDOT, and its blends with non-conducting polymers. What more, during research some very interested properties of tested materials has been discovered. PEDOT and its blends with PBTh and PTTh can be light activated, this phenomena increases overall electrode performance when light is introduced. This leads to new types of fuel cells, a hybrid of fuel cell and photovoltaic cell. This paper summarizes research and development of this innovative and alternative materials. Now when European Union proposed energy policy for member countries, this research can have great importance for Poland as well as for other countries.

PREFACE

This thesis work was carried out in the ARC Centre of Excellence for Electromaterials Science, which is part of Department for Materials Engineering at Monash University in Melbourne, Australia and supported by RES | the School for Renewable Energy Science in Akureyri, Iceland, which I both gratefully acknowledge.

Monash University is a public university based in Melbourne, Australia. It is Australia's largest university with about 55,000 students and the largest university in southern hemisphere. Monash University is a dynamic and internationally recognised university with a long established tradition of excellence in education and is one of the best universities in the world, distinctive because of its research intensive. The University has a total of eight campuses: six in Victoria, Australia (Clayton, Caulfield, Berwick, Peninsula, Parkville and Gippsland), one in Malaysia and one in South Africa. The university also has a centre in Prato, Italy. Monash University is a member of the prestigious 'Group of Eight', a group composed of some of the most research-intensive universities in Australia.

RES | the School for Renewable Energy Science in Akureyri is a private institution of higher learning offering an intensive one-year Master of Science program in renewable energy science and technologies. Degree is awarded jointly in cooperation with the University of Iceland and the University of Akureyri, as well as in partnership with a number of leading technical universities and institutions around the world. RES, because of its unique, attracts well known professors and specialists to come and share their knowledge and experience with students.

The subject was originally proposed by Prof. Douglas MacFarlane and the objective was to develop novel air electrode material for fuel cell using plasma polymerised PEDOT. The work of this MS.c. project was performed during the period from October 2010 to February 2011. During my work new, very interesting PEDOT properties has been discovered and that's how idea about solar activated fuel cells came out. Results of my work are shown in this paper. Dealing with electromaterials for fuel cell applications, was new experience for me and I won't deny that work done during my stay in Australia was

challenging, but fruitful. This research can give new light on both, fuel cells and solar panels and can be good material for further research and development.

I would like to thank Dr. Bjorn Wither-Jensen and Prof. Douglas MacFarlane for giving me opportunity to come to Monash, be part of their group and make this research, for their help, advices, guidelines and supervision given me during this project. I would like to thank also Ms. Tamara Wright for her administrative assistance during my stay in Australia and Ms. Orawan Winther-Jensen and the other members of the ARC Centre of Excellence for Electromaterials Science for their introduction and support with laboratory devices.

Last but not least I am grateful to the whole RES School administration and faculty staff, Dr. Björn Gunnarson, the Academic Director of RES, Dr. Thorsteinn Ingi Sigfusson, Dr. David Dvorak, the Academic Coordinators for the Fuel Cell Systems and Hydrogen concentration, Ms. Sigrun Loa Kristjansdottir, Chief of the RES office, all of whom gave me this marvellous opportunity to study for a year in Iceland which enlightened me and changed my outlook regarding the world's most important energy issues.

'Ancora imparo - I am still learning.'

—*Michelangelo (Monash University motto)*

Bartłomiej Kolodziejczyk

Clayton, 05.02. 2011

TABLE OF CONTENTS

1	Introduction.....	11
2	Background Informations	13
2.1	Fuel Cells	14
2.1.1	Fuel Cell Types	19
2.1.2	Fuel Cell Materials	27
2.2	Vapor Phase Polymerization.....	29
2.3	PEDOT Structure and Properties	31
2.4	Polythiophene Structure and Properties.....	32
2.5	Polyethylene Glycol Structure and Properties	34
3	PEDOT Manufacturing.....	35
3.1	PEDOT Manufacturing in Vapor Phase Polymerization Process.....	35
4	Testing – Experimental Procedure.....	38
4.1	Measuring Conductivity	38
4.1.1	Measuring Sheet Resistance (Four Point Test)	38
4.1.2	Measuring Thickness (Measuring Profile)	40
4.1.3	Conductivity Results	42
4.2	Ultraviolet-Visible Spectroscopy.....	44
4.3	Electrochemical Testing (Cyclic Voltammetry and Chronoamperometry).....	47
4.3.1	Introduction to Cyclic Voltammetry	47
4.3.2	Cyclic Voltammetry Test Cell Assembly.....	50
4.3.3	Cyclic Voltammetry Results for Thin Film Made of PEDOT, PBTh and PEG Blends	52
4.3.4	Cyclic Voltammetry Results for PEDOT/PTTh ‘1:0.5’ PEG ‘2’.....	68
4.3.5	Cyclic Voltammetry Results for PEDOT/PBTh ‘1:1’	69
4.3.6	Cyclic Voltammetry Results for PEDOT	71
4.3.7	Chronoamperometry.....	73
5	Importance and Implementation of Project in Poland	78
6	Conclusions.....	80
	References	82
	Appendix A - Leica KL 2500 LCD Light Source Calibration	1

LIST OF FIGURES

Figure 2.1 General concept of a hydrogen-oxygen fuel cell	15
Figure 2.2 Fuel cell polarization curve.....	15
Figure 2.3 Fuel cell polarization and power density curve.....	17
Figure 2.4 Schematic of phosphoric acid fuel cell	19
Figure 2.5 Schematic of polymer electrolyte membrane fuel cell.....	22
Figure 2.6 Schematic of alkaline fuel cell	23
Figure 2.7 Schematic of molten carbonate fuel cell	25
Figure 2.8 Schematic of solid oxide fuel cell	26
Figure 2.9 General concept of vapor phase polymerization (VPP) process.....	30
Figure 2.10 PEDOT chain structure	31
Figure 2.11 Computer modelled PEDOT chain structure	32
Figure 2.12 The monomer repeat unit of unsubstituted polythiophene.....	33
Figure 3.1 Reaction occurring during vapor phase polymerization process	36
Figure 3.2 Two standard PEDOT samples used for tests, on left PEDOT deposited on glass surface, on right PEDOT deposited on mylar coated with gold.....	36
Figure 4.1 Four point probe measurement technique (left). Probe near the edge of the sample, all current has to go through the left half plane (right)	39
Figure 4.2 Profiler test result for PEDOT/PBTh ,1:0.5' PEG ,2' sample. Scan length 500 um and 0.028 um/sample resolution.....	41
Figure 4.3 Profiler test result for PEDOT/PBTh ,1:0.5' PEG ,2' sample. Scan length 5000 um and 0.278 um/sample resolution.....	41
Figure 4.4 UV-Vis results for tested thin films normalized for thin film thickness.....	46
Figure 4.5 Typical excitation signal for cyclic voltammetry.....	48
Figure 4.6 Typical voltammogram plot.....	48
Figure 4.7 Effect of the increased scan rate.....	49
Figure 4.8 Change of the rate constant	49
Figure 4.9 The test electrode cross section, mylar with gold layer and polymerized PEDOT is laminated with a gold connector	50
Figure 4.10 The test cell layout, sample is laminated with a gold connector.....	51
Figure 4.11 3D test cell assembly model used in experiments.....	51
Figure 4.12 Comparison of PEDOT/PBTh ,1:1' PEG ,2' in different electrolytes, carried out with scan rate of 0.167 mV/s in presence of air and light	52

Figure 4.13 Comparison of PEDOT/PBTh ,1:1' PEG ,2' in different electrolytes, carried out with scan rate of 0.167 mV/s in presence of air in function of over-potential vs. current in presence of light	53
Figure 4.14 Comparison of PEDOT/PBTh ,1:3' PEG ,2' in different electrolytes, carried out with scan rate of 0.167 mV/s in presence of air	54
Figure 4.15 Comparison of PEDOT/PBTh ,1:3' PEG ,2' in different electrolytes, carried out with scan rate of 0.167 mV/s in presence of air	54
Figure 4.16 Test results in presence of bubbling air in 0.1 M NaPTS electrolyte with light	55
Figure 4.17 Test results in presence of bubbling air in 0.1 M NaPTS electrolyte in dark ..	56
Figure 4.18 Cyclic voltammetry test for PEDOT/ PBTh ,1:1' PEG ,2', sampling rate 20 mV/s, electrolyte 0.1 M NaPTS (pH 7). Blue graph test in presence of nitrogen, red graph in presence of air, tests were taken in dark.....	57
Figure 4.19 Cyclic voltammetry test for PEDOT/ PBTh ,1:1' PEG ,2', sampling rate 0.167 mV/s, electrolyte 0.1 M NaPTS (pH 7). Blue graph test in presence of nitrogen, red graph in presence of air, tests were taken in dark.....	57
Figure 4.20 Cyclic voltammetry test for PEDOT/ PBTh ,1:1' PEG ,2', in presence of bubbling air in 0.1 M NaPTS (pH 7) electrolyte, sampling rate 20 mV/s. Blue graph test with light shining (500 lm) on working electrode surface red graph taken for light intensity of 200 lm and green graph was taken in dark	58
Figure 4.21 Cyclic voltammetry test for PEDOT/ PBTh ,1:1' PEG ,2', in presence of bubbling nitrogen in 0.1 M NaPTS (pH 7) electrolyte, sampling rate 20 mV/s. Blue graph – dark, green – 1000 lm, red – 500 lm, purple – 200 lm	59
Figure 4.22 Cyclic voltammetry test for PEDOT/ PBTh ,1:1' PEG ,2', in presence of bubbling air in 0.1 M NaPTS (pH 7) electrolyte, sampling rate 0.167 mV/s. Blue graph – dark, green – 1000 lm, red – 500 lm, purple – 200 lm	60
Figure 4.23 Cyclic voltammetry test for PEDOT/ PBTh ,1:1' PEG ,2', in presence of bubbling nitrogen in 0.1 M NaPTS (pH 7) electrolyte, sampling rate 0.167 mV/s. Purple graph – dark, green – 1000 lm, red – 500 lm, blue – 200 lm	61
Figure 4.24 Cyclic voltammetry test for PEDOT/ PBTh ,1:1' PEG ,2', in presence of bubbling air (blue) and bubbling nitrogen (red), in 0.1 M H ₂ SO ₄ dissolved in water electrolyte (pH 1), sampling rate 50 mV/s, taken in dark	61
Figure 4.25 Cyclic voltammetry test for PEDOT/ PBTh ,1:1' PEG ,2', in presence of bubbling air (blue) and bubbling nitrogen (red), in 0.1 M H ₂ SO ₄ dissolved in water electrolyte (pH 1), sampling rate 0.167 mV/s, taken in dark.....	62
Figure 4.26 Cyclic voltammetry test for PEDOT/ PBTh ,1:3' PEG ,2', in presence of bubbling nitrogen in 0.1 M NaPTS (pH 7) electrolyte, scan rate 0.167 mV/s. Red plot – 1000 lm (3200K), blue - dark	63
Figure 4.27 Cyclic voltammetry test for PEDOT/ PBTh ,1:1' PEG ,2', in presence of bubbling nitrogen in 0.1 M H ₂ SO ₄ (pH 1) electrolyte, scan rate 0.167 mV/s. Red plot – 1000 lm (3200K), blue - dark	63
Figure 4.28 Cyclic voltammetry test for PEDOT/ PBTh ,1:1' PEG ,2', in presence of bubbling air in 0.1 M NaOH (pH 11) electrolyte, scan rate 0.167 mV/s. Red plot – dark, blue – 1000 lm (3200K)	64

Figure 4.29 Ratio of electrode current in light condition to electrode current in dark.....	65
Figure 4.30 Kinetics limits in light.....	65
Figure 4.31 Kinetics limits in dark	66
Figure 4.32 pH vs. electrode current plot for PEDOT/PBTh '1:0.5' PEG '2' ratio at two fixed voltage values -0.5V and -0.7V in presence of air, light intensity – 1000 lm....	66
Figure 4.33 pH vs. electrode current plot for PEDOT/PBTh '1:1' PEG '2' ratio at two fixed voltage values -0.5V and -0.7V in presence of air, light intensity – 1000 lm....	67
Figure 4.34 pH vs. electrode current plot for PEDOT/PBTh '1:2' PEG '2' ratio at two fixed voltage values -0.5V and -0.7V in presence of air, light intensity – 1000 lm....	67
Figure 4.35 pH vs. electrode current plot for PEDOT/PBTh '1:3' PEG '2' ratio at two fixed voltage values -0.5V and -0.7V in presence of air, light intensity – 1000 lm....	68
Figure 4.36 Comparison of PEDOT/PBTh ,1:0.5' PEG ,2' and PEDOT/PTTh ,1:0.5' PEG ,2' in 0.1M NaOH (~pH11) with bubbling air and light.....	69
Figure 4.37 Cyclic voltammetry test for PEDOT/ PBTh ,1:1', taken with very small sampling rate (0.167 mV/s). Blue graph – results for nitrogen, red graph – results for air	70
Figure 4.38 Cyclic voltammetry test for PEDOT/ PBTh ,1:1', taken with small sampling rate (0.167 mV/s). Blue graph – results in light, red graph – results in dark	71
Figure 4.39 Cyclic voltammetry test for pure PEDOT sample on mylar coated with gold for better conductivity. 0.1 M NaPTS (pH 7) was used as an electrolyte, during tests air was bubbling to electrolyte. Blue plot shows results for sampling rate 20 mV/s and red for 50 mV/s.....	72
Figure 4.40 Cyclic voltammetry test for pure PEDOT sample on mylar coated with gold for better conductivity. 0.1 M NaPTS (pH 7) was used as an electrolyte. Tests were taken in presence of nitrogen bubbling to electrolyte. Blue plot shows results for sampling rate 20 mV/s and red for 50 mV/s.....	72
Figure 4.41 Cyclic voltammetry test for pure PEDOT taken with very small sampling rate (0.167 mV/s). Blue graph – results for nitrogen, red graph – results for air	73
Figure 4.42 Chronoamperometry tests for pure PEDOT sample, in presence of bubbling air in 0.1 M NaPTS (pH 7) electrolyte, tests taken for fixed voltage values.....	74
Figure 4.43 Current at 0V	74
Figure 4.44 Chronoamperometry test for PEDOT/ PBTh ,1:1' in presence of bubbling air in 0.1 M NaPTS (pH 7) electrolyte, tests taken for fixed voltage values.....	75
Figure 4.45 Chronoamperometry test for PEDOT/ PBTh ,1:1' PEG ,2', in presence of bubbling air in 0.1 M NaOH (pH 11) electrolyte, tests taken for fixed voltage values. Red plot – -0.4V, blue – -0.3V	76
Figure 4.46 Chronoamperometry test with light filtration	77

LIST OF TABLES

Table 4-1 Sheet resistance data for different samples, collected during 4 point test on Jandel Model RM3. Data has been taken for current 4.5 uA (all values are in Ω/\square).. 40

Table 4-2 Thickness values for different samples, collected on Veeco DekTak 150 Profiler 42

Table 4-3 Conductivity values for different samples, calculated using sheet resistance and thickness values 43

Table 4-4 Conductivity values for common materials 44

1 INTRODUCTION

Fuel cells are a rapidly developing energy conversion technology. Offering higher efficiencies than conventional technologies, they also operate quietly and have a modular construction that is easily scalable. Fuel cells are considered as a future energy source, they are easy to manufacture and completely clean, only emission from fuel cell is pure water. Fuel cells can be used in various applications, from micro and small devices, such as mobile phones, laptop computers, through vehicles to big systems like submarines, households, hospitals, it is even possible to build fuel cell based power plant and supply whole city.

This vision is still more like a dream than reality and we still need to wait to commercialize this promising technology. Cost of fuel cell system is still very high comparing to traditional systems used in present, like for example internal combustion engines. Researchers are trying to improve performance of fuel cell by using complex designs of fuel cells or by dealing with new fuel cell materials. Main goal is to improve performance and lower total cost of fuel cell system.

Fuel cell electrode materials are still very expensive. One of the main barriers to the commercialization of fuel cell systems, especially for automotive use, is the high cost of the platinum electrocatalysts. Aside from the cost of the precious metal, concern has also been raised over the adequacy of the world supply of platinum, if fuel cell vehicles were to make a significant penetration into the global automotive fleet. Cost of platinum parts of fuel cell for car with 100 kW electric motor is higher than total cost of an 100 kW gasoline engine. Annual production of platinum is not able to supply all the cars produced per year. Current annual world production of platinum is only sufficient for about 3 million 100 kW vehicles, less than one-twentieth of the current annual global production of vehicles. Chemists are working toward the development of low-cost non-platinum electrocatalyst for the oxygen reduction reaction, durable materials that would be stable in the fuel cell's operating environment and retain high electrochemical activity over the design lifetime of the fuel cell.

Although platinum is used in both the anode and the cathode of the fuel cell, developing alternative oxygen reduction catalysts for the cathode is the more challenging of the two.

The idea is to find cheap and easy to manufacture material with similar performance to the one platinum has and without carbon monoxide poisoning. It can be done for example by using PEDOT^[1], conducting polymer material instead of platinum.

This project can bring new light on applications of conducting polymers in fuel cells. Knowledge gather during research can be used to build new, hybrid energy source – combination of fuel cell and photovoltaic cell in one device. Work of this hybrid energy source will be based on fuel cell principles, plus introduction of light to the electrode will increase overall performance.

2 BACKGROUND INFORMATIONS

The platinum in fuel cell anodes acts as an electrocatalyst, helping to separate hydrogen into protons and electrons. In the cathodes, the platinum helps the oxygen, protons, and electrons combine to produce water ^[19]. Over time, the performance of polymer electrolyte fuel cells with platinum or platinum alloy electrocatalysts degrades. This has been attributed to a loss of the electrochemically active surface area of the platinum. One proposed cause is that platinum oxidizes and dissolves at high potentials often encountered at the cathode, such a process would be exacerbated with repeated cycling between high and low cathode potentials, which lead to platinum oxidation and reduction, respectively ^[3]. The dissolved platinum then either deposits on existing platinum particles to form larger particles (often referred to as platinum ripening), or diffuses into an electrochemically inaccessible portion of the membrane-electrode assembly or its support structure, such as the gas diffusion layer. Measurements indicate that dissolution of platinum increases with increasing potentials that are encountered on the cathode of the fuel cell at low power output (for example, during idling) and possibly during start-up and shutdown. Other big problem coming with platinum is platinum poisoning of carbon monoxide which refers to the effect that a platinum can be 'poisoned' if it reacts with another compound (carbon monoxide) that bonds chemically (similar to a reaction inhibitor) but does not release, or chemically alters the catalyst. This effectively reduces the usefulness of the catalyst, (i. e. the number of active sites) as it cannot participate in the reaction with which it was supposed to catalyze ^[5].

Scientists at Monash University in Australia have come up with an alternative based on a highly conductive polymer deposited onto a hydrophobic, breathable membrane (Gore-Tex). The conductive polymer, poly(3,4-ethylenedioxythiophene) (PEDOT), acts as both the fuel cell electrode and the catalyst ^[1]. Conducting polymers have lately become serious candidates for catalysts for a range of electro-catalytic reactions, including oxygen reduction (for fuel-cells and metal-air batteries) and proton reduction (hydrogen production). Very recently has been proved that some blends of different conducting polymers (with different reduction potentials) can work for photo-enhanced electro-catalysis of e.g. oxygen^[19].

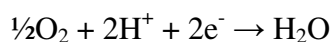
This discovery is thought to be of greatest importance and further investigation of the phenomena is required.

2.1 Fuel Cells

The basic operation of fuel cell is simple. Fuel cell is a device which ‘burn’ or combust fuel in the simple chemical reaction to produce electricity and heat and pure water as long as it is supplied with fuel. The main difference between the fuel cell and a combustion engine depends on energy conversion. In internal combustion engines, heat generated from combusted fuel is converted into mechanical energy and then into electrical energy, causing losses at each level of transformation. In fuel cells, electricity and heat are produced in chemical reaction. In a simple hydrogen fuel cell, two half reactions process occur as follow:



At the fuel cell’s anode hydrogen gas ionises, releasing electrons and creating H^+ ions (or protons). This reaction releases energy. The protons migrate through the electrolyte and combine with the oxygen, usually from atmospheric air, at the cathode side to form water.



To proceed both reactions continuously, electrons produced at anode has to migrate through electrical circuit to the cathode, producing direct current. Also, H^+ ions must pass through electrolyte. Electrolyte must only allow H^+ ions to pass through it, and not electrons. Otherwise, the electrons would go through electrolyte, not through electrical circuit and energy will be lost. Fuel cells can reach electrical efficiency from 40% to even 70%.

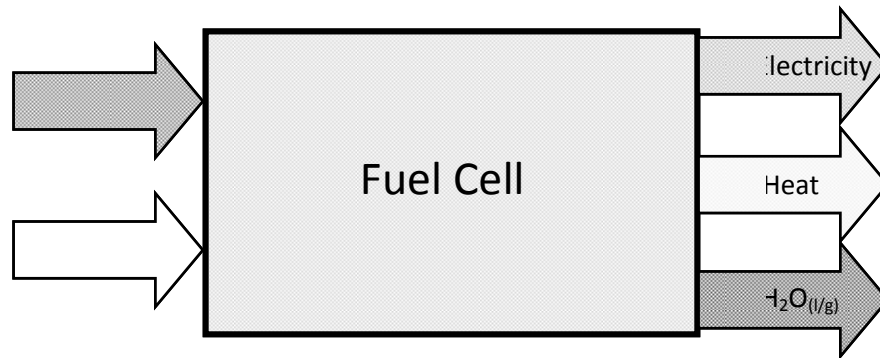


Figure 2.1 General concept of a hydrogen-oxygen fuel cell

The performance of the fuel cell can be described by the dependence of current vs. voltage. This representation is called a current-voltage (i-V) curve. The voltage output is a function of current, normalized by the area of the fuel cell, giving current density. An ideal fuel cell would supply any amount of current, while working with the constant voltage, determined by thermodynamics. In real fuel cells, the actual voltage output is sometimes less than the ideal thermodynamically predicted voltage and the more current is drawn from a fuel cell, the lower the voltage output of the cell due to unavoidable losses, limiting the power of fuel cell.

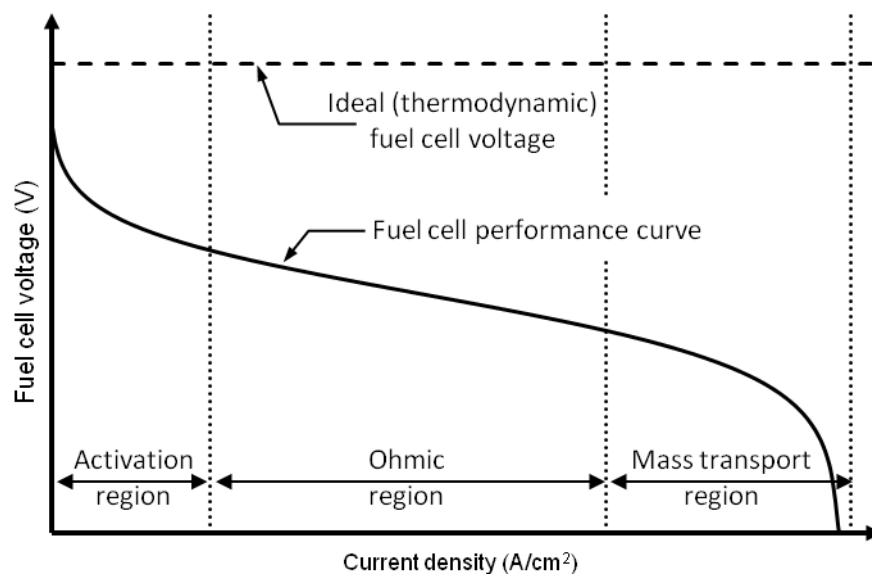


Figure 2.2 Fuel cell polarization curve^[6]

With increasing current drawn from the cell, the irreversible losses are increasing, causing a decrease in voltage output of fuel cell. Three major types of fuel cell losses are described below:

- Activation losses – due to electrochemical reaction,
- Ohmic losses – due to ionic and electronic conduction,
- Concentration losses – due to mass transport.

The real voltage output of a fuel cell is a function of thermodynamically predicted open circuit voltage minus losses and can be described by formula:

$$V = E_{\text{thermo}} - \eta_{\text{act}} - \eta_{\text{ohmic}} - \eta_{\text{conc}},$$

where:

V – real output voltage,

E_{thermo} – thermodynamically predicted open circuit voltage,

η_{act} – activation losses,

η_{ohmic} – ohmic losses,

η_{conc} – concentration losses.

The power of the fuel cell is determined by the equation:

$$P = i \cdot A \cdot V,$$

where:

P – power (W),

i – current density (A/cm^2),

A – cell area (cm^2),

V – voltage (V).

The other characteristic of a fuel cell is a power density curve, which gives view on the power density delivered by a fuel cell as a function of fuel cell current density. Schematic performance and power density curves are shown in Figure 2.3.

Fuel cell power density is simply fuel cell voltage multiplied by current density. Power density increases with increasing current density, reaches a maximum, and then falls down together with fuel cell voltage, caused by concentration losses. At current above maximum power density, both voltage and power fall, so it is preferred to operate fuel cell below or at maximum power density point. At current densities below the power density maximum point, voltage increases, but power density decreases. It is very hard to find optimal working point for fuel cell.

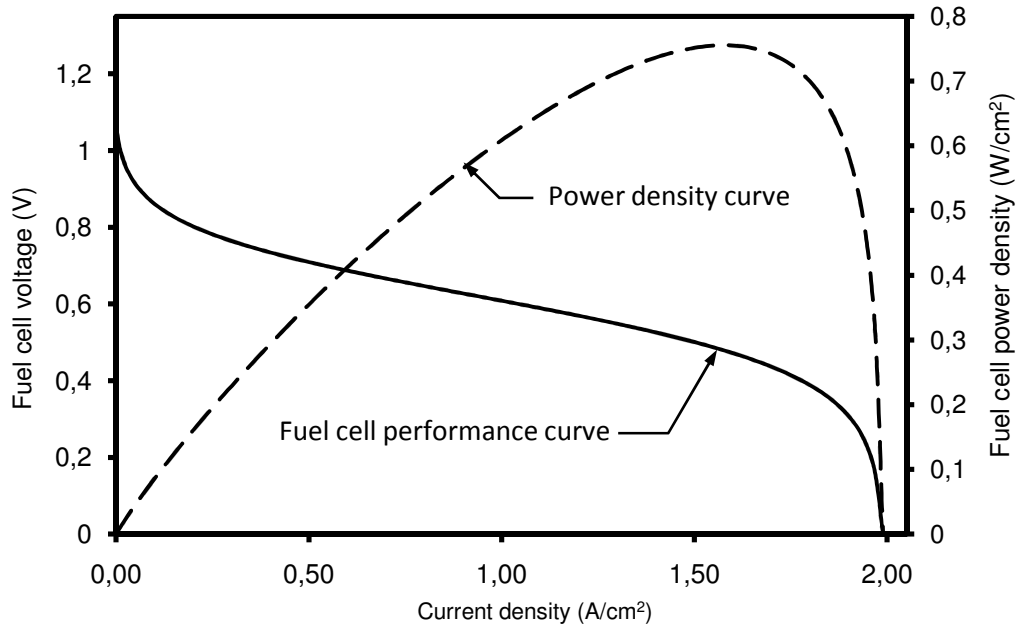


Figure 2.3 Fuel cell polarization and power density curve

If the system is reversible (or has no losses), then electrical work (E) done by fuel cell will be equal to the Gibbs free energy released Δg_f .

$$\Delta g_f = -n \cdot F \cdot E,$$

thus

$$E = - \Delta g_f / n \cdot F,$$

where:

Δg_f – Gibbs free energy released,

n – number of moles of electrons transferred,

F – Faraday's constant.

This fundamental equation gives the electromotive force (EMF) or reversible open circuit (OCV) voltage of the hydrogen fuel cell. At standard conditions, the highest possible voltage to yield for hydrogen-oxygen fuel equals 1.23 V. Gibbs free energy changes, the reversible fuel cell voltage is highly dependent on operating conditions such as temperature, pressure and activities of the species.

Change of the reversible cell voltage with pressure is related to the volume change of the reaction. Pressure and temperature have a minimal effect on reversible voltage. Chemical activity has a more significant influence, which can be described by the Nernst equation:

$$E = E^0 - R \cdot T / n \cdot F \cdot \ln(\prod a_{\text{products}}^{v_i} / \prod a_{\text{reactants}}^{v_i}),$$

The Nernst equation provides a relationship between the ideal standard potential (E^0) for the fuel cell reaction and the ideal equilibrium potential (E) at different temperatures and partial pressures of products and reactants. When the ideal potential at standard conditions is known, the ideal voltage can be determined at other temperatures and pressures using Nernst equation. The Nernst equation does not fully describe all the processes occurring in fuel cell, but is giving estimation good enough to calculate fuel cell voltage.

2.1.1 Fuel Cell Types

Fuel cells are classified primarily by the kind of electrolyte they employ. This classification determines the kind of chemical reactions that take place in the cell, the kind of catalysts required, the temperature range in which the cell operates, the fuel required, and other factors. These characteristics, affect the applications for which these cells are most suitable. There are several types of fuel cells currently under development, each with its own advantages, limitations, and potential applications. Below are described five major types of fuel cells.

Phosphoric Acid Fuel Cell (PAFC)

Phosphoric acid fuel cells use liquid phosphoric acid as an electrolyte. Phosphoric acid (H_3PO_4) with a concentration ranging up to 100% is contained in a Teflon bonded silicone carbide matrix. Electrodes in PAFC are made of porous carbon and contain platinum catalyst. Pure phosphoric acid solidifies at 42°C and the ionic conductivity of phosphoric acid is low at low temperatures, so phosphoric acid fuel cells have to be operated above this temperature. Optimal performance occurs at temperatures from 150°C to 220°C [6].

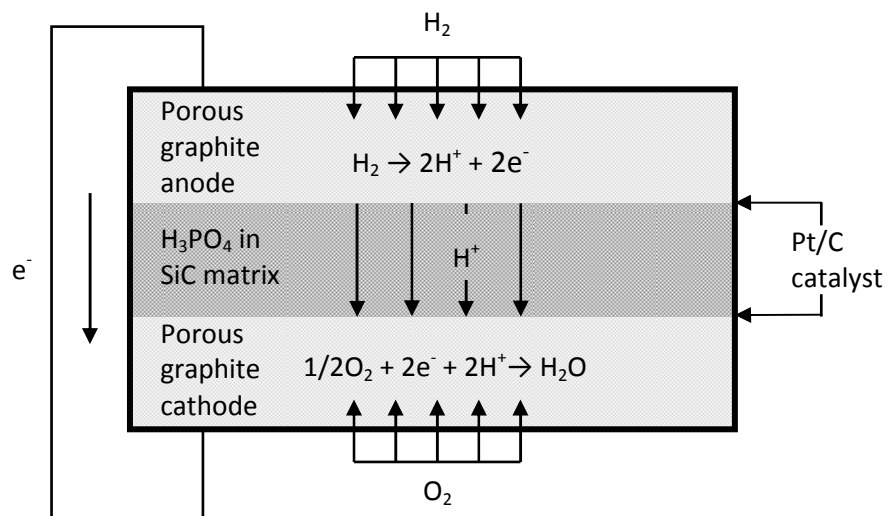


Figure 2.4 Schematic of phosphoric acid fuel cell

The charge carrier is the hydrogen ion. The hydrogen introduced at the anode is split into its protons and electrons. The protons migrate through the electrolyte and combine with the oxygen, usually from atmospheric air, at the cathode to form water. The electrons are routed through an external circuit where they can perform useful work and generate heat.

Anode Reaction: $2\text{H}_2 \rightarrow 4\text{H}^+ + 4\text{e}^-$

Cathode Reaction: $\text{O}_2 + 4\text{H}^+ + 4\text{e}^- \rightarrow 2\text{H}_2\text{O}$

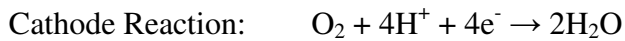
Overall reaction: $2\text{H}_2 + \text{O}_2 \rightarrow 2\text{H}_2\text{O}$

PAFC are 85% efficient when used for the co-generation of electricity and heat but less efficient at generating electricity alone (37%–42%). The waste heat is capable of heating hot water or generating steam at atmospheric pressure. Simple construction, low electrolyte volatility and long-term stability are additional advantages. PAFCs are less powerful than other fuel cells, given the same weight and volume. As a result, these fuel cells are typically large and heavy. PAFCs are also expensive. Similar to PEM fuel cells, PAFCs require an expensive platinum catalyst, which raises the cost of the fuel cell and make PAFC susceptible to carbon monoxide and sulphur poisoning. This type of fuel cell is usually implemented in stationary power generation systems, but some PAFCs have been used to power large vehicles such as city buses ^[3].

Proton Exchange Membrane Fuel Cell (or Polymer electrolyte membrane fuel cell) PEMFC.

Proton exchange membrane fuel cells, also called polymer electrolyte membrane fuel cells, deliver high power density and offer low volume and weight, compared with other fuel cells. PEMFCs employ thin solid polymer layer as a membrane, usually perfluorinated sulfonic acid polymer also known as Nafion®. This polymer is a proton conductor when it is saturated with water, but it does not conduct electrons ^[3].

At the anode, the hydrogen molecule is split into hydrogen ions and electrons. The protons (H^+) permeate across the membrane to the cathode while the electrons flow through an external circuit and produce electric power. Oxygen from the air, is supplied to the cathode where it combines with the electrons and the hydrogen ions to produce water. The reactions occurring in proton exchange membrane fuel cell are as follows:



PEMFC operate at low temperature, typically from 80° C to 100° C, which allows for a rapid start-up, because of shorter warm-up time and results in less wear on system components, resulting in enhanced durability, but because of low operating temperature, platinum-based materials are the only practical catalyst currently suitable. Platinum with loadings of about 0.3 mg/cm² makes these fuel cells expensive. The platinum catalyst is also extremely sensitive to CO and sulphur poisoning, making it necessary to employ an additional reactor to reduce impurities in the fuel gas if the hydrogen is derived from an alcohol or hydrocarbon fuel. When the hydrogen fuel contains small amounts of CO, then platinum-ruthenium alloys can be used to decrease the sensibility of the catalyst ^[6].

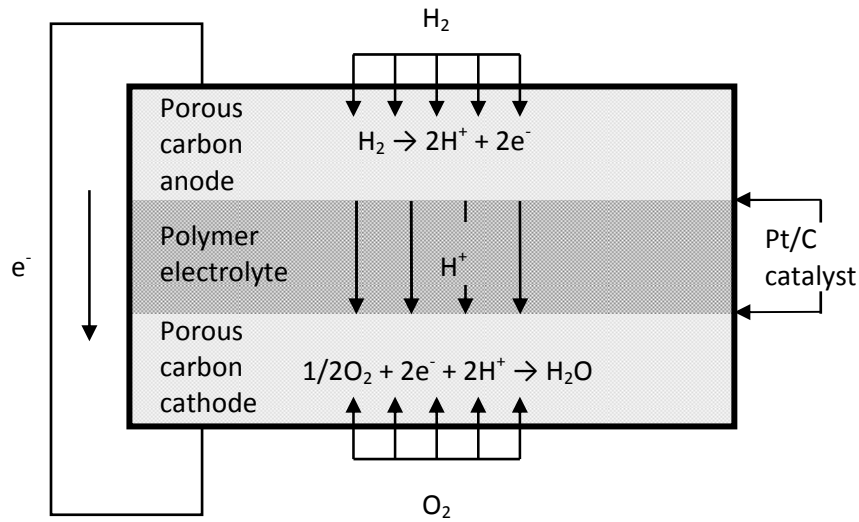


Figure 2.5 Schematic of polymer electrolyte membrane fuel cell

Operating temperatures of 100° C are not allowing to use PEMFC in combined heat and power applications. Also, since the electrolyte is required to be saturated with water, careful water management control is important to operate optimally, especially when operating below the freezing point.

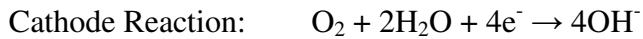
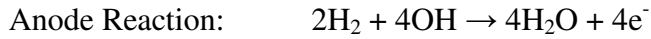
PEM fuel cells have the highest power density of all the fuel cell classes, which it makes them compact and lightweight. Solid electrolyte material makes PEMFC easier to seal, and therefore, less expensive to manufacture. Low-temperature operation gives better start-stop capabilities ^[3].

PEM fuel cells are used primarily for transport and portable applications, some are used for stationary applications.

Alkaline Fuel Cell (AFC)

Alkaline fuel cells use a solution of potassium hydroxide (KOH) as an electrolyte. The concentration of KOH can vary with the fuel cell's operating temperature. High-temperature AFCs operate at temperatures between 100° C and 250° C, when newer AFCs

operates at lower temperatures of roughly 23° C to 70° C. The charge carrier for an alkaline fuel cell is the hydroxyl ion (OH⁻) that migrates from the cathode to the anode where they react with hydrogen to produce water and electrons. Water formed at the anode migrates back to the cathode to regenerate hydroxyl ions ^[6]. Chemical reactions which occur in alkaline fuel cell are shown below:



The technology of alkaline fuel cell is well developed and their efficiency reaches up to 60%. Its good performance is due to the rate at which chemical reactions take place in the cell. However, they are very sensitive to carbon dioxide (CO₂), which can be present in hydrogen or in air, poisoning it rapidly, degrading the fuel cell performance and shortening the cell's lifetime. Therefore, those kinds of fuel cells are limited to closed environments, such as outer space and submarines. This type of fuel cell must use pure hydrogen and oxygen ^[6].

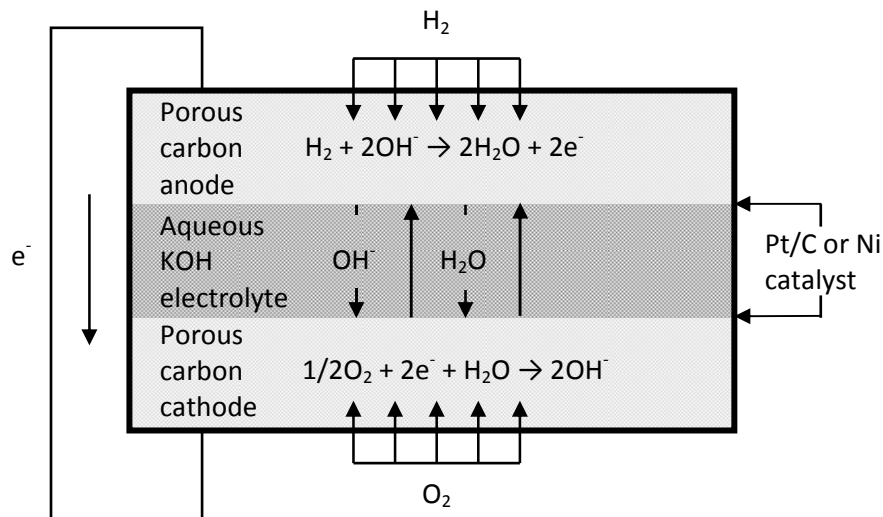


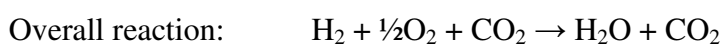
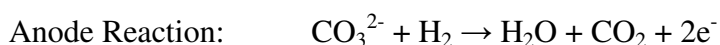
Figure 2.6 Schematic of alkaline fuel cell

Furthermore, molecules such as CO, H₂O and CH₄, which are harmless or even work as fuels to other fuel cells, are poisons to an alkaline fuel cell. KOH electrolyte may need occasional replenishment and water must be removed from anode side. Because they don't need expensive catalyst they are cheap to manufacture. AFC have been used in space technology. The fuel cells on board spacecrafts provide electrical power for on-board systems, as well as drinking water. AFC stacks have been shown to maintain sufficiently stable operation for more than 8000 operating hours ^[16].

Molten Carbonate Fuel Cell (MCFC)

Molten carbonate fuel cells (MCFCs) are currently being developed for natural gas and coal-based power plants. MCFCs are high-temperature fuel cell that use an electrolyte composed of a molten mixture of carbonate salts suspended in a porous ceramic matrix. Two mixtures are currently used: lithium carbonate with potassium carbonate, or lithium carbonate with sodium carbonate. Because to melt the carbonate salts and achieve high ion conductivity through the electrolyte, MCFCs operate at high temperatures (650° C and above) and non-precious metals can be used as catalyst reducing overall cost of fuel cell. Molten carbonate fuel cells are not sensitive to sulphur, carbon monoxide or carbon dioxide poisoning, what more they can even use carbon oxides as fuel, making them more attractive for fuelling with gases made from coal ^[16].

When heated to a temperature of around 650° C, salts melt and become conductive to carbonate ions (CO₃²⁻). Ions flow from the cathode to the anode where they combine with hydrogen to produce water, carbon dioxide and electrons ^[6].



Electrical efficiency of typical molten carbonate fuel cell unit can reach up to 50%, when in combined heat and power it can be as high as 90%. MCFC produces high-quality waste heat for cogeneration applications. The higher operating temperature of MCFCs has

both, advantages and disadvantages compared to the lower temperature fuel cells. At the higher operating temperature, fuel reforming of natural gas can occur internally, eliminating the need for an external fuel processor. Additional advantages include the ability to use standard materials for construction, such as stainless steel sheets, and allow the use of nickel-based catalysts on the electrodes, reducing total costs.

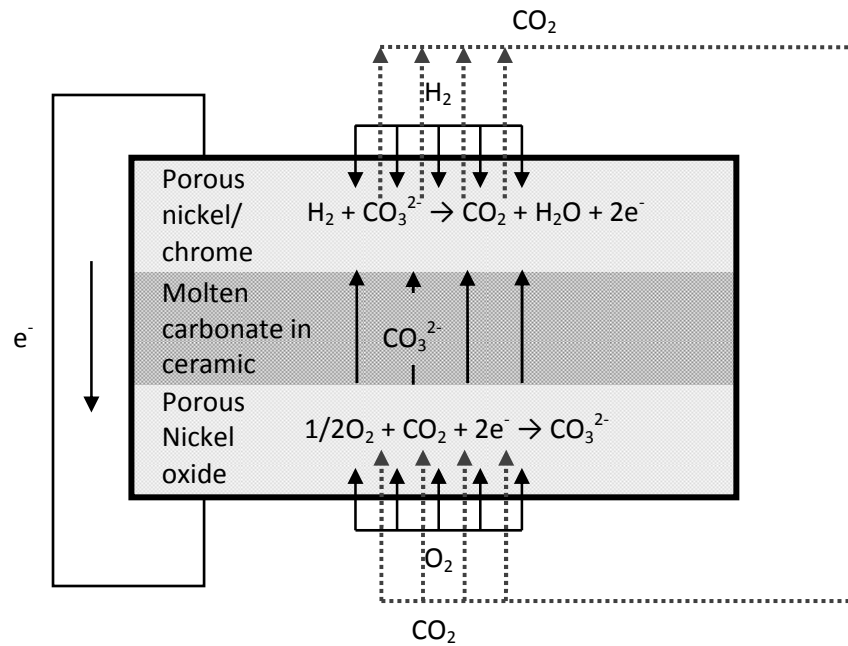


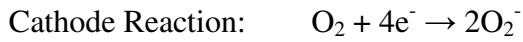
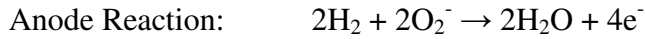
Figure 2.7 Schematic of molten carbonate fuel cell

Disadvantages of MCFC are implementation of carbon dioxide recycling, corrosive environment, and degradation/lifetime issues. It requires significant time to reach operating conditions and responds slowly to transients. These characteristics make MCFCs more suitable for steady power purposes.

Solid Oxide Fuel Cell (SOFC)

Solid oxide fuel cell employs a ceramic, nonporous metal oxide electrolyte, usually Y_2O_3 -stabilized ZrO_2 . In SOFC ionic charge carriers are O_2^- ions. At the cathode side, the oxygen molecules from the air are split into oxygen ions with the addition of four electrons. The oxygen ions are conducted through the ceramic electrolyte and combine with hydrogen at the anode side, releasing four electrons, which travel an external circuit

providing electric power and producing waste heat ^[16]. Reactions occurring in solid oxide fuel cell are as follow:



The operating temperature of solid oxide fuel cell is between 600° C and 1000° C, which provides both challenges and advantages. The challenges include long start-up time due to the time needed to reach operating temperature, slow respond to transients in electricity demand, stack hardware, stack sealing and interconnect issues. Because of high operating temperature, slow respond to the transients and slow start-up time, SOFC are considered for high-power applications including industrial and large-scale central-electricity generating-stations and CHP systems. Electrical efficiency in SOFC reaches from 50% to 60%, and in co-generation configuration even 90% can be achieved. The advantages include fuel flexibility, no precious metal as a catalyst and high power density [23].

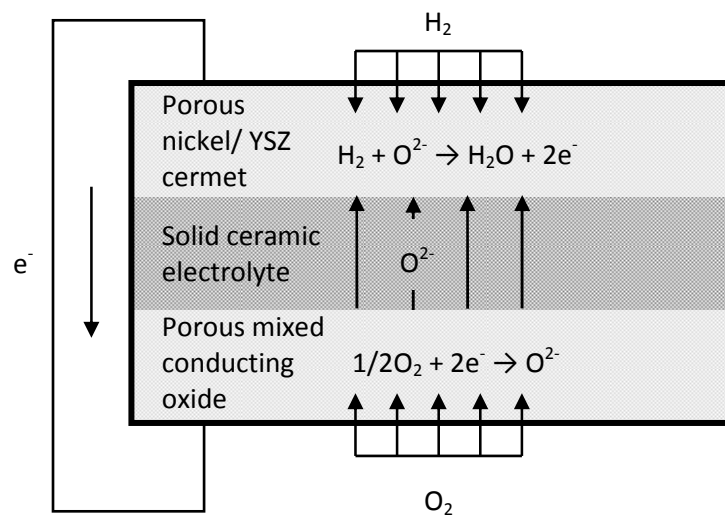


Figure 2.8 Schematic of solid oxide fuel cell

The very high operating temperature of the SOFC enables them to tolerate relatively impure fuels, such as those obtained from the gasification of coal or gasses from industrial process and other sources. Fuels polluted with CO, CO₂, S are not a problem for SOFC.

2.1.2 Fuel Cell Materials

Development and design of novel fuel cell materials is in area of intensive research all over the world. There are a lot of new material ideas for fuel cells, but so far old and well known materials are still in use. It is because research is still running or brilliant idea turned out to be not sufficient for fuel cell application for some reasons. So far in proton exchange membrane fuel cells, nafion-electrolyte based membranes with combination with Pt and C catalysts are in use. In SOFC, yttria stabilized zirconia (YSZ) is the main material. Researchers are still trying to find optimal solution for fuel cells, this goal can be hard to achieve, trying to improve one property of material in many cases we lower the other, sometimes very important property. To achieve optimal result is almost impossible, since we have to deal with many properties, like durability, mechanical strength, conductivity, low resistance, thickness, high stability and high performance just to name a few. Optimal material should be also cheap and easy to manufacture. Fuel cell environment is very harsh sometimes and meeting all mentioned requirements is a big challenge ^{[3][21]}.

Fuel cells are assembly devices which consists many parts, such as electrodes, electrolyte, bipolar plates, end plates. Since there is no moving parts they are quiet and very durable, but it is still developing technology. Research in design, construction and manufacturing process is running in many institutions all over the world. But the main concentration should be put in fuel cell material aspect. Most materials used in fuel cells today, is very 'old' – some of them has been chosen more than 25 years ago, when fuel cells started to be developed. With today's technology most of them can be upgraded or replaced by new materials, with better performance, durability, mechanical strength, higher conductivity, etc. Since bipolar plate and end plate materials are not so important, most research goes to upgrade MEA (Membrane Electrode Assembly) materials. MEA is heart of fuel cell, the place where conversion takes place, and that's why it is so important ^[22].

Research is running, trying to implement new processes and new materials to improve work of fuel cell. Researchers are using plasma polymerisation, vapor phase polymerisation, nanotechnology and other techniques, together with new materials to improve properties and work of fuel cell, but still old and well known materials are in common use.

Electrolyte Materials

Requirements given to fuel cell electrolyte materials are high ion conductivity, but not electrons. Electrolyte must be also gas impermeable, to prevent gasses mixing and as thin as possible to minimize resistance ^[3].

Many electrolyte materials are based on thin polymeric membranes, most of these polymer materials relay on water based transport mechanisms for ions. Water is very often involved in the ionic transport, therefore ionic conductivity is very sensitive to the level of hydration. Operating fuel cell in dry environment is limited or even impossible. Because of this phenomena complex water management solutions are required to use for many fuel cell systems. Ionic transport looks a bit different it comes to deal with solid ceramic electrolyte materials for example. Ceramic electrolyte materials conduct ions via defect hopping mechanisms, it requires high temperatures. Ceramic electrolytes are not sensitive to hydration level, therefore in most cases complex water management system is not necessary. Ionic conductivity in oxide ceramic electrolytes is much worse than in polymeric electrolytes, so to obtain high ionic conductivity fuel cell has to be operated at high temperatures, from 700° C to 800° C, sometimes even up to 1000° C ^{[30][31][33]}.

Designing polymer electrolyte material able to work above 100°C has big importance, as it simplify water management, improve overall performance and increase tolerance to impurities in fuel. Good polymer electrolyte material must have high ionic conductivity, good mechanical properties, so it is possible to manufacture thin, durable membranes. Polymer electrolyte must be also highly stably in fuel cell environment and inexpensive ^[23].

Electrode and Catalyst Materials

Fuel cell electrodes must have high electrical conductivity and high porosity to collect (or deliver) electrons released during chemical reaction and collect (deliver) products or reactants from fuel cell. Other requirement given to fuel cell material is high catalytic activity. Many fuel cell catalysts are based on platinum, noble metal which makes catalyst one of the most expensive parts of fuel cell. Double layer design of electrode/catalyst is most common one, thicker layer of inexpensive, highly conductive, porous electrode is bonded on the top of expensive thin and highly active catalyst layer creating membrane electrode assembly (MEA) ^{[3][6][35]}.

Same requirements are given to SOFC materials, but high temperature of SOFC environment makes it impossible to use the same materials as for example materials used in PEMFC, because they are unstable in high temperatures. Together with high temperature come mechanical strength, thermal stress and corrosion issues. Most of SOFC electrode materials are high conductive ceramic materials or ceramic-metal composites, called cermets ^[23].

New approach in alkaline fuel cells is anion-exchange membrane (AEM). Anion-exchange membranes are solid polymer electrolyte membranes that contain positive ionic groups and mobile negatively charged anions. This new kind of membranes for alkaline fuel cells seems to be very promising, but so far they are still in development phase. Very intensive research in this field is run by Prof. Robert Slade from University of Surrey in UK.

Development of better and/or cheaper catalyst materials and better high surface area materials for electrodes are in the area of intensive research.

2.2 Vapor Phase Polymerization

Vapor phase polymerization (VPP) is similar to physical vapor deposition, but during this process some chemical reactions occur as well, VPP combine some parts of physical and chemical vapor deposition. VPP is fundamentally a vaporisation coating technique, involving transfer of material on an atomic level and polymerization process occurring in vacuum environment ^{[40][41]}. Vapor phase polymerization is method to deposit and

polymerize thin films by the condensation of a vaporized form of the material onto various surfaces. The coating method involves purely physical processes such as high temperature vacuum evaporation, transportation, deposition, concentration and polymerization ^[40].

During evaporation stage, a target, consisting of the material to be deposited is heated, this dislodges atoms from the surface of the target, vaporising them. Transport stage, simply consists of the movement of vaporised atoms from the target to the substrate to be coated and will generally be a straight line affair ^[41]. In some cases coatings can consist of metal oxides, nitrides, carbides and other materials as catalysts. The atoms of metal will then react with the appropriate gas during the transport stage, reactive gases may be oxygen, nitrogen and methane. In cases where the coating consists of the target material alone, this step would not be part of the process. Deposition is the process of coating build up on the substrate surface. Depending on the actual process, some reactions between target materials and the reactive gases may also take place at the substrate surface simultaneously with the deposition process ^[39]. The last stage is polymerization where monomers creating bonds, become polymer chains deposited on the target surface.

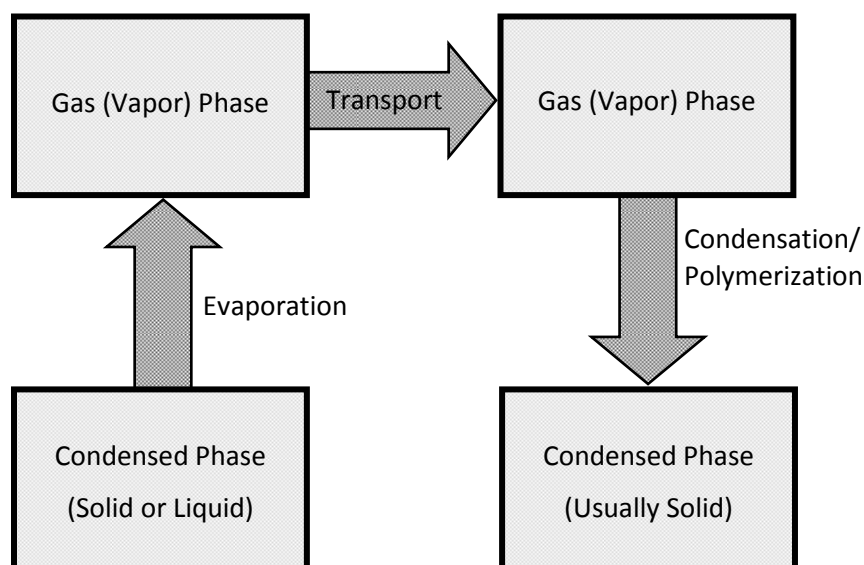


Figure 2.9 General concept of vapor phase polymerization (VPP) process

Vapor phase polymerization is used in the manufacture of items including semiconductor and organic-semiconductors devices, aluminized PET film for balloons and

snack bags, and coated cutting tools for metalworking, VPP found great importance in thin film deposition, nanotechnology and material sciences. It is possible to achieve extremely thin films like atomic layers. VPP is very simple, but powerful process which with help of special evaporators can deposit mono-layers of virtually all materials with melting points up to 3500°C ^{[40][11]}. VPP process can change target surface for numerous reasons, such as improving hardness and wear resistance, friction reduction, improved oxidation resistance. The use of such coatings is aimed at improving efficiency through improved performance and longer component life. They may also allow coated components to operate in harsh environments that the uncoated component would not otherwise have been able to perform ^[39].

2.3 PEDOT Structure and Properties

Poly(3,4-ethylenedioxythiophene) or PEDOT (also known as PEDT, PDOT) is a conducting polymer based on 3,4-ethylenedioxythiophene or EDOT monomer, its empirical formula is C₆H₆O₂S. PEDOT is optically transparent in its conducting state, has high stability, low redox potential and moderate band gap. A large disadvantage is poor solubility ^[11].

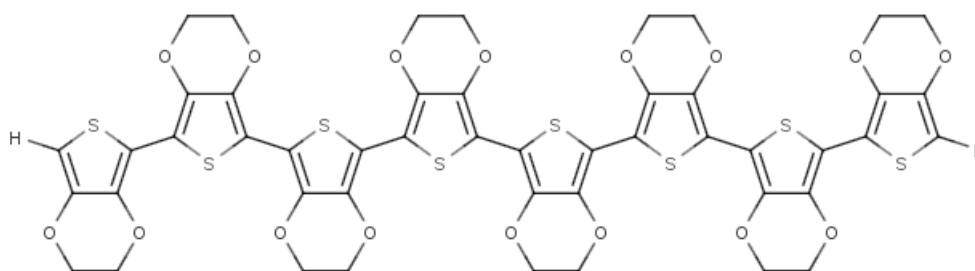


Figure 2.10 PEDOT chain structure

In the field of electroanalysis, conductive polymers are widely employed as coatings conferring the electrode systems antifouling properties and possibly activating electrocatalytic redox processes. Among different conducting polymers, PEDOT has emerged in recent years, thanks to characteristics previously reported. In addition, PEDOT coatings possess high stability over different charge and discharge cycles and can be electrogenerated directly on a conductive support (Pt, Au, glassy carbon, indium tin oxide, etc.) in organic solvents or in aqueous solution. The enhancement of the electrochemical

signals relative to the oxidation of different analytes, when using PEDOT modified electrodes with respect to bare support has been reported in recent publications ^{[1][11]}.

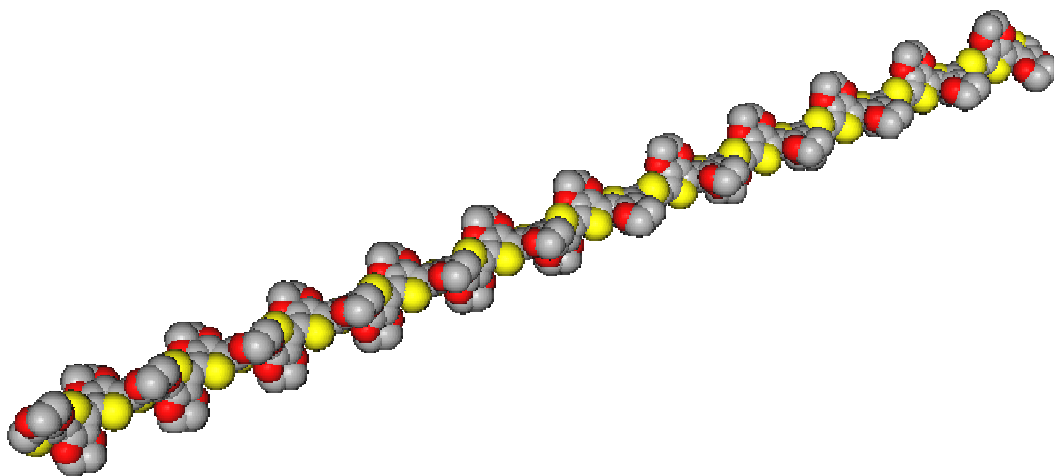


Figure 2.11 Computer modelled PEDOT chain structure

2.4 Polythiophene Structure and Properties

Polythiophenes (PTs) are result from the polymerization of thiophenes, a sulfur heterocycle, that can become conducting when electrons are added or removed from the conjugated orbitals via doping.

The study of polythiophenes has become point of interest since Alan Heeger, Alan MacDiarmid, and Hideki Shirakawa awarded the Nobel Prize in Chemistry in 2000, “for the discovery and development of conductive polymers”. Electrical conductivity is result from the delocalization of electrons along the polymer backbone. However, electrical conductivity is not the only interesting property resulting from electron delocalization. Other properties of these materials are optical properties. Rapid color shifts are response to changes in solvent, temperature, applied potential, and binding to other molecules. Both electrical conductivity and color changes are caused by the same mechanism — deviation (twisting) of the polymer backbone ^{[47][48]}.

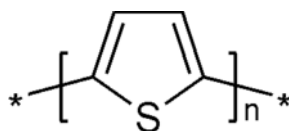


Figure 2.12 The monomer repeat unit of unsubstituted polythiophene

Mechanism of conductivity and doping is pretty easy and can be explained as follows. In conducting polymers electrons are delocalized along the conjugated backbones, by adding or removing electrons from the system, a charged unit called a bipolaron is formed. The bipolaron moves as a unit up and down the polymer chain, and is responsible for the macroscopically observed conductivity of the polymer. Conductivity of conducting polymers is much lower than conductivity of most metals, such as copper or aluminium, but high conductivity is not necessary for many applications of conducting polymers^[49].

The number of coplanar rings determines the conjugation length, the longer the conjugation length, the longer the absorption wavelength, because of the lower the separation between adjacent energy levels. Deviation from coplanarity may be both, permanent or temporary. Permanent deviation is a result from mislinkages during synthesis. Temporary deviation is a result from changes in the environment or binding. Twist in the backbone highly reduces the conjugation length, and the separation between energy levels is increasing which results in a shorter absorption wavelength. Latest studies show that it is possible to synthesize 48 – and even 96 – mer oligothiophenes. A variety of environmental factors can cause the conjugated backbone to twist, reducing the conjugation length and causing an absorption band shift, including solvent, temperature, application of an electric field, and dissolved ions^{[47][50]}.

Many applications have been proposed for polythiophene, but so far none has been commercialized. Most common applications of polythiophene include solar cells, batteries, field-effect transistors^[51], electroluminescent devices, nonlinear optic devices^[52], photochemical resistors, diodes and chemical sensors^[53].

In this research two kinds of polythiophene were used. First was polybithiophene – built of two thiophene mers, and second polyterthiophene – built of three thiophene mers.

Bithiophene is easier to deal with, it has lower evaporation temperature than terthiophene, so polymerization process takes less time and can be carried out in lower temperature. What more, terthiophene is ten times cheaper than bithiophene. However, polyterthiophene has much better properties, because it is built using polymers with three conjugated coplanar thiophene rings, instead of two coplanar thiophene rings, so chance for deviation decreases, and resulting film made of terthiophene is less twisted. In appendix F, comparison of thiophene, bithiophene and terthiophene can be found.

2.5 Polyethylene Glycol Structure and Properties

Polyethylene glycol (PEG) is a polyether compound and is used in variety of applications from industrial manufacturing to medicine. Polyethylene glycol is also known as polyethylene oxide (PEO) or polyoxyethylene (POE). Basically polyethylene glycol is an oligomer or polymer of ethylene oxide. PEG is very flexible and water soluble polymer. It binds water and very often is used as a support to keep uniform state of substances. PEG has low toxicity and is used as an alternative to the traditional highly poisonous ethylene glycol solutions. PEG and PEO are liquids or low-melting solids, depending on their molecular weights. Polyethylene glycols are prepared by polymerization of ethylene oxide and are commercially available over a wide range of molecular weights from 300 g/mol to 10,000,000 g/mol. Polyethylene glycols are also available with different geometries. PEG is produced by the interaction of ethylene oxide with water, ethylene glycol, or ethylene glycol oligomers. Ethylene glycol and its oligomers are preferable as a starting material instead of water, because they allow the creation of polymers with a low molecular weight distribution. Chain length depends on the reactants ratio. Polyethylene glycol is also used as polymer host for many solid polymer electrolytes which can be used in various applications such as batteries, fuel cells and other electrical devices.

3 PEDOT MANUFACTURING

Purpose of this chapter is to provide general introduction to the various PEDOT manufacturing processes depending what kind of properties are demanded. Type of PEDOT manufacturing process depends strongly on target material on which surface PEDOT is going to be deposited.

Mixing PEDOT or depositing it on other materials is sometimes necessary and desired in order to gain better electrical or mechanical properties. PEDOT mechanical strength is very weak, so to get material which will be able to work in demanding environment, like the one in fuel cells or batteries, PEDOT must be mixed with other polymers (conducting or not). Some tests showed that PEDOT when mixed with some non conducting polymers, becomes even better conductor than in its pure form. This phenomena is being investigated.

3.1 PEDOT Manufacturing in Vapor Phase Polymerization Process

Vapor phase polymerization is carried out in a simple single chamber setup. The chamber can be flushed with air, nitrogen, or argon during polymerization, and a heater provides the possibility to increase the temperature of the monomer reservoir in order to speed up the process. The samples are initially coated with the oxidant, Fe(III) tosylate in 40% butanol solution mixed with pyridine, to make oxidant less acidic. Process has to be carried out in pH higher than one offered by Fe(III) tosylate, using alkaline inhibitor (pyridine). Pyridine increases the pH of the Fe(III) tosylate in butanol solution, but in the same time redox activity of Fe(III) will decrease. In too acidic environment EDOT bonds can break, affecting on final results. The optimal results can be achieved by adding 0.5 mol of pyridine per mol of Fe(III) tosylate. The Fe(III) tosylate/pyridine solution was applied to the substrates and dried in air at room temperature until the solvent, butanol, had evaporated. The samples were then further dried for 3 min in an oven at 70 °C in air, later the samples are transferred to the polymerization chamber in this case vacuum desiccator was used, and heated up to 70°C to speed up the process ^{[11][40]}. Normally from 30 to 45 minutes is needed to finalize the deposition and polymerization. Next step is to wash obtained samples in water, twice and later in ethanol to remove all impurities from film

surface, washing process has to be carried out very carefully, trying not to scratch delicate PEDOT surface. Washed samples have to be dried in standard room conditions.

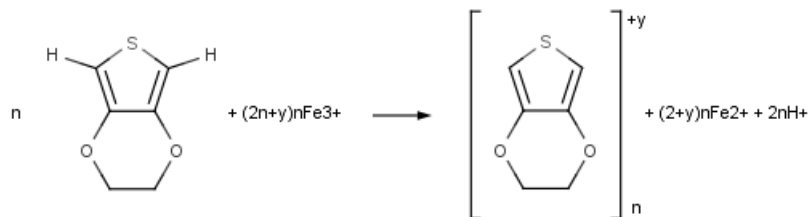


Figure 3.1 Reaction occurring during vapor phase polymerization process

It is possible to deposit many PEDOT layers, one on another. To achieve multilayer PEDOT surface, washing process has to be skipped after vapor phase polymerization. Coating next layer of oxidant (Fe(III) tosylate) on PEDOT surface and repeating whole process again gives possibility to deposit next PEDOT layer ^{[11][40]}. Process needs to be repeated as many times as many layers are desired to achieve. Samples have to be washed after depositing last layer of PEDOT and dried in room conditions.

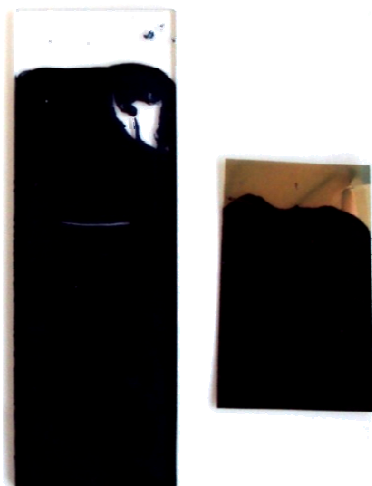


Figure 3.2 Two standard PEDOT samples used for tests, on left PEDOT deposited on glass surface, on right PEDOT deposited on mylar coated with gold

During vapor phase polymerization sample color is changing, starting from yellow (Fe(III) tosylate), through green (combination of yellow and blue – Fe(III) tosylate with PEDOT) to blue (PEDOT), time of the process may depend on many parameters so

experienced scientist can evaluate when process has finalized by visual test. Obtained samples are shown above, intensive blue color is PEDOT film. Sample on glass (Fig. 3.2) was used for conductivity and UV-Vis tests, small scratch for test on profilometer can be visible above, and sample on mylar (Fig. 3.2) covered with gold (one side) was used for electrochemical tests - cyclic voltammetry and chronoamperometry.

4 TESTING – EXPERIMENTAL PROCEDURE

Testing is very important part of each research. Measuring parameters give a quantitative comparison, distinguishing good from bad results. Some sophisticated techniques not only give results, but also indicate why results are so good or bad.

This chapter describes techniques used to investigate PEDOT parameters. All the techniques are very simple and easily understandable, but give all necessary data to compare parameters of developed material with other materials and distinguish good material from the bad one.

4.1 Measuring Conductivity

Conductivity is one of the major parameters of fuel cell. Conductivity quantifies the ability of material to permit the flow of charge when driven by an electric field. A material's conductivity (σ) depends on two factors, quantity of carries available to transport charge the mobility of those carries within the material. The following equation defines conductivity in condition of resistivity and thickness:

$$\sigma = 1/(\rho \cdot t),$$

where:

σ – conductivity (S/m),

ρ – sheet resistance (Ω/\square),

t – thickness (m).

To measure sheet resistance of material and film thickness, two methods has been used, four point test and profile measuring, both described below.

4.1.1 Measuring Sheet Resistance (Four Point Test)

The four point probe technique is one of the most common methods for measuring sheet resistance. The classic arrangement is to have four needle-like electrodes in a linear

arrangement and constant distance with a current injected into the material via the outer two electrodes. The resultant electric potential distribution is measured via the two inner electrodes by using separate electrodes for the current injection and for the determination of the electric potential, the contact resistance between the metal electrodes and the material will not show up in the measured results. Because the contact resistance can be large and can strongly depend on the condition and materials of the electrodes, it is easier to interpret the data measured by the four-point probe technique than results gathered by two point probe techniques.

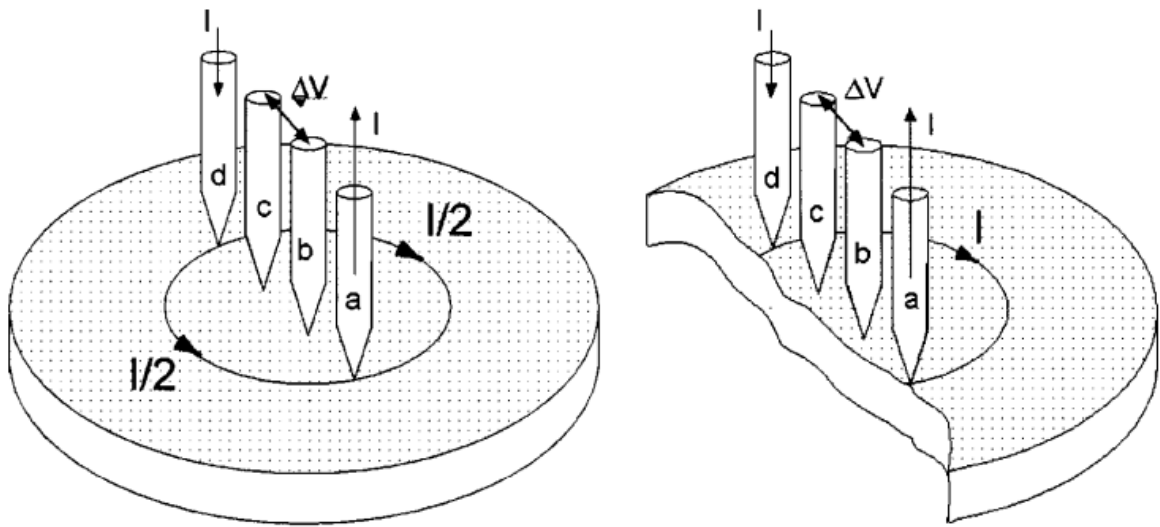


Figure 4.1 Four point probe measurement technique (left). Probe near the edge of the sample, all current has to go through the left half plane (right)

In general, the material's sheet resistance, ρ , can be calculated by the relation:

$$\rho = \alpha(V_{\text{measured}} / I_{\text{measured}})$$

The sheet resistance correction factor (α) counts the size of the test structure, the thickness of the material, the size of the electrodes, and the position of the electrodes with respect to the boundary of the test structure into account. Figure above illustrates the effect of the position of the electrodes with respect to the boundaries of the test structure. By placing the electrodes at the edge rather than in the middle of the test structure, the measured voltage over the inner electrodes will be two times larger because all current has to take the right-half plane.

Table 4-1 Sheet resistance data for different samples, collected during 4 point test on Jandel Model RM3. Data has been taken for current 4.5 uA (all values are in Ω/\square)

Material	Test 1	Test 2	Test 3	Test 4	Average
PEDOT	24.61	20.59	21.42	20.99	21.903
PEDOT/PBTh ,1:1‘	286.72	312.04	325.33	308.63	308.18
PEDOT/PBTh ,1:0.5‘ PEG ,2‘	38.45	40.12	35.07	36.86	37.625
PEDOT/PBTh ,1:1‘ PEG ,2‘	1328	1304	1540	1357	1382.3
PEDOT/PBTh ,1:2‘ PEG ,2‘	1732	1502	1740	1813	1696.75
PEDOT/PBTh ,1:3‘ PEG ,2‘	1951	1905	1838	1855	1887.25
PEDOT/PBTh ‘1:4‘ PEG ‘2‘	3893	3937	3954	3786	3892.5
PEDOT/PBTh ‘1:5‘ PEG ‘2‘	2430	2878	2587	2323	2554.5
PEDOT/PTTh ‘1:0.5‘ PEG ‘2‘	193.27	186.38	165.97	231.25	194.22

Table above shows sheet resistance values for all tested samples. Four point test was carried out using Jandel Model RM3 device, test was performed four times for each sample in different places and average value calculated. Sheet resistance depends mostly on PEDOT ratio in sample, more PEDOT lower sheet resistance.

4.1.2 Measuring Thickness (Measuring Profile)

The easiest way to measure thickness is by using profilometer, a measuring device used to measure a surface's profile, in order to quantify its roughness. Vertical resolution is usually in the nanometre level, though lateral resolution is usually poorer. There are two types of profilometers, contact and non-contact. More common are contact profilometers, where diamond needle is moved vertically in contact with a sample and then moved laterally across the sample for a specified distance and specified contact force. A profilometer can measure small surface variations in vertical stylus displacement as a function of position, typical profilometer can measure small vertical features ranging in height from 10 nanometres to 1 millimetre, special profilometers can be even more precise. Small changes in height position of the diamond needle are affecting on piezoelectric actuator which generates an analog signal and is converted into a digital signal stored,

analyzed and displayed. The radius of diamond needle ranges from 10 nanometres to 25 μm , and the horizontal resolution is controlled by the scan speed and data signal sampling rate. The needle tracking force can range from less than 1 to 50 milligrams.

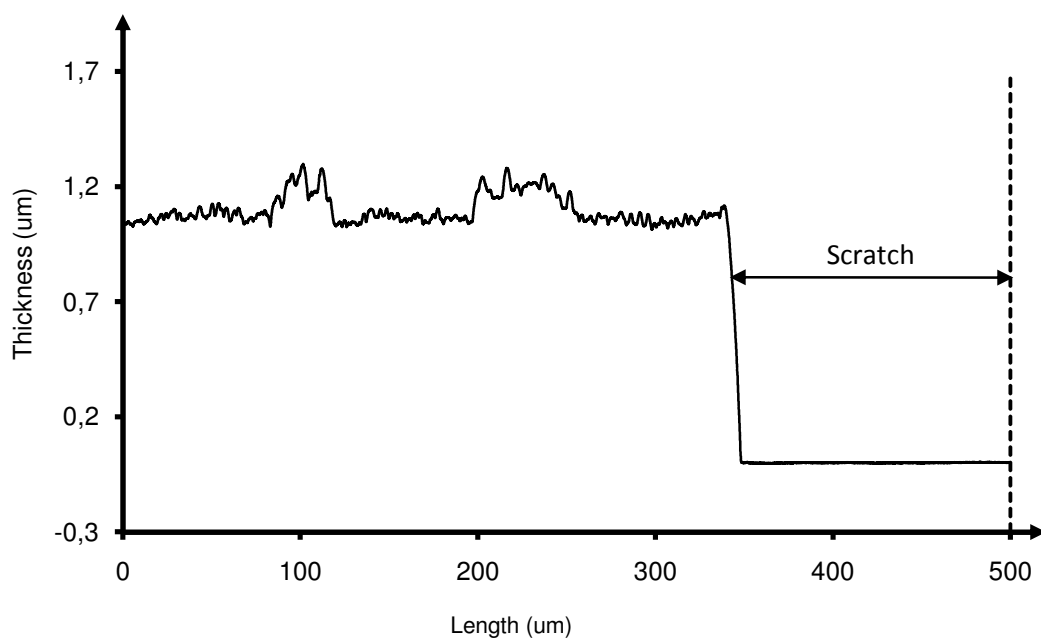


Figure 4.2 Profiler test result for PEDOT/PBTh ,1:0.5' PEG ,2' sample. Scan length 500 μm and 0.028 $\mu\text{m}/\text{sample}$ resolution

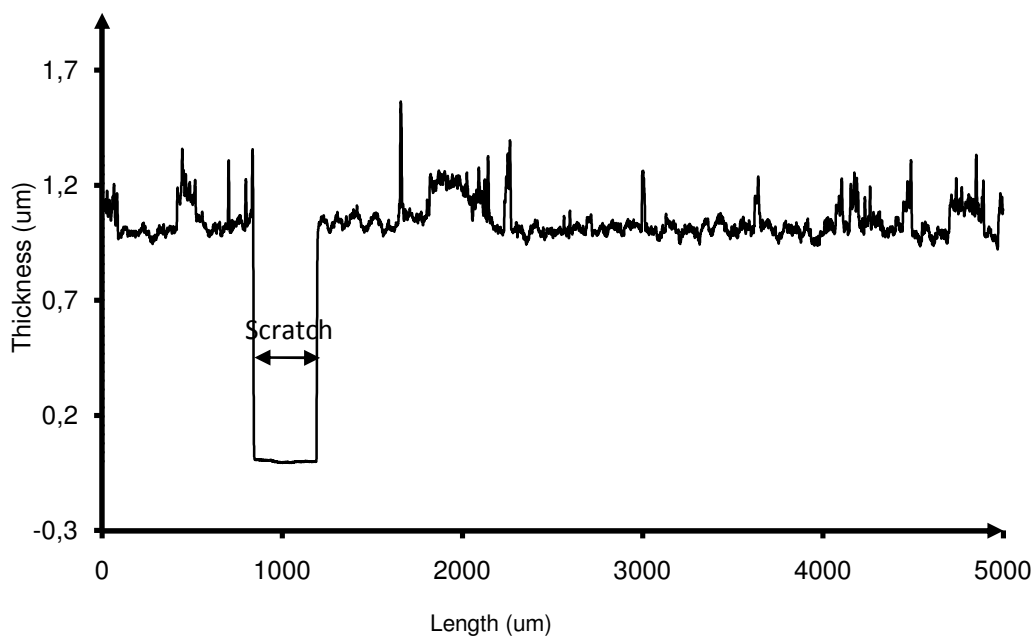


Figure 4.3 Profiler test result for PEDOT/PBTh ,1:0.5' PEG ,2' sample. Scan length 5000 μm and 0.278 $\mu\text{m}/\text{sample}$ resolution

Profilometer can be used for measuring both, roughness and thickness of PEDOT layer. It is important to have surface as flat as possible, so is possible to achieve same parameters along PEDOT layer. The simplest way to measure thickness of PEDOT layer, is to make small scratch in PEDOT sample polymerized on a glass surface. Making small gap in PEDOT layer and measuring distance between PEDOT and glass surfaces, gives layer thickness.

Table 4-2 Thickness values for different samples, collected on Veeco DekTak 150 Profiler

Material	Thickness [nm]
PEDOT	875
PEDOT/PBTh ,1:1‘	385
PEDOT/PBTh ,1:0.5‘ PEG ,2‘	1005
PEDOT/PBTh ,1:1‘ PEG ,2‘	260
PEDOT/PBTh ,1:2‘ PEG ,2‘	950
PEDOT/PBTh ,1:3‘ PEG ,2‘	1755
PEDOT/PBTh ,1:4‘ PEG ,2‘	1293
PEDOT/PBTh ,1:5‘ PEG ,2‘	685
PEDOT/PTTh ‘1:0.5’ PEG ‘2’	890

Tests were performed on Bruker DekTak 150 Surface Profiler, giving view on surface roughness and layer thickness.

4.1.3 Conductivity results

Having film thickness and its sheet resistance values, conductivity of each sample has been calculated. Conductivity values are as follows:

Table 4-3 Conductivity values for different samples, calculated using sheet resistance and thickness values

Material	Conductivity [S/m]
PEDOT	47619.05
PEDOT/PBTh ,1:1‘	8428.20
PEDOT/PBTh ,1:0.5‘ PEG ,2‘	26445.84
PEDOT/PBTh ,1:1‘ PEG ,2‘	2782.43
PEDOT/PBTh ,1:2‘ PEG ,2‘	620.38
PEDOT/PBTh ,1:3‘ PEG ,2‘	298.52
PEDOT/PBTh ,1:4‘ PEG ,2‘	198.69
PEDOT/PBTh ,1:5‘ PEG ,2‘	571.48
PEDOT/PTTh ‘1:0.5’ PEG ‘2’	5785.24

Again, in samples with higher PEDOT ratio, conductivity values are higher. Conductivity values for common materials are shown in table below, just for comparison. For PEDOT/PBTh ‘1:5’ PEG ‘2’ ratio conductivity is much higher than for PEDOT/PBTh ‘1:4’ PEG ‘2’ ratio, and even higher than for PEDOT/PBTh ‘1:3’ PEG ‘2’. Cyclic voltammetry tests of PEDOT/PBTh ‘1:5’ PEG ‘2’ gives much lower performance than samples with lower ratios. Only explanation is that in PEDOT/PBTh ‘1:5’ PEG ‘2’ sample ratio of PBTh to PEDOT is to high so this blend doesn’t create interpenetrating networks, but separated phases occur in this thin film. Using other words, heterogeneous film instead of homogeneous film is result of polymerization in this case. Some tests show that PEDOT together with PEG create thin with conductivity higher even conductivity of pure PEDOT, it is very surprising since PEG is non conducting polymer. When PBTh (or PTTh) are added to the blend during VPP process, conductivity of resulting film is decreasing.

Table 4-4 Conductivity values for common materials

Material	Conductivity [S/m]
Silver	6.29×10^7
Copper	5.69×10^7
Annealed copper	5.80×10^7
Gold	4.52×10^7
Aluminium	3.50×10^7
Iron	1.03×10^7
Platinum	0.943×10^7
PEDOT	1×10^5
Sea water	4.8
Drinking water	0.0005 to 0.05
Deionized water	5.5×10^{-6}
Air	$3 \text{ to } 8 \times 10^{-13}$
Jet A-1 kerosene	$0.5 \text{ to } 4.5 \times 10^{-14}$
n-hexane	1×10^{-14}

4.2 Ultraviolet-visible spectroscopy

Ultraviolet-visible spectroscopy or ultraviolet-visible spectrophotometry (UV-Vis or UV/Vis) is absorption spectroscopy or reflectance spectroscopy in the ultraviolet-visible spectral region, sometimes near-infrared (NIR) ranges. The absorption or reflectance in the visible range directly affects the perceived color of the chemicals involved. In this region of the electromagnetic spectrum, molecules undergo electronic transitions.

The instrument used in ultraviolet-visible spectroscopy is called a UV/Vis spectrophotometer. UV/Vis spectrophotometer measures the intensity of light passing through a sample and compares it to the intensity of light before introduction to the sample.

The ratio of light intensity after passing the sample to light intensity before is called the transmittance. The light absorbance of the sample can be calculated as:

$$A = -\log(T/100),$$

where:

A – light absorbance,

T – transmittance.

It is possible to configure the UV-Vis spectrophotometer to measure reflectance. In this configuration, the spectrophotometer measures the intensity of light reflected from a tested sample and compares it with the intensity of light which reflects from a reference material. The ratio between light intensity of sample and light intensity of reference material is called the reflectance.

The spectrophotometer consists of a sample holder, reference holder (double beam spectrophotometer), a light source, a diffraction grating monochromator to separate the different wavelengths of light and a light detector. Older spectrophotometers use couple of light sources in one device, the radiation source is often a tungsten filament with wavelengths from 300 to 2500 nm and a deuterium arc lamp, which produce continuous ultraviolet light in range from 190 to 400 nm, a newer spectrophotometers use xenon arc lamps, which can produce continuous light from 160 to 2,000 nm or more. Photomultiplier tube is used typically as the detector, sometimes it can be a photodiode or a photodiode array, newer devices has a charge-coupled device (CCD). Basically, the monochromator swipes through each wavelength and changing light intensity can be measured by detector.

A spectrophotometer can be either single beam or double beam. In a single beam configuration, light passes first through reference material and later through sample material and later two measurements are compared. In double beam configuration, the light is split into two beams before it reaches the sample. Light passes through, both sample and reference material simultaneously. The reference beam intensity is taken as 100% transmission or 0 absorbance, and the measurement displayed is the ratio of the two beam intensities.

Below results of UV-Vis spectroscopy for different samples are shown:

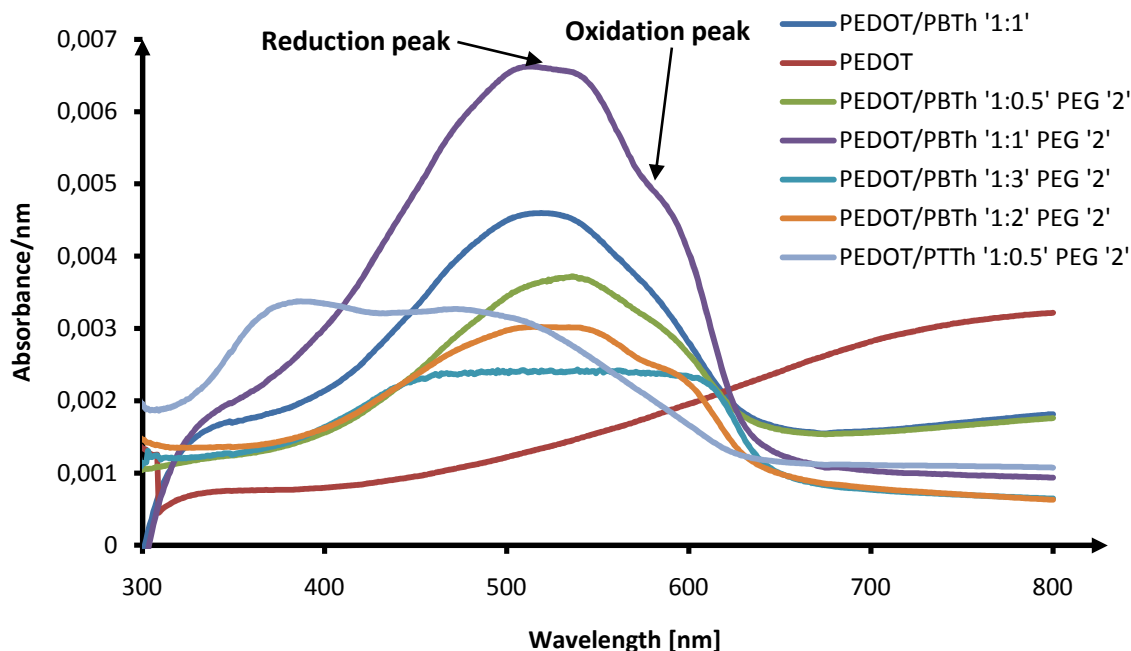


Figure 4.4 UV-Vis results for tested thin films normalized for thin film thickness

UV-Vis test show that PEDOT is not oxidised when comes together with other polymers in blends. Absorption in pure PEDOT is growing with increasing wavelength, but in tested blends absorption is growing very rapidly at the beginning, reaches highest possible absorption point and then is decreasing. Two peaks can be visible for PEDOT, PBTh, PTTh and PEG blends, one is reduction peak, other one is oxidation peak when absorbance is decreasing. Light absorbance is much higher for blends with PBTh (or PTTh) than PEDOT itself. In pure PEDOT light activation effect can be observed, but PBTh greatly increases this phenomena. UV-Vis data gathered from tests was corrected for thickness. Tested samples had different thickness and more thicker film, more light it absorbs, so to compare samples normalization for thickness has been done for each sample.

4.3 Electrochemical Testing (Cyclic Voltammetry and Chronoamperometry)

Cyclic voltammetry (CV) is the most effective and versatile electroanalytical technique available for the mechanistic study of redox systems. It enables the electrode potential to be rapidly scanned in search of redox couples ^[5]. When located, a couple can then be characterized from the potentials of peaks on the cyclic voltammogram and from changes caused by variation of the scan rate. Cyclic voltammetry is often the first experiment performed in an electrochemical study ^{[20][21]}.

However, the basis of the chronoamperometry (CA) technique is measurement of current change in time at fixed potential value.

4.3.1 Introduction to Cyclic Voltammetry

The repetitive triangular potential excitation signal for cyclic voltammetry, shown on figure below, causes the potential of the working electrode to sweep back and forth between two designated values (the switching potentials) ^{[5][21]}. To obtain a cyclic voltammogram, the current at the working electrode is measured during the potential scan.

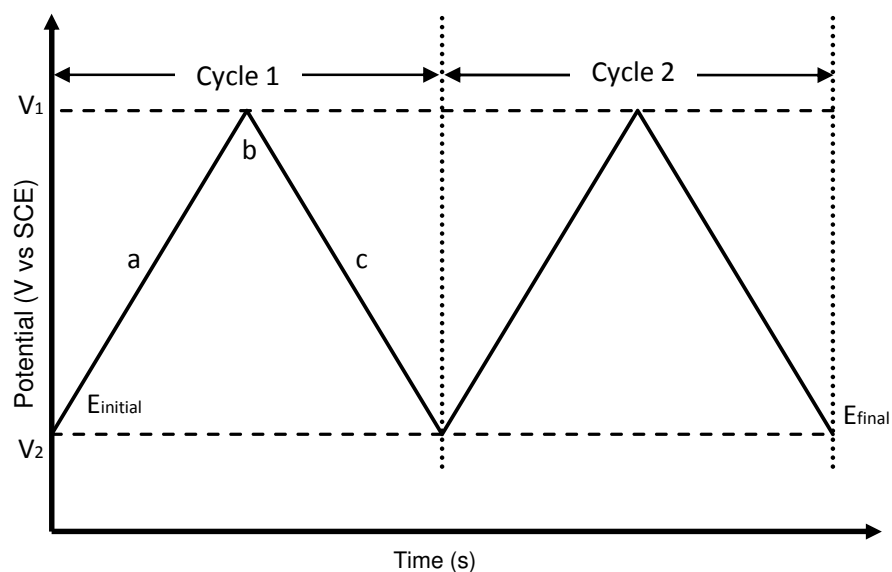


Figure 4.5 Typical excitation signal for cyclic voltammetry

A typical cyclic voltammogram recorded for a reversible single electrode transfer reaction is shown in below.

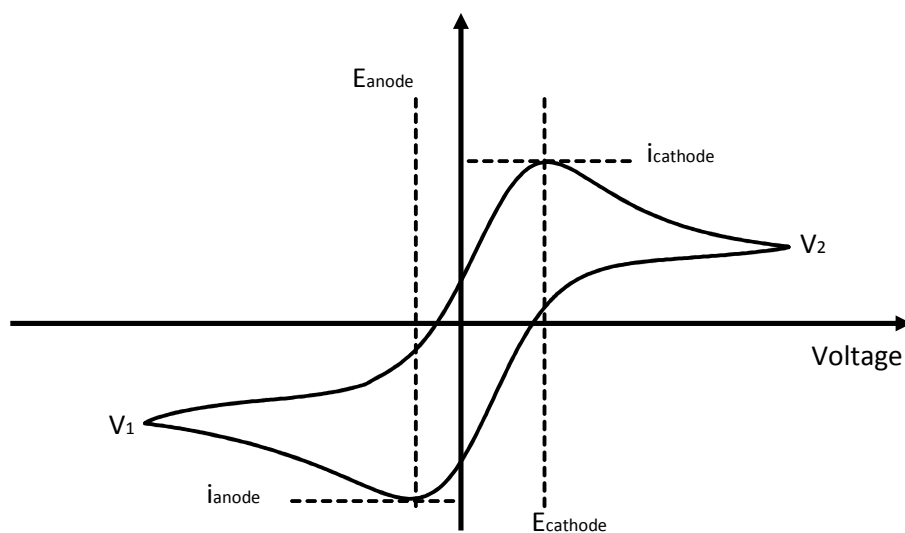


Figure 4.6 Typical voltammogram plot

The forward sweep produces a current response which is plotted on V-i graph. When the scan is reversed it simply moves back through the equilibrium positions gradually converting electrolysis product. When the current flow is reversed, flowing from the

solution species back to the electrode and occurs in the opposite sense to the forward seep, but otherwise principles don't change ^[22]. The voltage scan rate influence on the current for a reversible electron transfer is shown below.

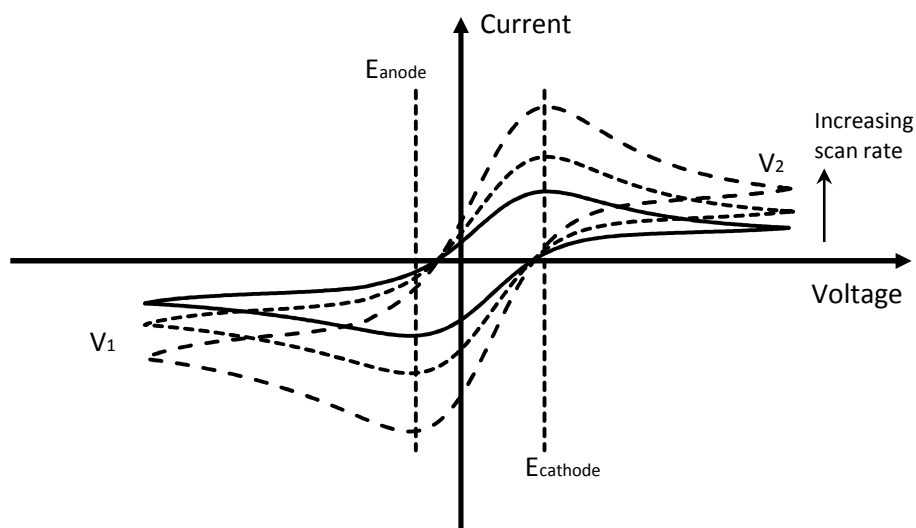


Figure 4.7 Effect of the increased scan rate

The cyclic voltammetry shows different behaviour for cases where the electron transfer is not reversible ^{[22][23]}. Figure below shows voltammogram for a reversible reaction, for different values of the reduction and oxidation rate constants.

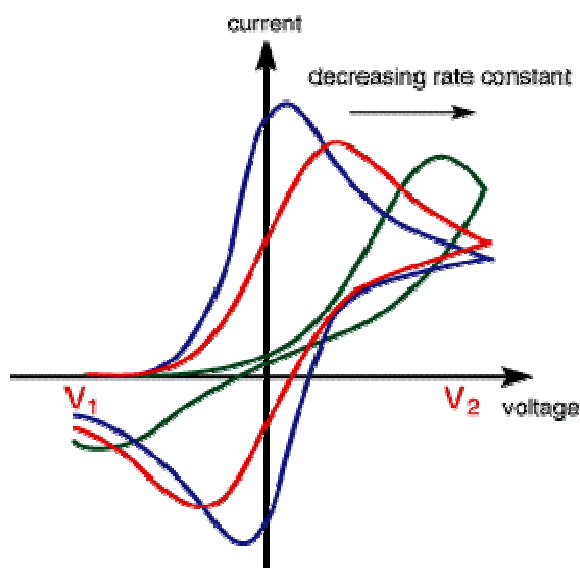


Figure 4.8 Change of the rate constant

First case where both the oxidation and reduction rate constants are fast, but when the rate constants are lowered the curves shift and reaction become more reductive ^[23]. The equilibrium at the surface is no longer establishing so rapidly. Analysing the variation of peak position as a function of scan rate it is possible to estimate the electron transfer rate constants.

4.3.2 Cyclic Voltammetry Test Cell Assembly

Figure below shows real test PEDOT electrode deposited on Mylar and laminated with gold connector, all the electrodes used during tests look similar to the one below.

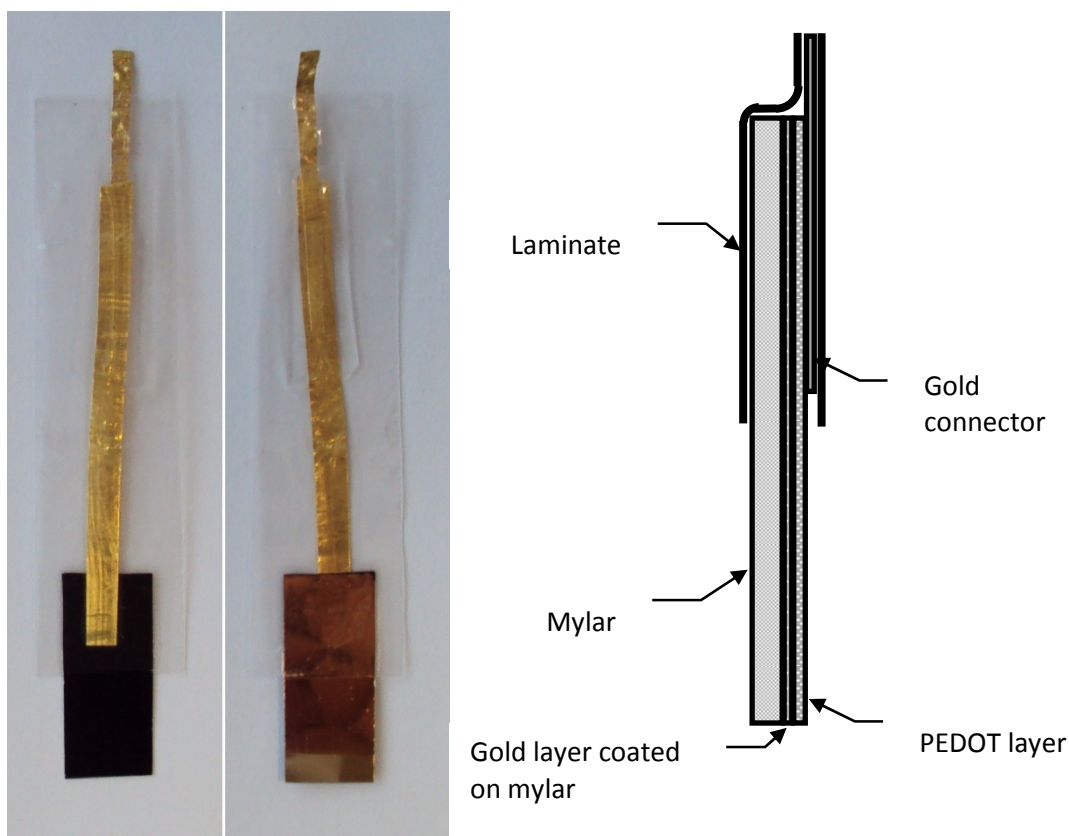


Figure 4.9 The test electrode cross section, mylar with gold layer and polymerized PEDOT is laminated with a gold connector

Figure below shows standard test cell. System consist of three electrodes (counter electrode, reference electrode and working electrode) in electrolyte, cell is sealed to make closed environment for tests. However, electrode shown above is not optimal electrode

design for fuel cells. Tests has been performed on simple electrode geometry only to evaluate material properties, for future fuel cell GDE (Gas Diffusion Electrode) electrode has to be build.

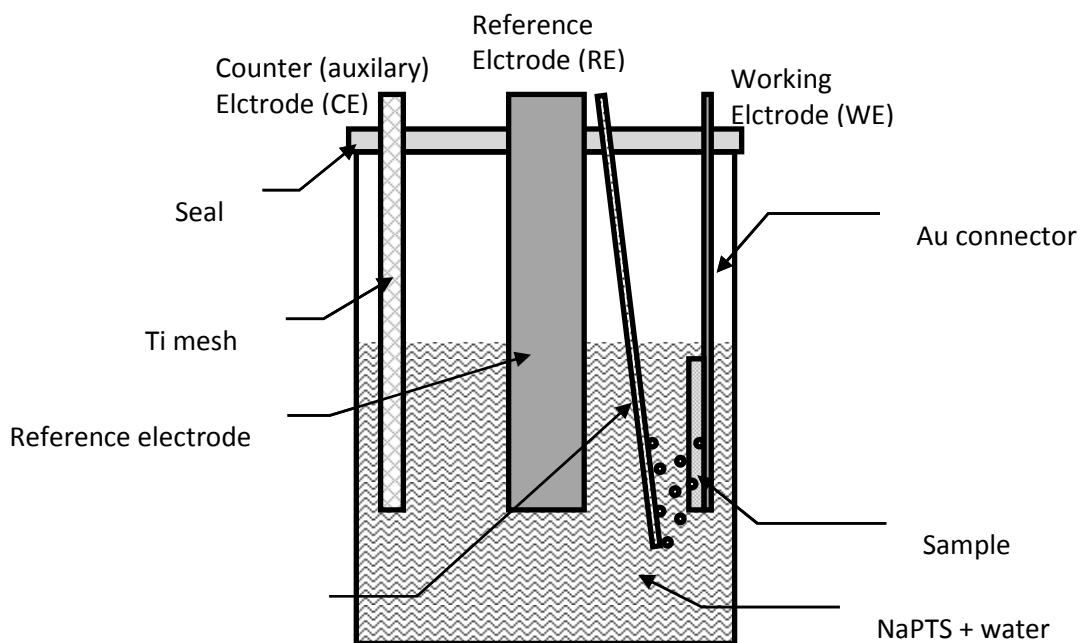


Figure 4.10 The test cell layout, sample is laminated with a gold connector

As working electrode, PEDOT electrode shown before has been used. Counter electrode is simply titanium mesh, and reference electrode is used to record reaction data.

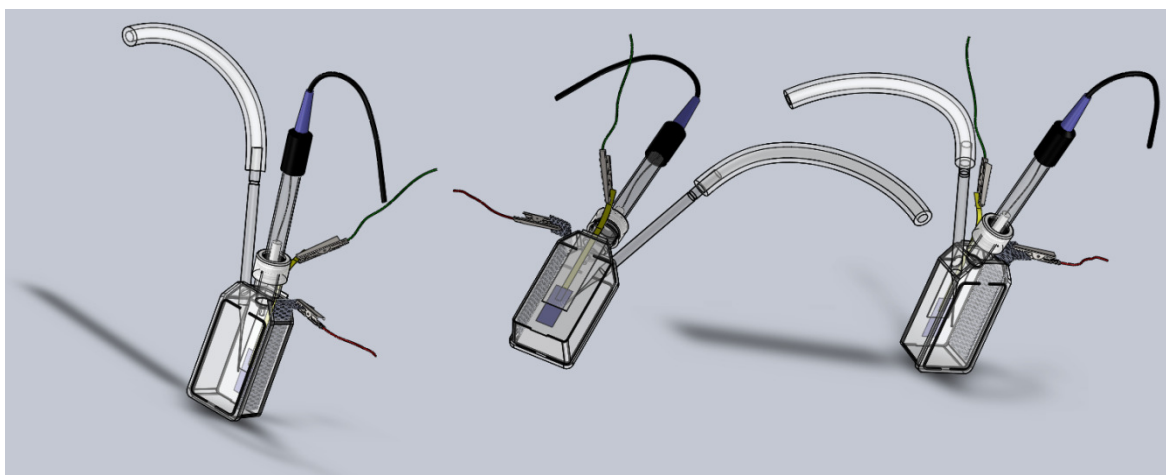


Figure 4.11 3D test cell assembly model used in experiments

Cyclic voltammetry tests for thin film made of PEDOT, PBTh and PEG with different ratios of components are shown below. Tests were performed for different ratios of the components, different light concentrations, in presence of nitrogen and in presence of air, with different scan rates and in different electrolytes with pH 1, 4, 7, 11, 14.

4.3.3 Cyclic Voltammetry Results for Thin Film Made of PEDOT, PBTh and PEG blends

Tested electrodes consisted PEDOT and PBTh in ratios 1:0.5, 1:1, 1:2, 1:3 and PEG in ratio '2'. Material was tested with bubbling nitrogen and with bubbling air to the test cell, with three different scan rates (50 mV/s, 20 mV/s, 0.167 mV/s), four light concentration (dark, 300 lm, 500 lm, 1000 lm) and in different electrolytes (pH 1, 4, 7, 11, 13), to indicate electrode parameters and best work environment for future electrode.

It is rather impossible to show all results of performed testes, so only the most interesting results have been shown.

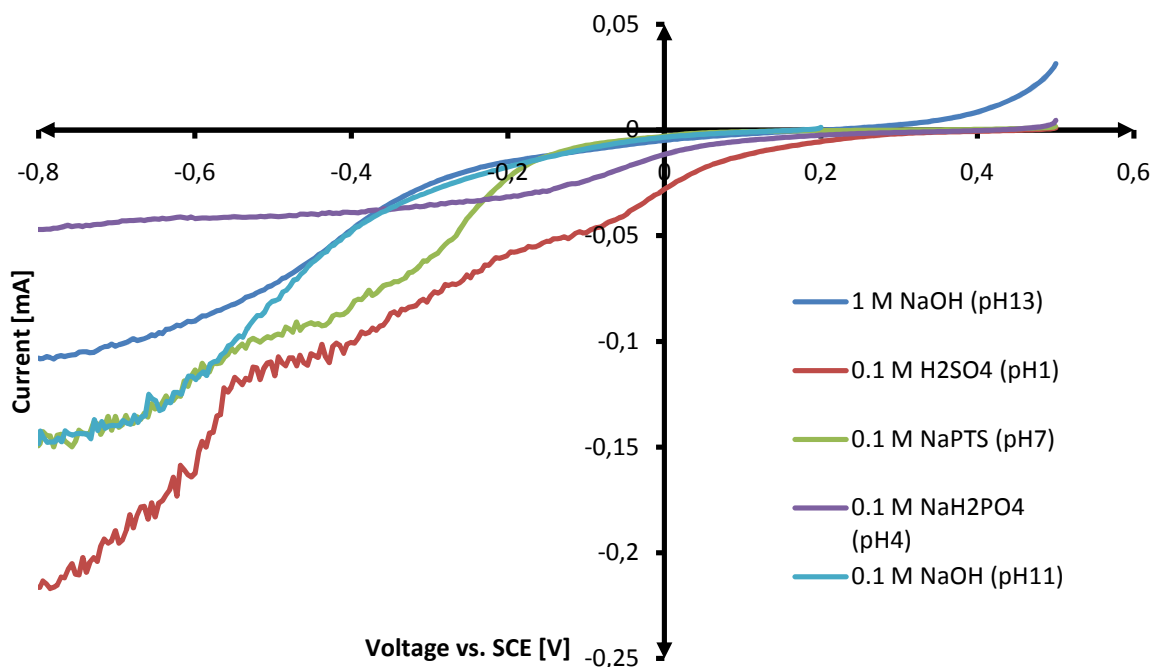


Figure 4.12 Comparison of PEDOT/PBTh ,1:1' PEG ,2' in different electrolytes, carried out with scan rate of 0.167 mV/s in presence of air and light

Figure 4.12 compares results of tests carried out in presence of air, with scan rate 0.167 mV/s and light concentration of 1000 lm (~2 suns). The variable in this test was type of electrolyte. Tests proved that best results can be achieved using acidic electrolyte (0.1 M H₂SO₄) with pH 1. Again current instability can be visible for voltage values above – 0.4V.

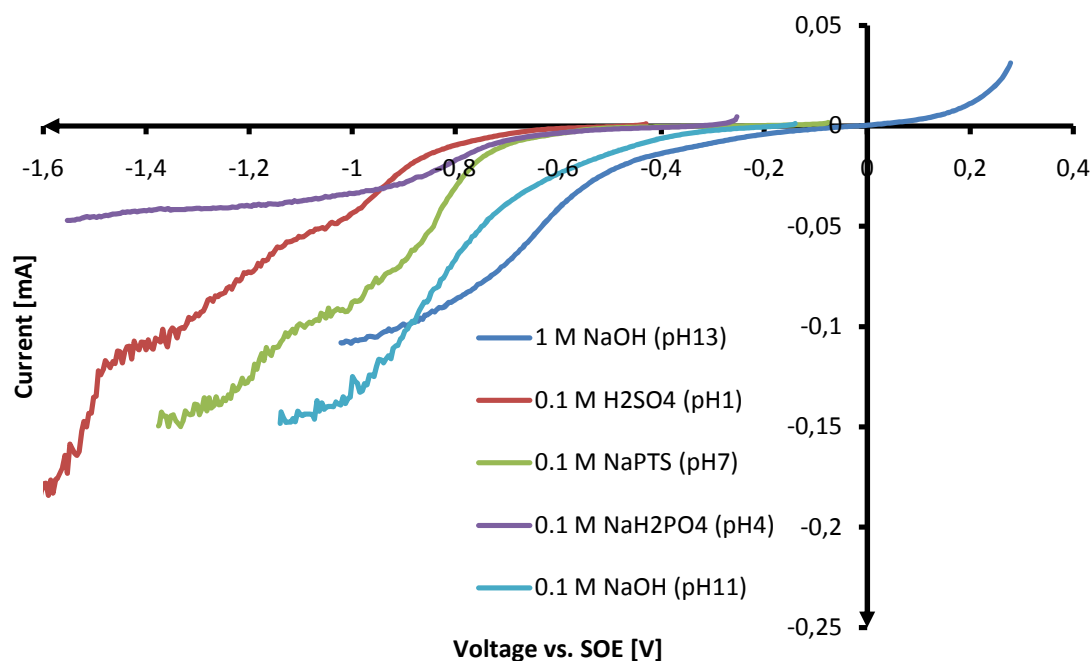


Figure 4.13 Comparison of PEDOT/PBTh ,1:1‘ PEG ,2‘ in different electrolytes, carried out with scan rate of 0.167 mV/s in presence of air in function of over-potential vs. current in presence of light

Figure above presents results of cyclic voltammetry in function of over-potential vs. current. In electrolytes with different pH values reduction reaction occurs at different potential values. Appendix B, shows potential values for reactions at different pH. Function of over-potential vs. current proves that electrode is more efficient in alkaline electrolytes. At fixed voltage, the highest current can be drawn from electrode in electrolyte with highest pH. Similar results are observed for other ratios of tested polymer blends.

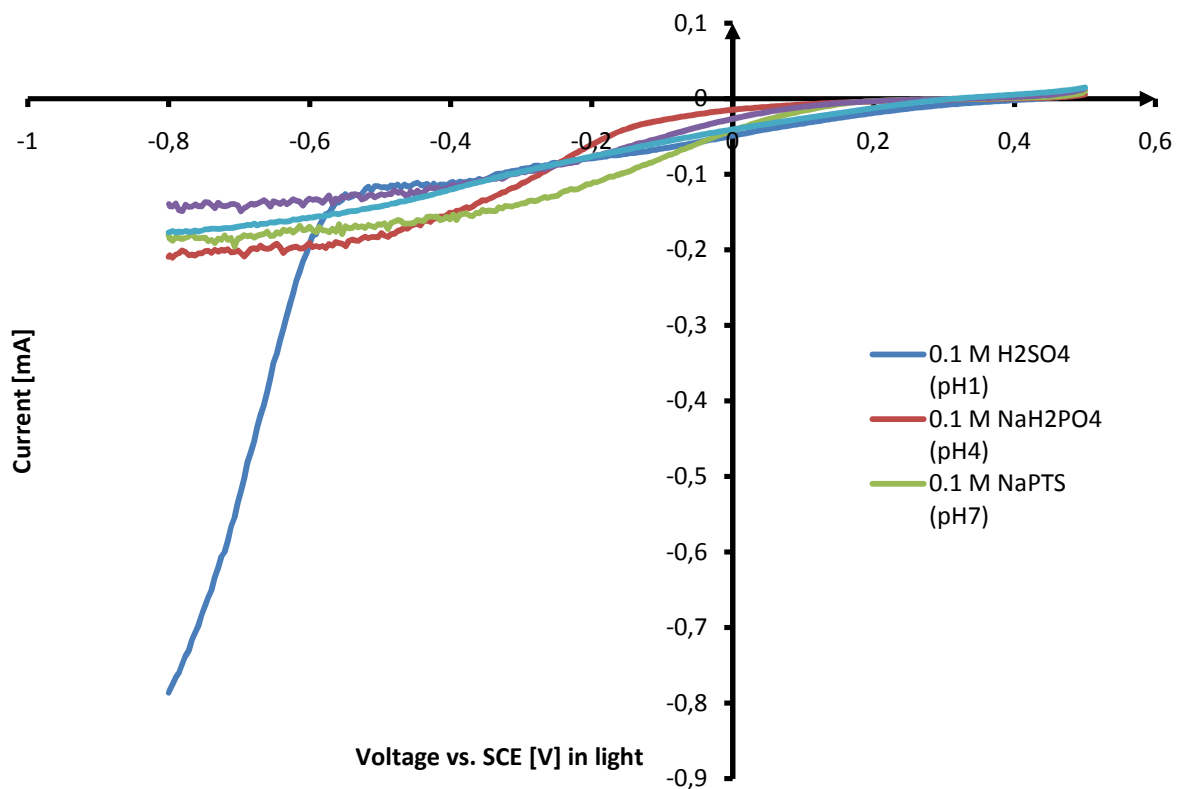


Figure 4.14 Comparison of PEDOT/PBTh ,1:3' PEG ,2' in different electrolytes, carried out with scan rate of 0.167 mV/s in presence of air

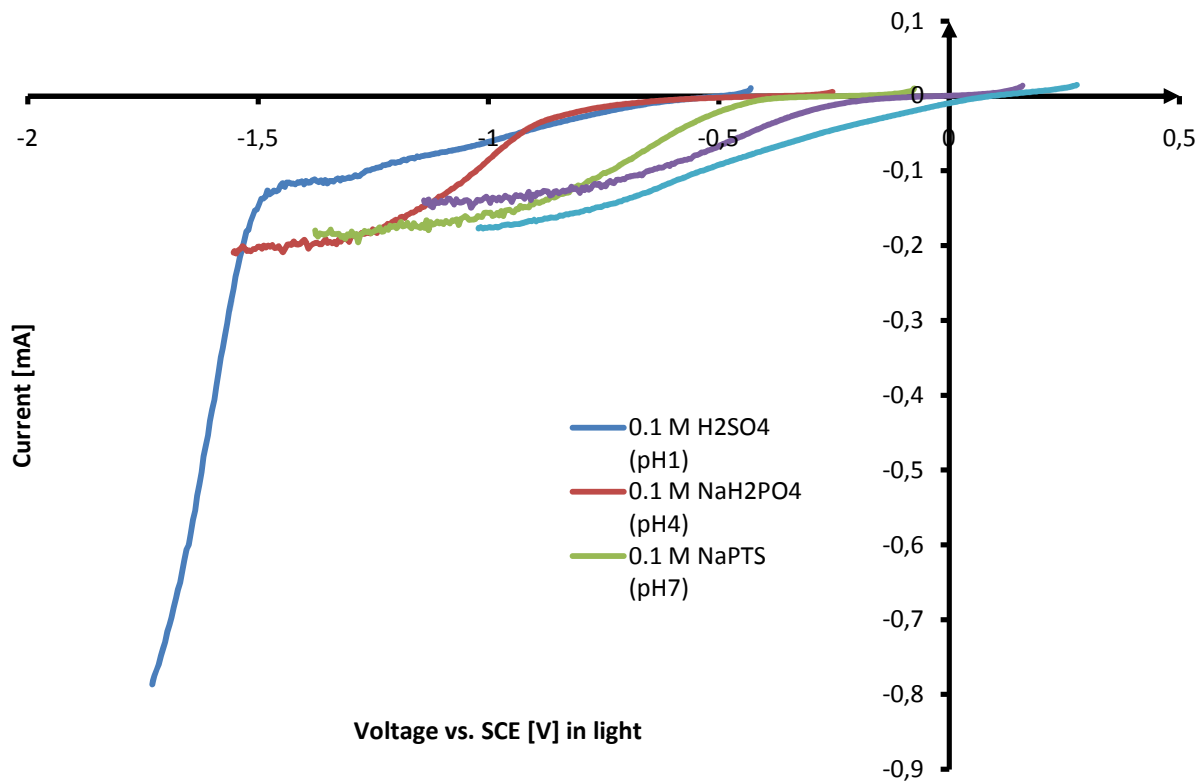


Figure 4.15 Comparison of PEDOT/PBTh ,1:3' PEG ,2' in different electrolytes, carried out with scan rate of 0.167 mV/s in presence of air

Two graphs above are similar to graphs before, but compare PEDOT/PBTh performance in ratio 1:3 and PEG '2'. Tests show that blends with higher amounts of PBTh have higher light performance. For test carried out in acidic (0.1M H₂SO₄) electrolyte proton reduction can be visible.

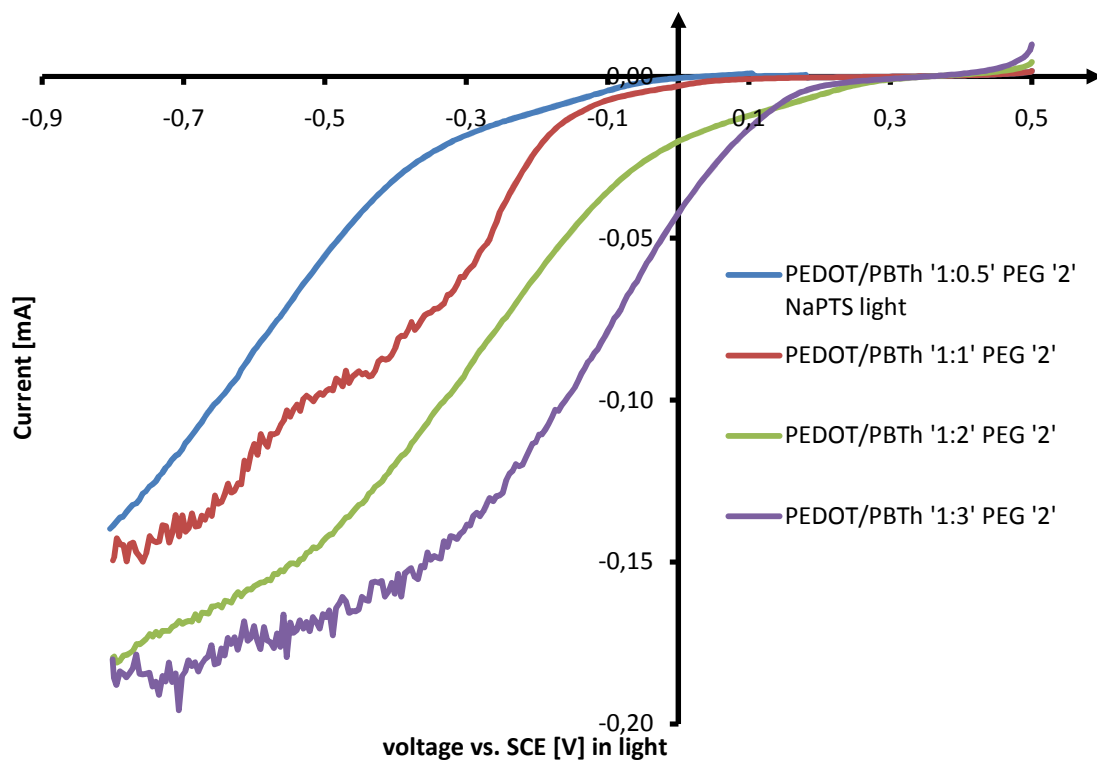


Figure 4.16 Test results in presence of bubbling air in 0.1 M NaPTS electrolyte with light

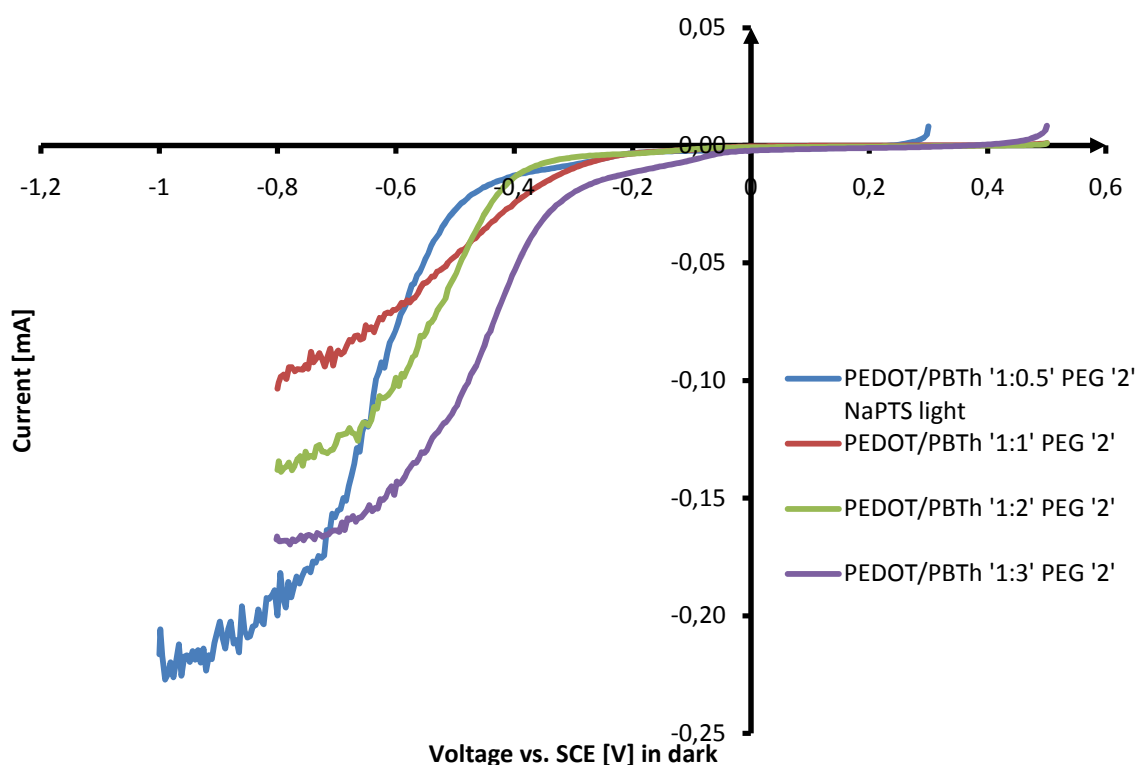


Figure 4.17 Test results in presence of bubbling air in 0.1 M NaPTS electrolyte in dark

Plots above proves that better results can be achieved for blends with higher ratios of PBTh. With increasing PBTh concentration in blend reduction reaction swipes, more PBTh in blend less potential is needed to draw desired current. In tested polymer blends, polymers create interpenetrating networks, but there is limitation. When limitation will be reached polymers will create 'islands' – polymers will create concentrated formations, not interpenetrating networks, it results in heterogeneous properties of thin film or even some properties can be vanished, since polymers are not supporting each other.

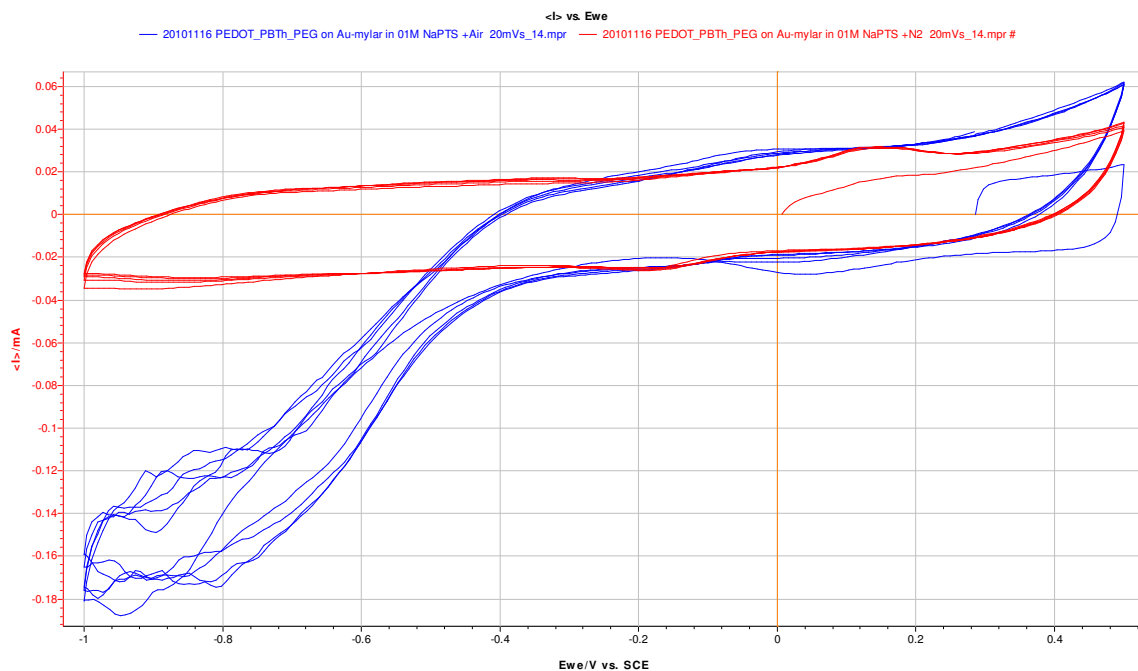


Figure 4.18 Cyclic voltammetry test for PEDOT/ PBTh ,1:1' PEG ,2', sampling rate 20 mV/s, electrolyte 0.1 M NaPTS (pH 7). Blue graph test in presence of nitrogen, red graph in presence of air, tests were taken in dark

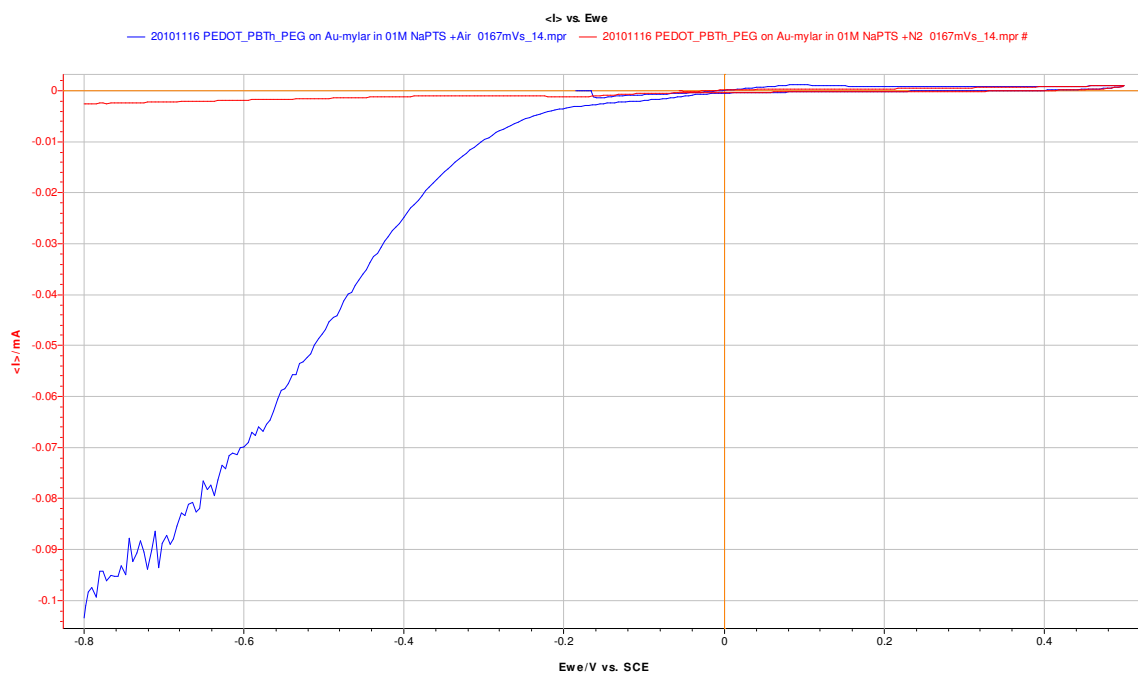


Figure 4.19 Cyclic voltammetry test for PEDOT/ PBTh ,1:1' PEG ,2', sampling rate 0.167 mV/s, electrolyte 0.1 M NaPTS (pH 7). Blue graph test in presence of nitrogen, red graph in presence of air, tests were taken in dark

Figures above only prove that much better results can be achieved in presence of bubbling air which is obvious, because in reduction process electrons are added to an atom or ion by removing oxygen or adding hydrogen, so number of active sites is proportional to the current. In fuel cells, this means that the voltage will be higher for a given current, or the current higher for a given voltage.

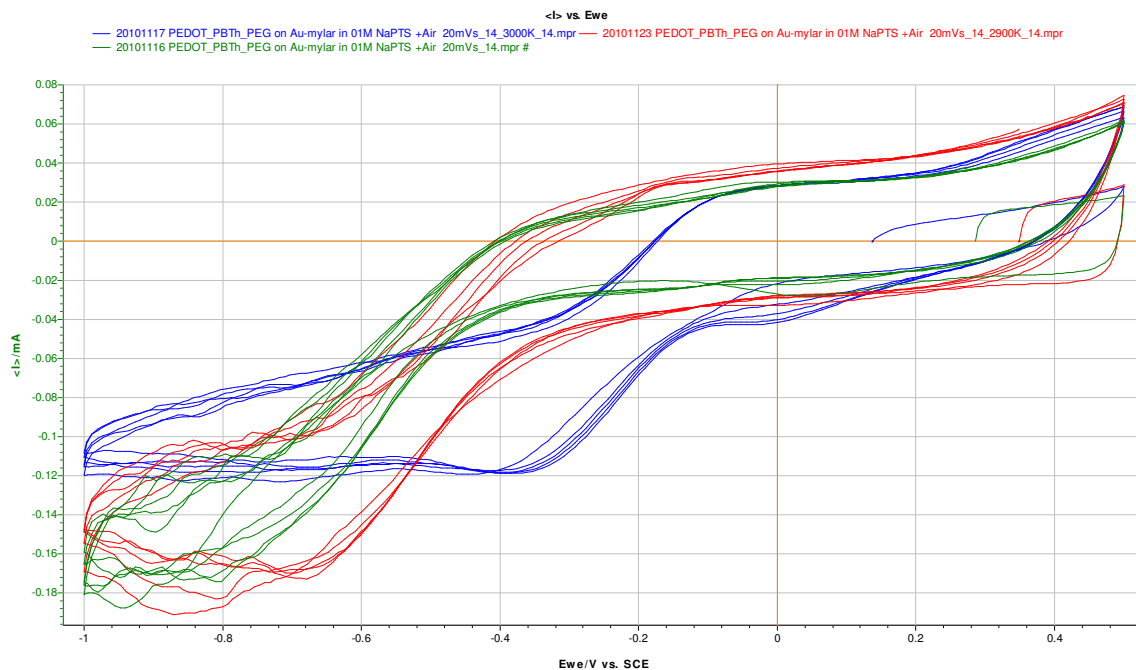


Figure 4.20 Cyclic voltammetry test for PEDOT/ PBTh ,1:1' PEG ,2', in presence of bubbling air in 0.1 M NaPTS (pH 7) electrolyte, sampling rate 20 mV/s. Blue graph test with light shining (500 lm) on working electrode surface red graph taken for light intensity of 200 lm and green graph was taken in dark

Figure above shows that light concentration has huge influence on electrode performance. Higher light intensity, higher performance. Electrode degradation can be visible on blue plot, part of thin film deposited on mylar got off, because of long electrode operation, smaller electrode surface results in lower current.

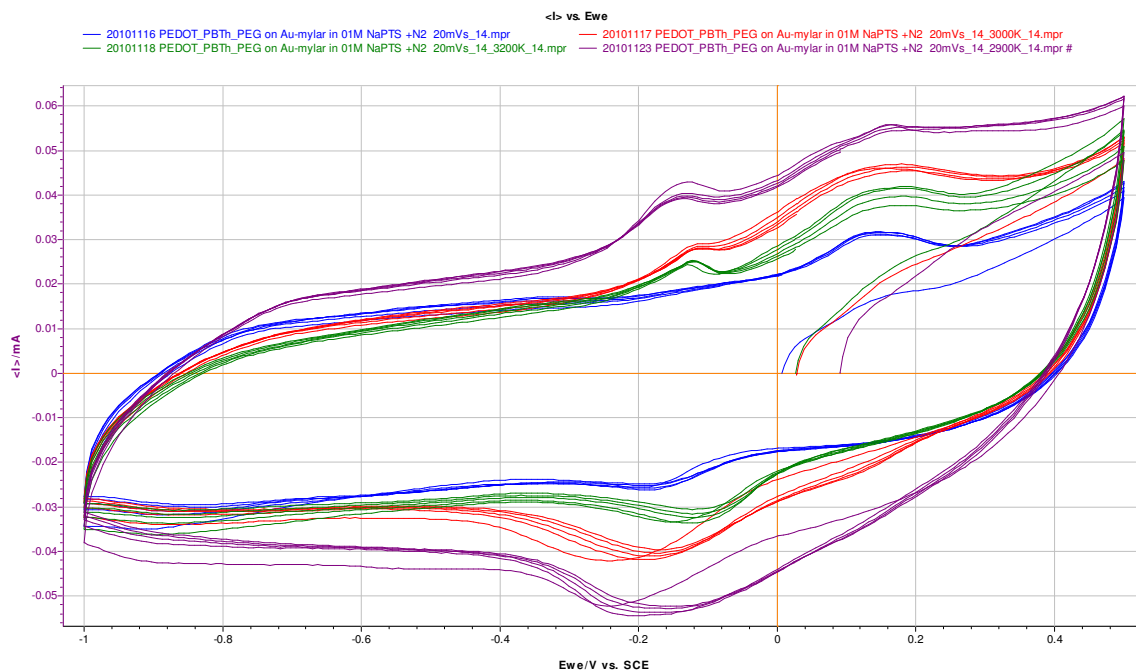


Figure 4.21 Cyclic voltammetry test for PEDOT/ PBTh ,1:1 ' PEG ,2', in presence of bubbling nitrogen in 0.1 M NaPTS (pH 7) electrolyte, sampling rate 20 mV/s. Blue graph – dark, green – 1000 lm, red – 500 lm, purple – 200 lm

Figure above again proves light activation of the electrode, this time in presence of nitrogen for different light intensity.

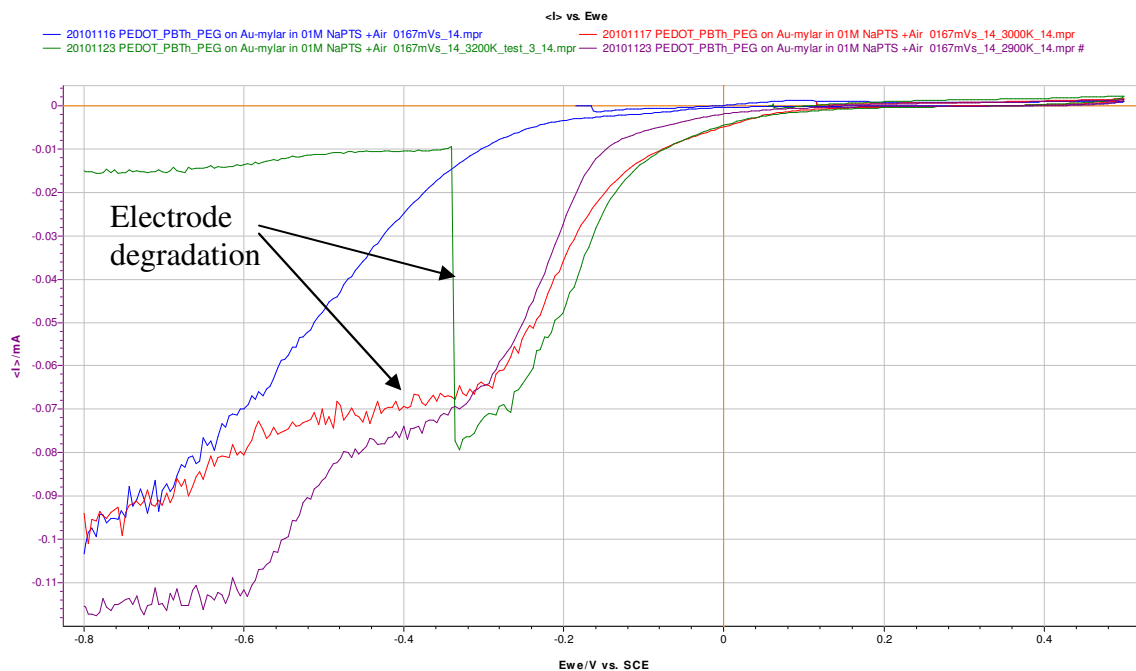


Figure 4.22 Cyclic voltammetry test for PEDOT/ PBTh ,1:1 ' PEG ,2', in presence of bubbling air in 0.1 M NaPTS (pH 7) electrolyte, sampling rate 0.167 mV/s. Blue graph – dark, green – 1000 lm, red – 500 lm, purple – 200 lm

Test results shown on figure above and below were carried out in presence of air and nitrogen with very small scan rate (0.167 mV/s). Very interesting is visible step from higher current level to the lower, electrode was operating for long time and after many test simply died.

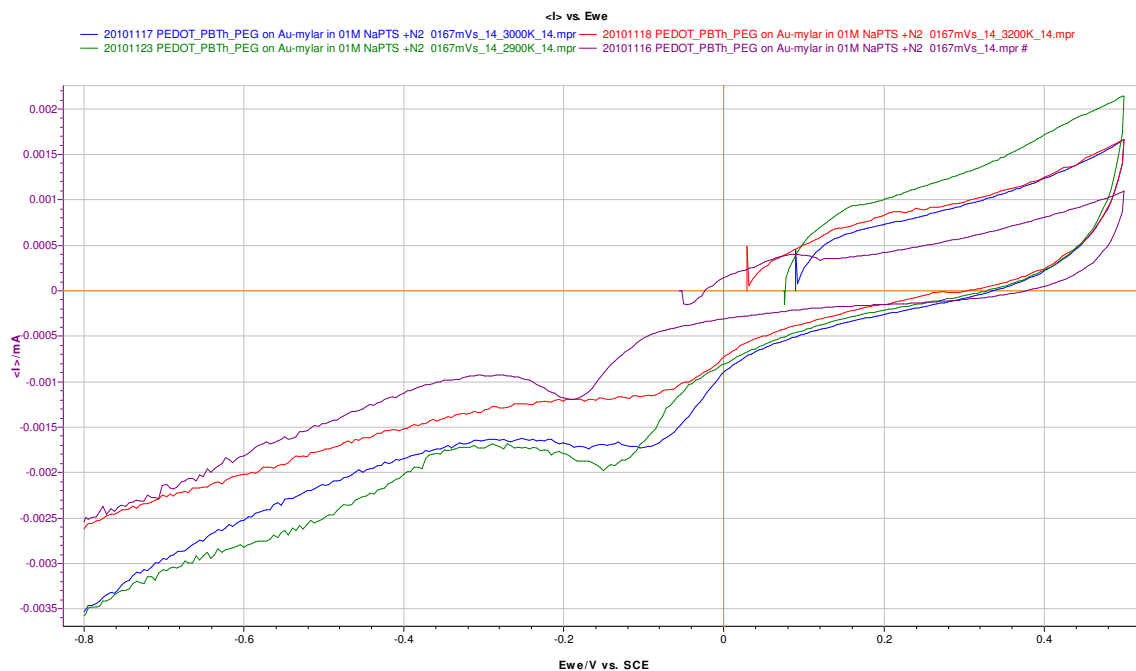


Figure 4.23 Cyclic voltammetry test for PEDOT/ PBTh ,1:1' PEG ,2', in presence of bubbling nitrogen in 0.1 M NaPTS (pH 7) electrolyte, sampling rate 0.167 mV/s. Purple graph – dark, green – 1000 lm, red – 500 lm, blue – 200 lm

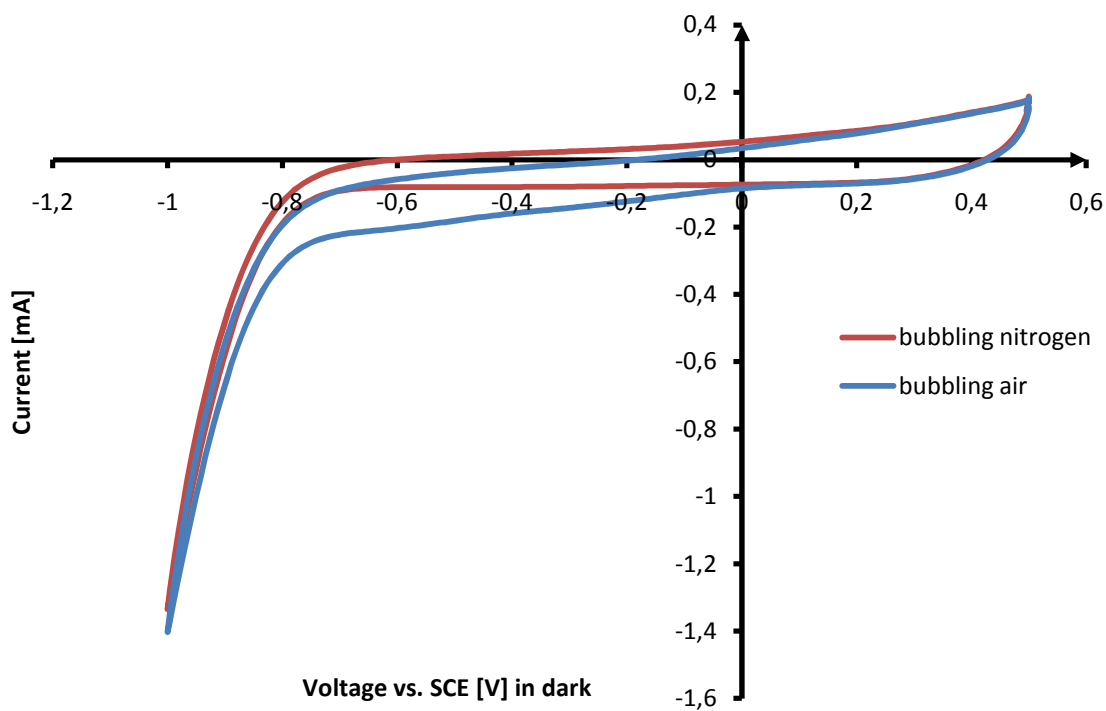


Figure 4.24 Cyclic voltammetry test for PEDOT/ PBTh ,1:1' PEG ,2', in presence of bubbling air (blue) and bubbling nitrogen (red), in 0.1 M H₂SO₄ dissolved in water electrolyte (pH 1), sampling rate 50 mV/s, taken in dark

The figure above shows cyclic voltammetry test results carried out in presence of bubbling nitrogen (red) and air (blue) in 0.1 M H_2SO_4 electrolyte. Big peak visible at the end of reduction process is a proton reduction peak.

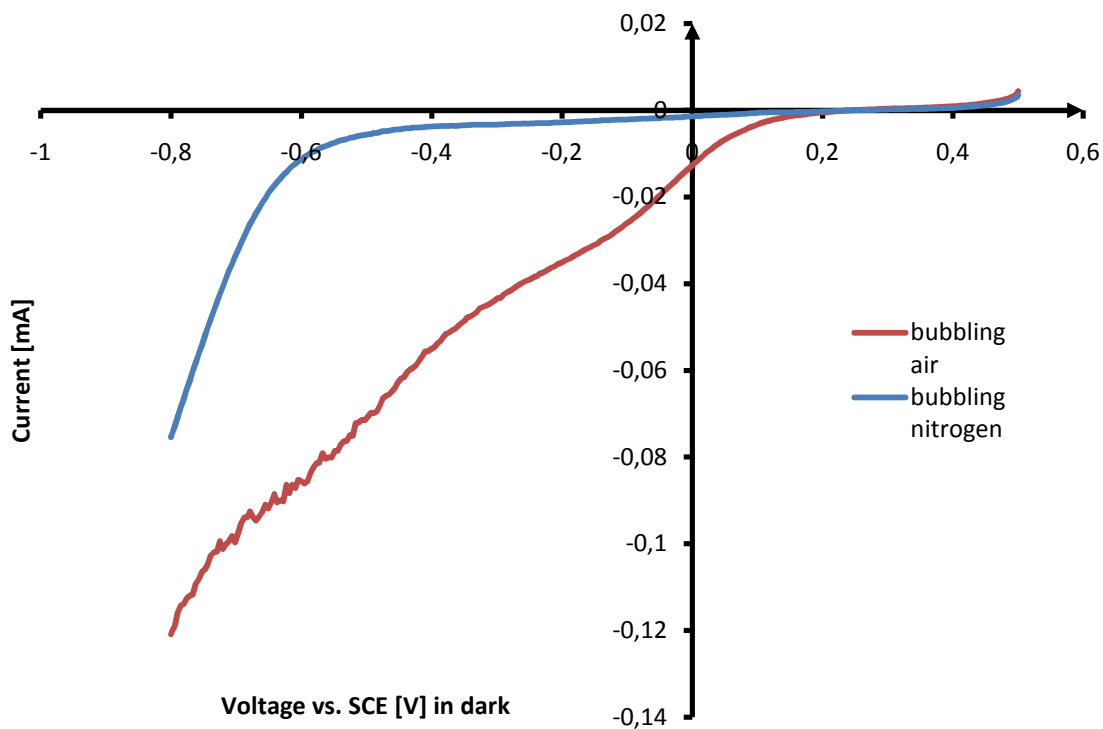


Figure 4.25 Cyclic voltammetry test for PEDOT/ PBTh ,1:1' PEG ,2', in presence of bubbling air (blue) and bubbling nitrogen (red), in 0.1 M H_2SO_4 dissolved in water electrolyte (pH 1), sampling rate 0.167 mV/s, taken in dark

Figure above shows result of the same experiment as before but with more precise scan rate of 0.167 mV/s, giving better view on reduction reactions.

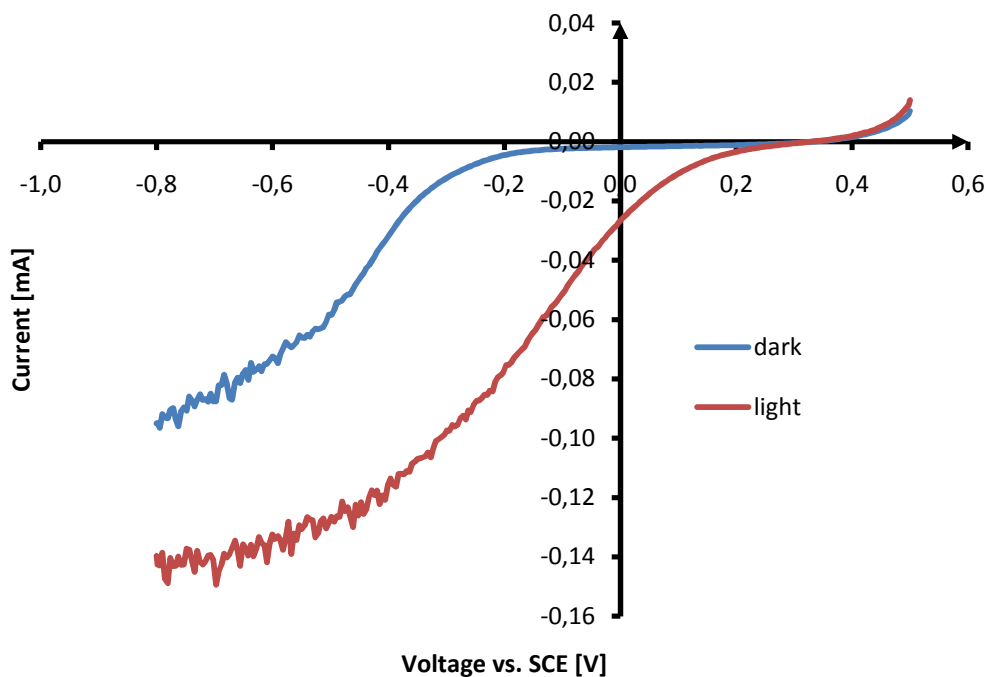


Figure 4.26 Cyclic voltammetry test for PEDOT/ PBTh ,1:3' PEG ,2', in presence of bubbling nitrogen in 0.1 M NaPTS (pH 7) electrolyte, scan rate 0.167 mV/s. Red plot – 1000 lm (3200K), blue - dark

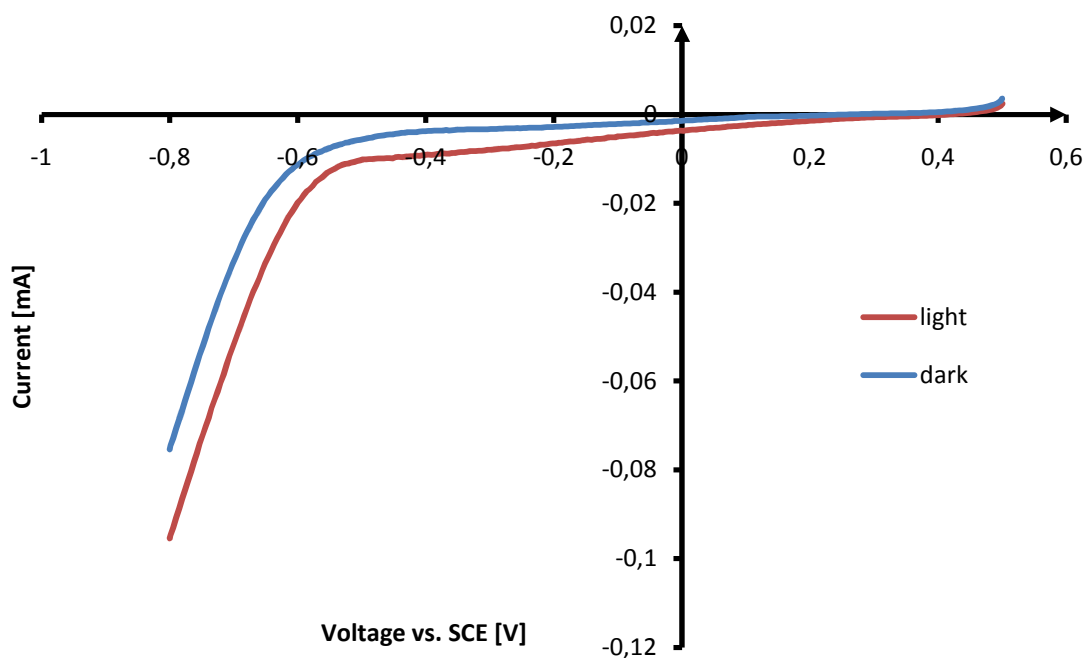


Figure 4.27 Cyclic voltammetry test for PEDOT/ PBTh ,1:1' PEG ,2', in presence of bubbling nitrogen in 0.1 M H₂SO₄ (pH 1) electrolyte, scan rate 0.167 mV/s. Red plot – 1000 lm (3200K), blue - dark

Figure 4.26 shows solar activation for PEDOT/PBTh '1:1' PEG '2' electrode in presence of bubbling nitrogen in H₂SO₄ dissolved in water electrolyte (pH 1). Tests were carried out with light and without light (light intensity of 1000 lm or ~2 suns). Tests show that light activation has big influence on overall electrode performance.

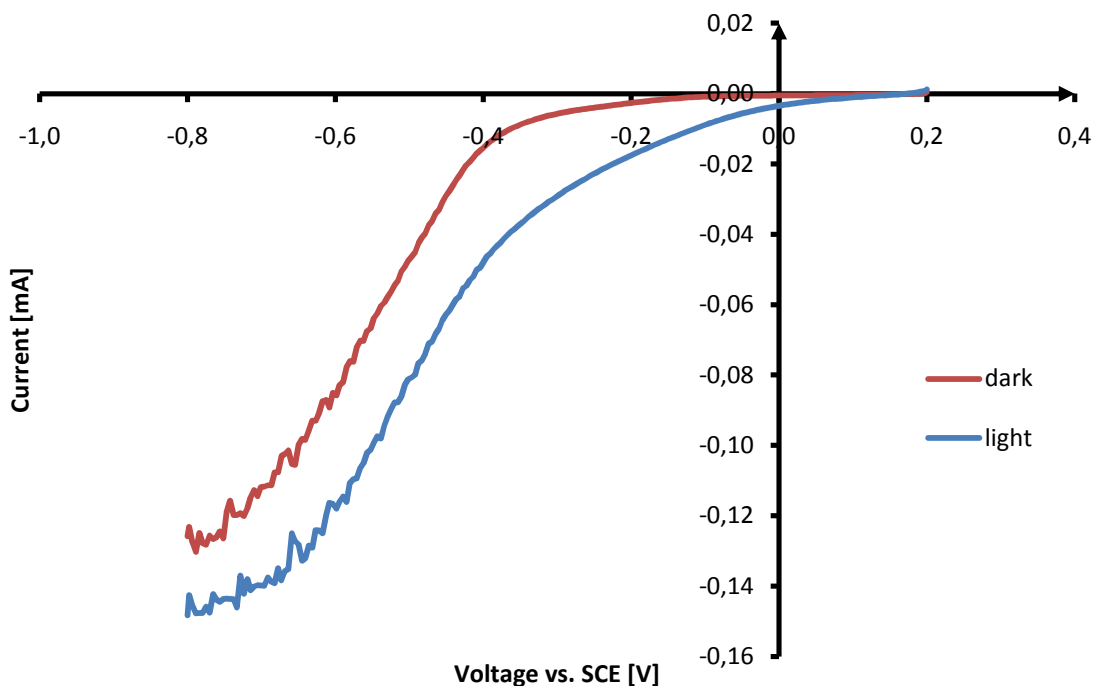


Figure 4.28 Cyclic voltammetry test for PEDOT/ PBTh ,1:1' PEG ,2', in presence of bubbling air in 0.1 M NaOH (pH 11) electrolyte, scan rate 0.167 mV/s. Red plot – dark, blue – 1000 lm (3200K)

Figure 2.47 shows similar test like the one before, but this time tests were carried out in presence of air and in 0.1 NaOH (pH 11) electrolyte. At the end of reduction process in both cases electrode instability is visible, current is not increasing smoothly, but changes very rapidly. It might be caused by bubbling air, together with current growth air flow in electrolyte can be an issue, because of diffusion limitations. The other explanation of this instability is film thickness, together with growing voltage and current, power delivered to the system is growing, thin film may not manage to big powers. The best idea to avoid this unwanted behaviour is to operate on lower voltage values, where current is stable or make electrode thicker.

Plot below shows ratio of electrode current in dark conditions to electrode current in light conditions - 1000 lm. At the beginning ratio is growing very fast, but later is decreasing to reach constant level at the end. Electrode current in dark is taken as 100%, current in light conditions is percentage of current in dark.

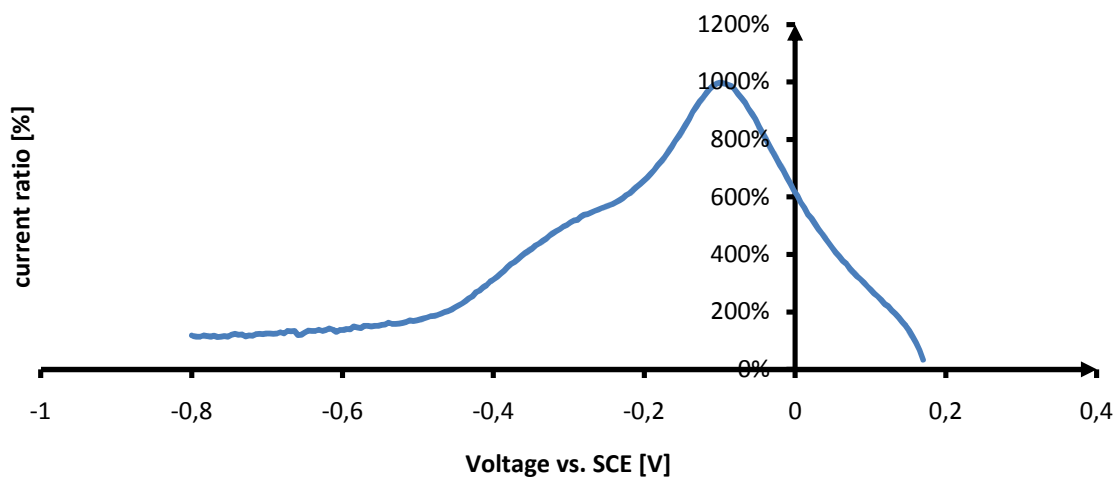


Figure 4.29 Ratio of electrode current in light condition to electrode current in dark

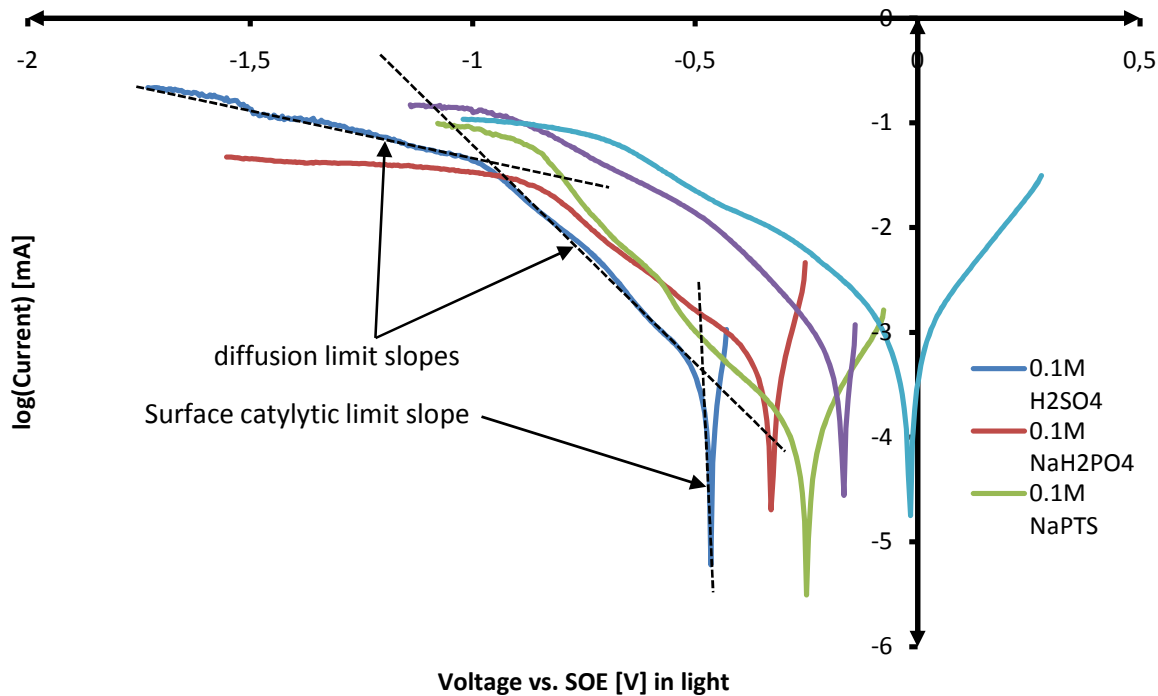


Figure 4.30 Kinetics limits in light

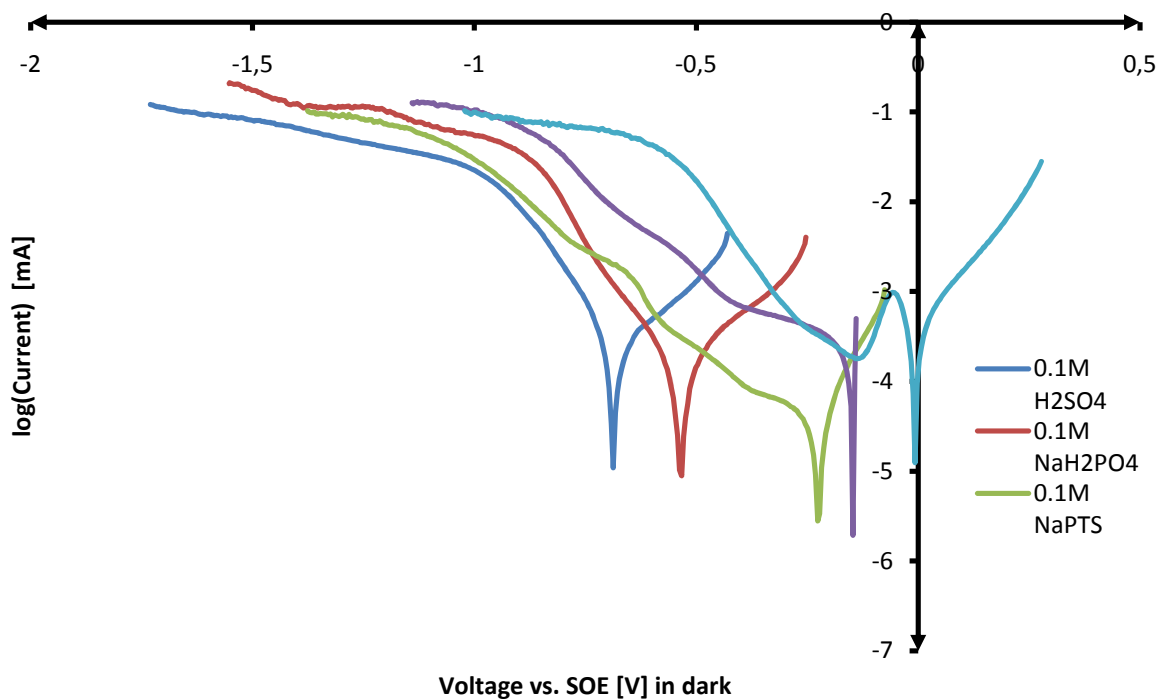


Figure 4.31 Kinetics limits in dark

On above graphs current values are plotted in function of logarithm. On all the plots three slopes can be distinguished, all of them correspond to different kinetics limits. First slope is a surface catalytic limit, and two other are diffusion limits.

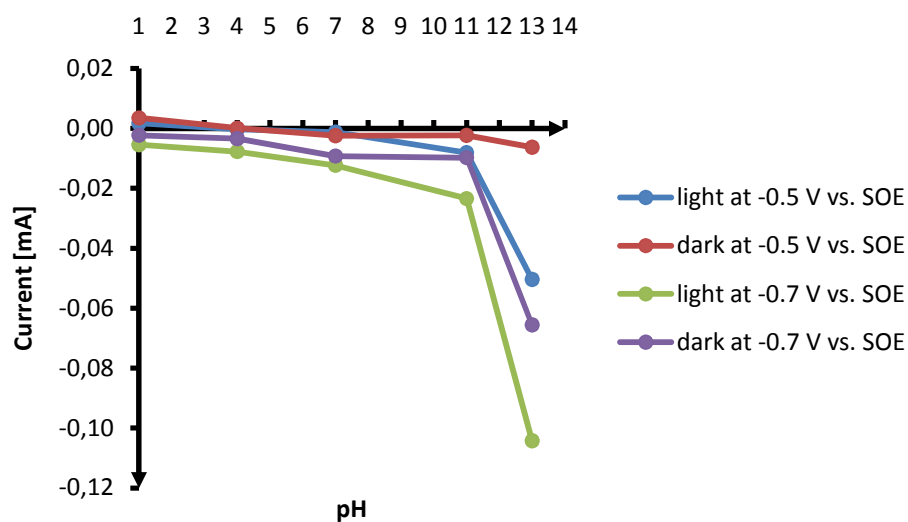


Figure 4.32 pH vs. electrode current plot for PEDOT/PBTh '1:0.5' PEG '2' ratio at two fixed voltage values -0.5V and -0.7V in presence of air, light intensity – 1000 lm

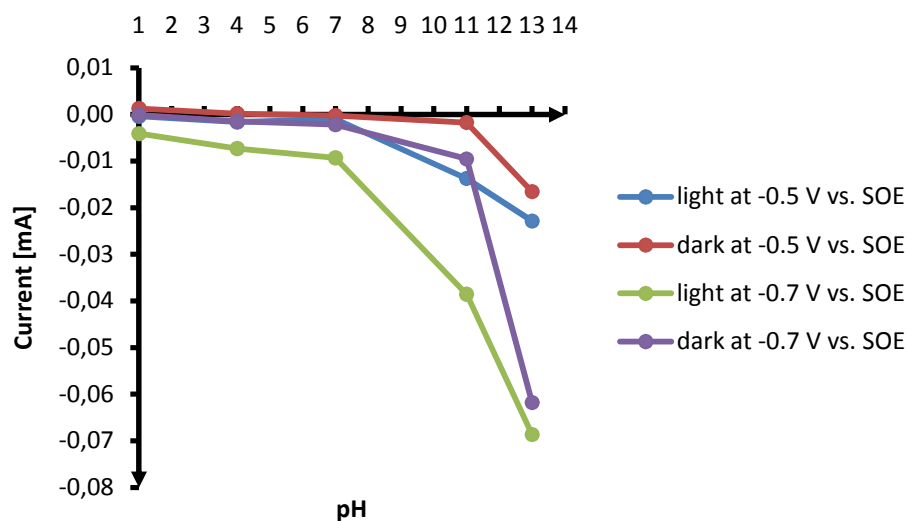


Figure 4.33 pH vs. electrode current plot for PEDOT/PBTh '1:1' PEG '2' ratio at two fixed voltage values -0.5V and -0.7V in presence of air, light intensity – 1000 lm

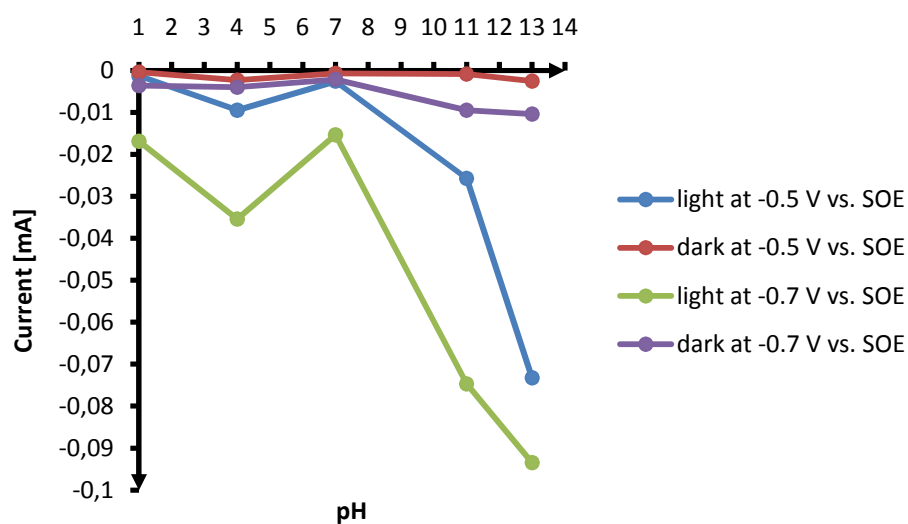


Figure 4.34 pH vs. electrode current plot for PEDOT/PBTh '1:2' PEG '2' ratio at two fixed voltage values -0.5V and -0.7V in presence of air, light intensity – 1000 lm

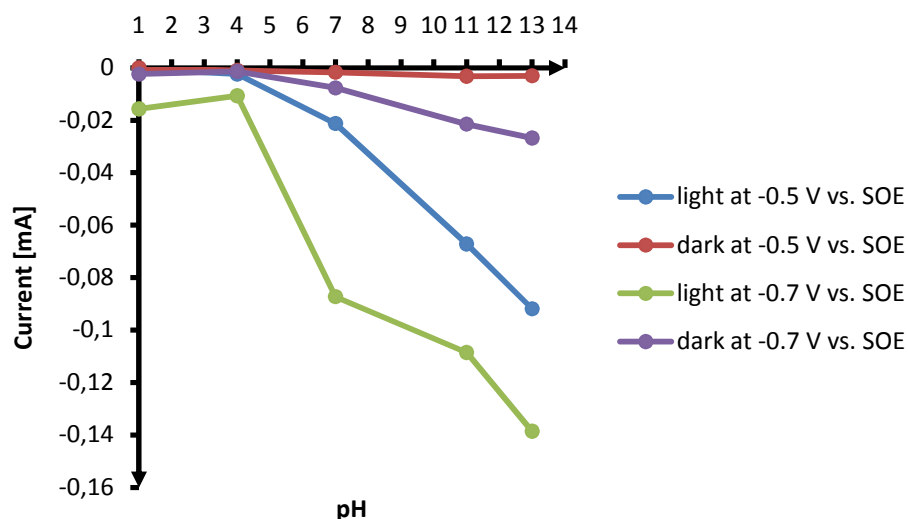


Figure 4.35 pH vs. electrode current plot for PEDOT/PBTh '1:3' PEG '2' ratio at two fixed voltage values -0.5V and -0.7V in presence of air, light intensity – 1000 lm

Four plots above prove that same effect occurs for all tested blends. Together with increase of pH value of electrolyte electrode performance is growing. Tests show that the best results can be achieved for alkaline environments.

4.3.4 Cyclic Voltammetry Results for PEDOT/PTTh '1:0.5' PEG '2'

Plot below compares two polymer blends, first is blend consisting PEDOT/PBTh '1:0.5' PEG '2', second PEDOT/PTTh '1:0.5' PEG '2'. Both tests were carried out in the same conditions. 0.1 M NaOH was used as electrolyte, light was introduced to the electrode during test and air was bubbling into electrolyte.

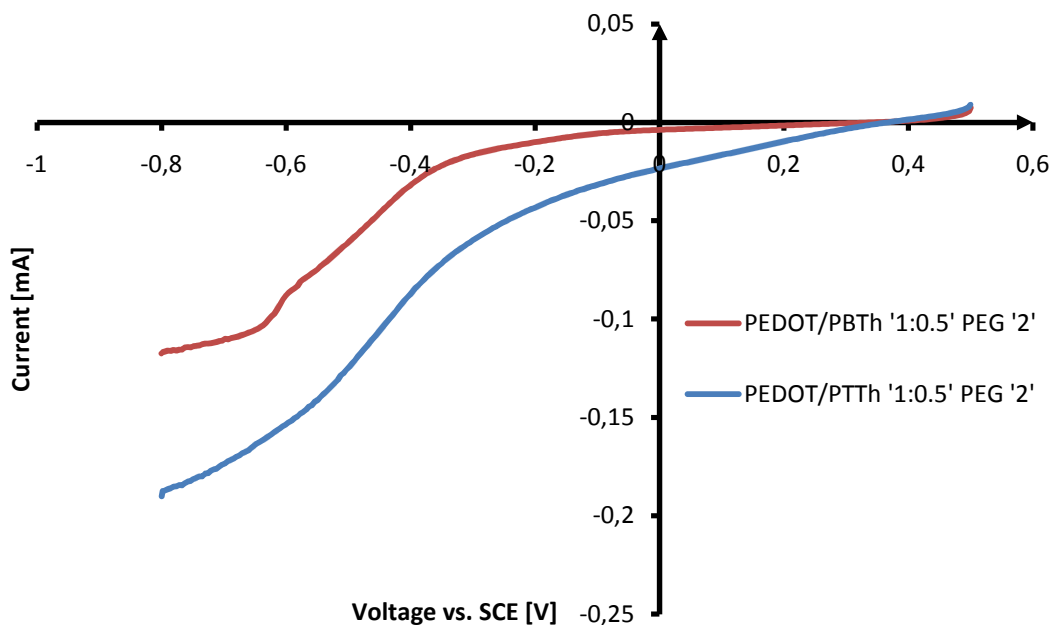


Figure 4.36 Comparison of PEDOT/PBTh ,1:0.5' PEG ,2' and PEDOT/PTTh ,1:0.5' PEG ,2' in 0.1M NaOH (~pH11) with bubbling air and light

Blend of PEDOT, PTTh and PEG has much higher performance comparing to blend with PEDOT, PBTh and PEG, it is caused by higher order in conjugation of PTTh. The conjugation length is determined by the number of coplanar rings — the longer the conjugation length, the longer the absorption wavelength. Deviation from coplanarity may be permanent and be result of mislinkages during synthesis. Temporary deviations are results of from changes in the environment or binding. This twist in the backbone reduces the conjugation length, and the separation between energy levels is increased. This results in a shorter absorption wavelength.

4.3.5 Cyclic Voltammetry Results for PEDOT/PBTh '1:1'

Cyclic voltammetry test results for PEDOT and PBTh material in ratio '1:1' are similar to results gathered for pure PEDOT. Tests performed in complete darkness and in presence of light makes difference in results, it means that solar activation occurs for this material, but further chronoamperometry tests shows that response time of PEDOT and PBTh only is much slower without PEG.

Tests were performed in presence of bubbling nitrogen and bubbling air, as electrolyte 0.1 NaPTS dissolved in water has been used. Tests were carried out for scan rates of 50 mV/s, 20 mV/s and 0.167 mV/s.

Test results for sampling rate of 0.167 mV/s, in presence of nitrogen and air, in complete dark are shown below.

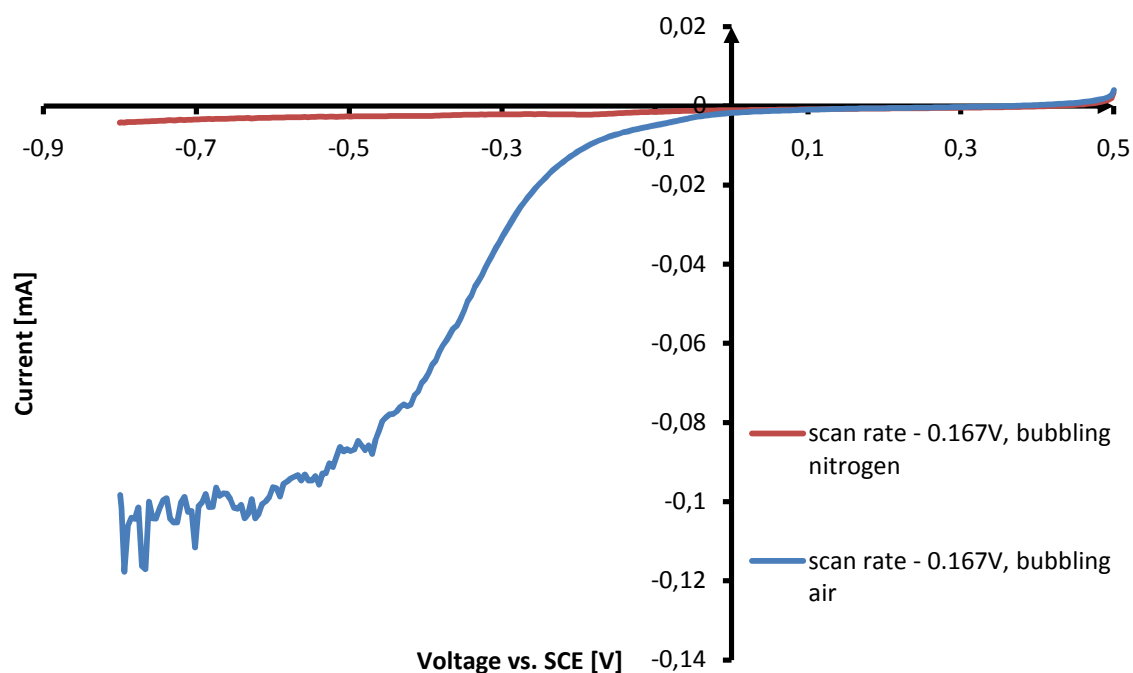


Figure 4.37 Cyclic voltammetry test for PEDOT/ PBTh ,1:1', taken with very small sampling rate (0.167 mV/s). Blue graph – results for nitrogen, red graph – results for air

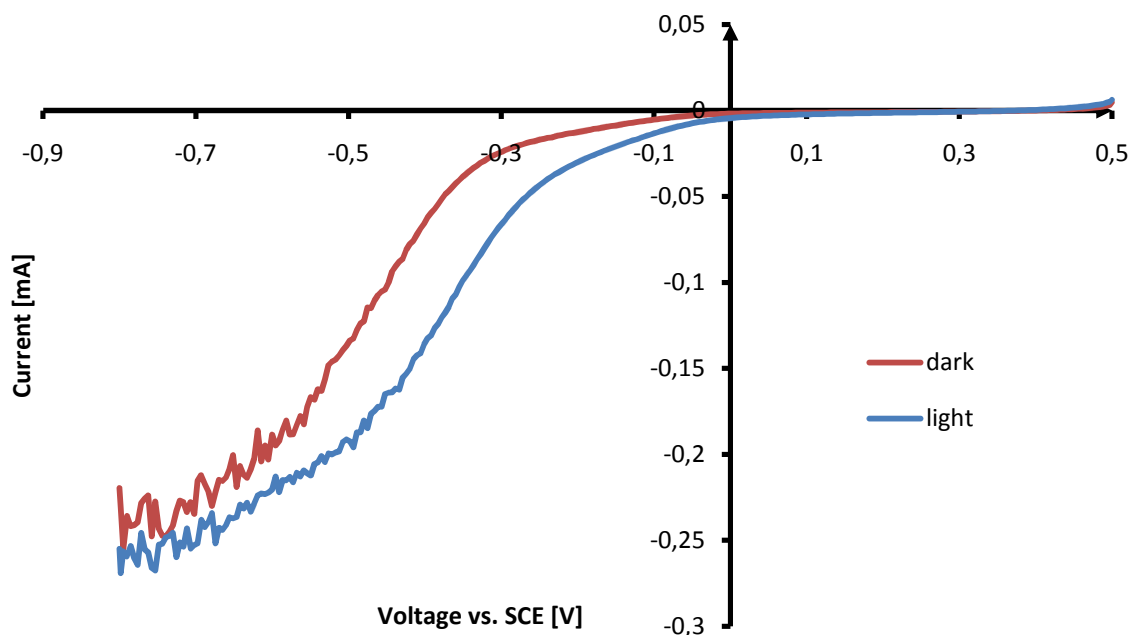


Figure 4.38 Cyclic voltammetry test for PEDOT/ PBTh ,1:1', taken with small sampling rate (0.167 mV/s). Blue graph – results in light, red graph – results in dark

Plot above proves that light activation phenomena occurs also for blends with PEDOT and PBTh only, however PEG supports ionic conductivity and improves mechanical properties of electrode.

4.3.6 Cyclic Voltammetry Results for PEDOT

Plots below show cyclic voltammetry results for pure PEDOT electrode. Tests were performed just to get idea about electrochemical properties of PEDOT in order for comparison of pure PEDOT electrode with electrodes made of PEDOT and other polymers. Tests were carried out with air and nitrogen and scan rates of 0.167 mV/s, 20 mV/s and 50 mV/s, giving six plots total.

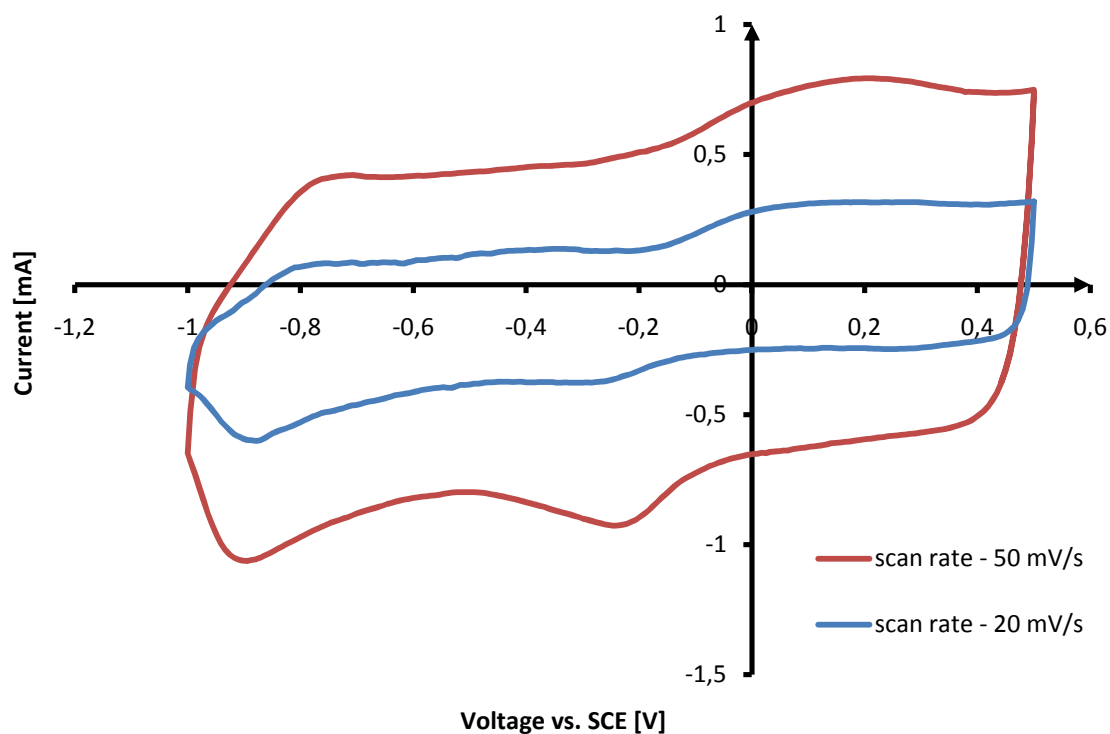


Figure 4.39 Cyclic voltammetry test for pure PEDOT sample on mylar coated with gold for better conductivity. 0.1 M NaPTS (pH 7) was used as an electrolyte, during tests air was bubbling to electrolyte. Blue plot shows results for sampling rate 20 mV/s and red for 50 mV/s

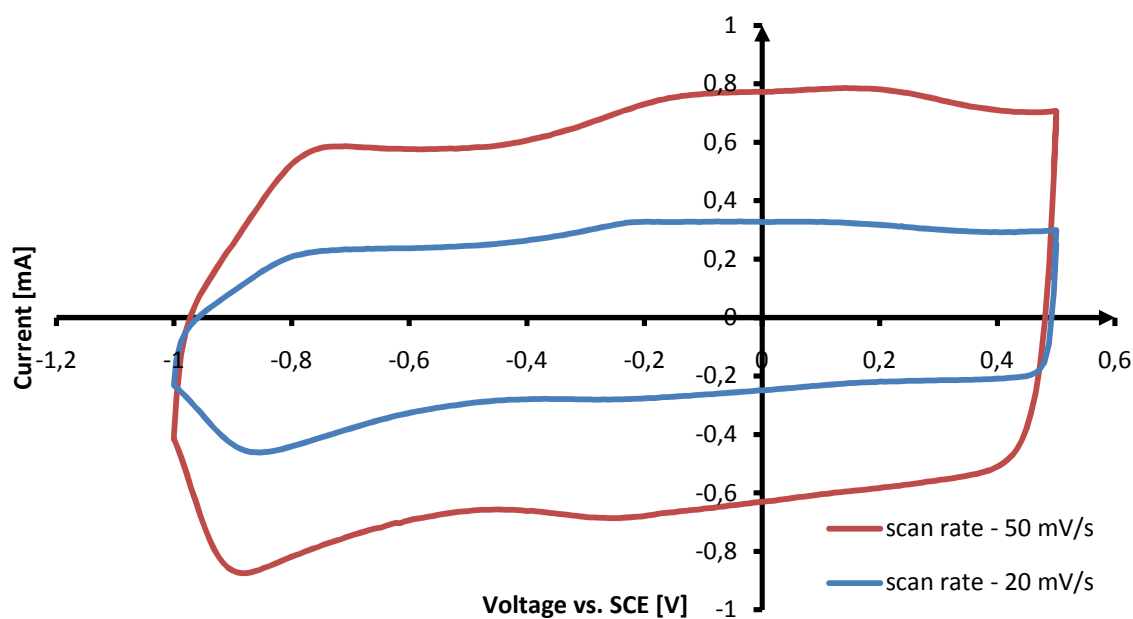


Figure 4.40 Cyclic voltammetry test for pure PEDOT sample on mylar coated with gold for better conductivity. 0.1 M NaPTS (pH 7) was used as an electrolyte. Tests were taken

in presence of nitrogen bubbling to electrolyte. Blue plot shows results for sampling rate 20 mV/s and red for 50 mV/s

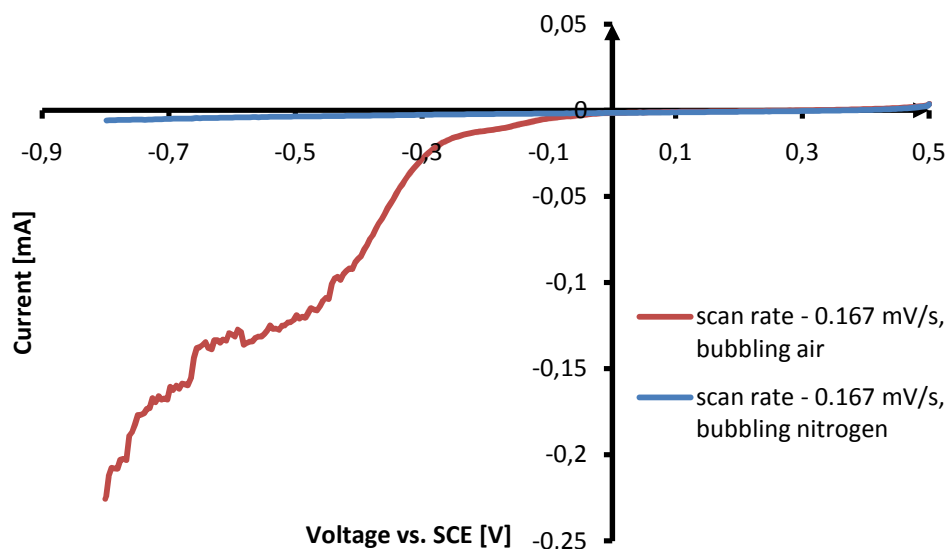


Figure 4.41 Cyclic voltammetry test for pure PEDOT taken with very small sampling rate (0.167 mV/s). Blue graph – results for nitrogen, red graph – results for air

4.3.7 Chronoamperometry

Chronoamperometry (CA) involves stepping the potential of the working electrode from an initial potential, at which generally no faradic reaction occurs, to a potential value at which the faradic reaction occurs. The current-time response reflects the change in the concentration gradient in the vicinity of the surface. In other words, the basis of this technique is measurement of current change in time at fixed voltage (potential) value. Chronoamperometry is often used for diffusion coefficient measuring of electroactive species or the surface area of the working electrode, but this technique can be also applied to the study of electrode processes mechanisms. An alternative and very useful mode for recording the electrochemical response is to integrate the current, so that one obtains the charge passed as a function of time. This mode is used for measuring the quantity of adsorbed reactants. Chronoamperometry can be also used to test electrode reaction on changing parameters, at fixed potential value drawn current should be the same all the time, by changing some external parameters, such as light intensity shining on electrode, and record changes caused by this change.

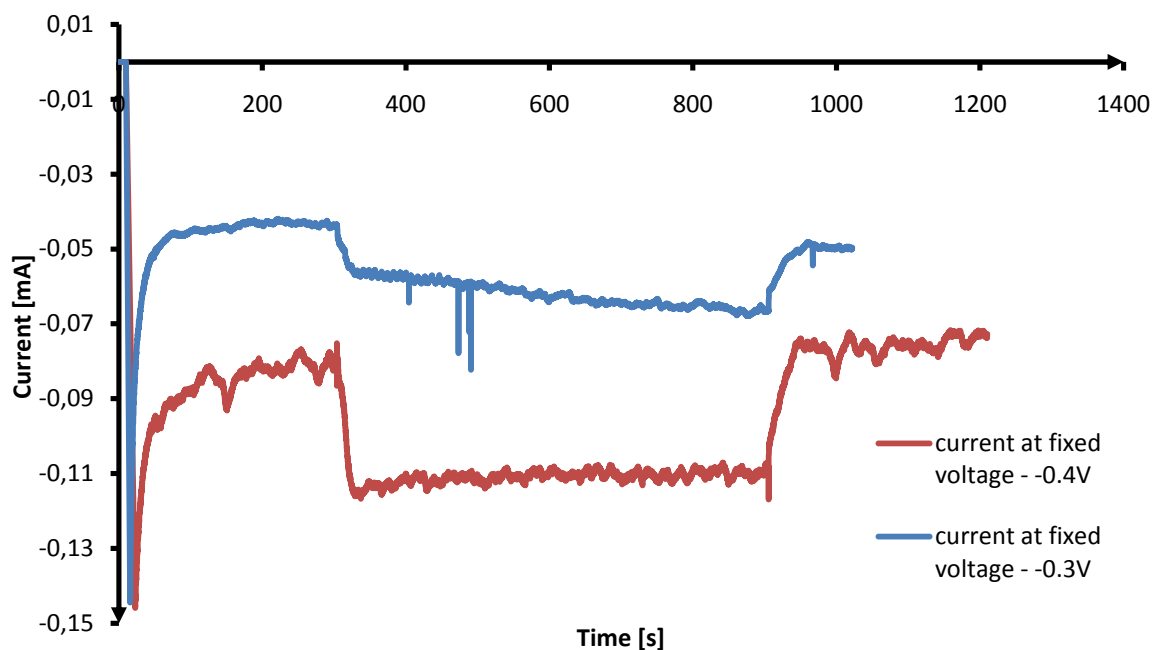


Figure 4.42 Chronoamperometry tests for pure PEDOT sample, in presence of bubbling air in 0.1 M NaPTS (pH 7) electrolyte, tests taken for fixed voltage values.

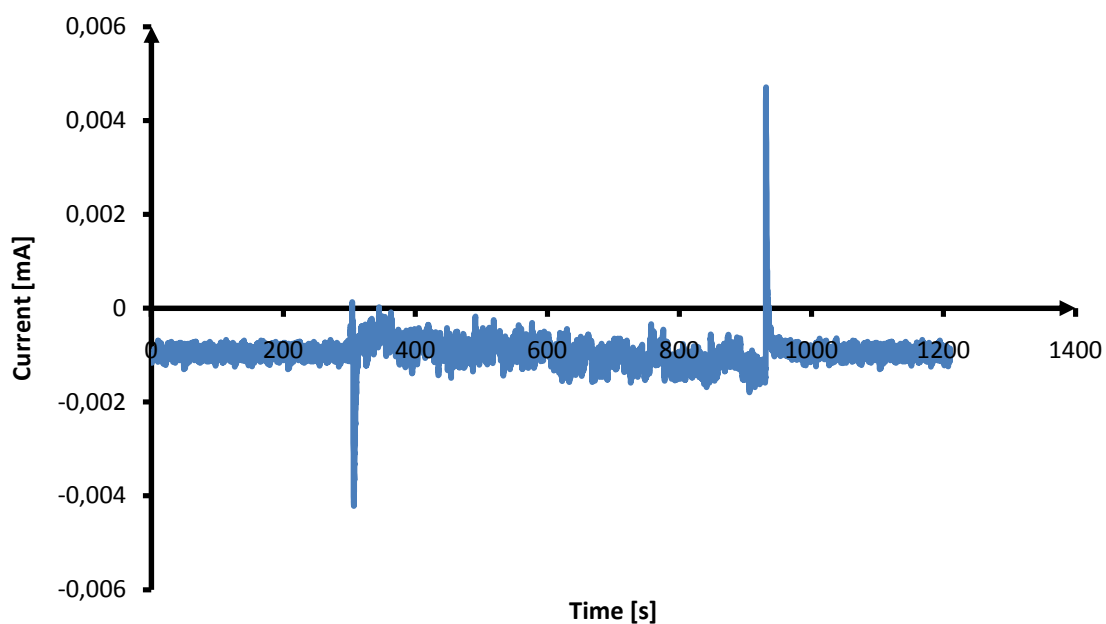


Figure 4.43 Current at 0V

Light activation occurs even in pure PEDOT, but current is unstable with growing voltage and growing light intensity. Pure PEDOT has longer response time to changes in light intensity and needs more time to reach steady-state. What is very interesting, even if

there is no voltage delivered to the system, PEDOT is still light active, two small peaks can be visible at 0V when light is switched on and off.

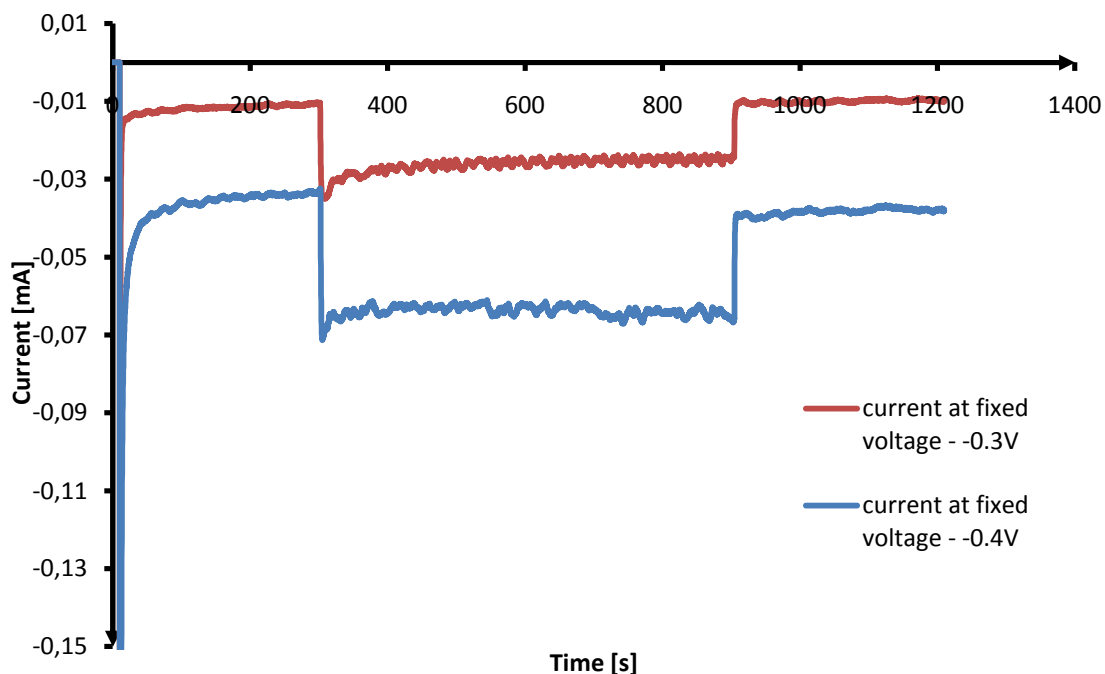


Figure 4.44 Chronoamperometry test for PEDOT/ PBTh ,1:1' in presence of bubbling air in 0.1 M NaPTS (pH 7) electrolyte, tests taken for fixed voltage values

Response time for PEDOT and PBTh blends is much faster, but drawn current is still not completely stable. Adding PEG 2000 to PEDOT and PBTh, helps to solve instability problem, moreover PEG 2000 supports ionic conductivity.

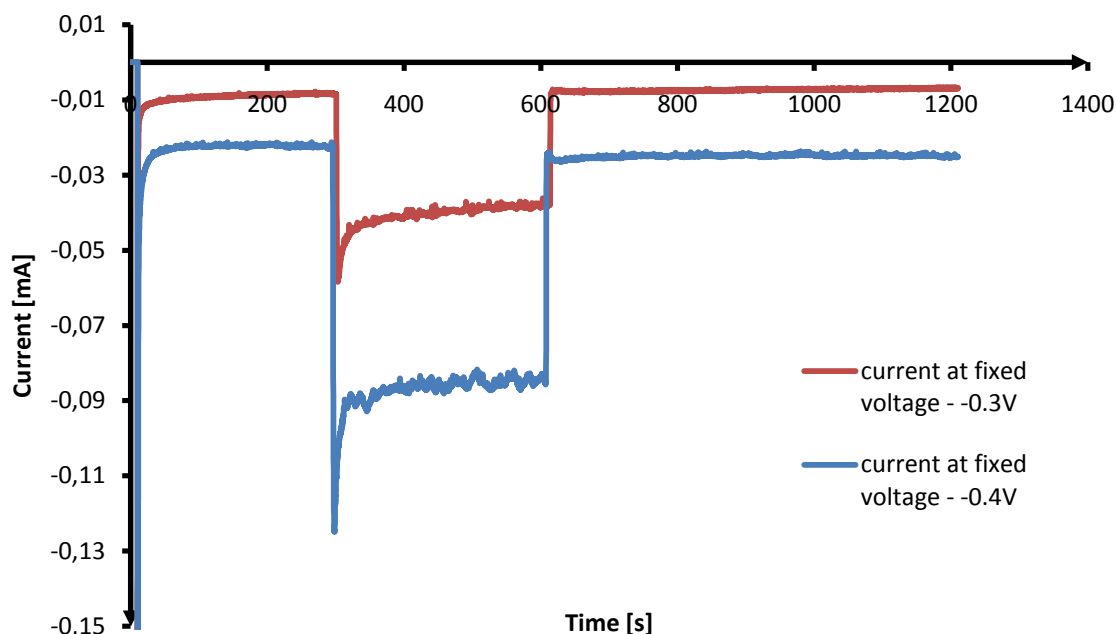


Figure 4.45 Chronoamperometry test for PEDOT/ PBTh ,1:1' PEG ,2', in presence of bubbling air in 0.1 M NaOH (pH 11) electrolyte, tests taken for fixed voltage values. Red plot – -0.4V, blue – -0.3V

Chronoamperometry tests above show light activation effect at fixed voltage values. Difference between current for two voltage values without light and with light is not the same, it means that together with voltage increase light effect is not constant, but increases affecting on current. Electrode shows very stable behaviour over time, and its response on change of light concentration is very rapid not like it was in pure PEDOT. What more, after turning off the light again, current rapidly comes back to same steady-state as it was before light introduction.

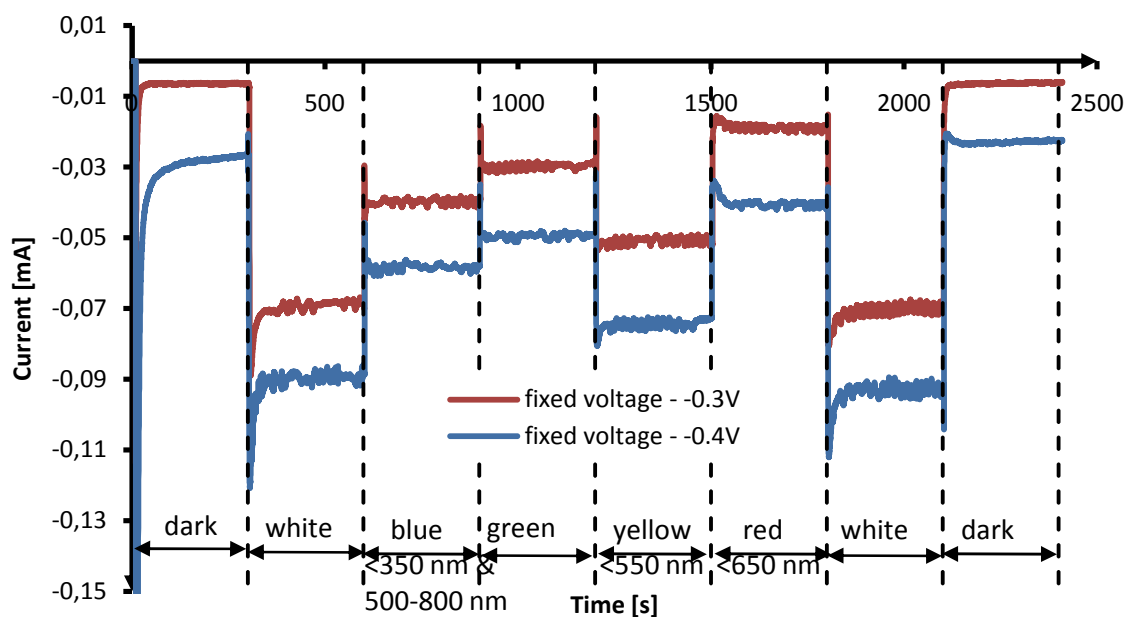


Figure 4.46 Chronoamperometry test with light filtration

Transmission curves for Leica KL2500 LCD are included in appendix E. Test above prove results gathered from UV-Vis test. Yellow filter transmits light from 550 nm wavelength and above, UV-Vis graph shows that 550 nm is the place just after the biggest peak. Red filter transmits light from 650 nm wavelength and above, below this value light is blocked by filter, transmission range of red filter is the place on UV-Vis graph, where absorbance of tested materials is the lowest. Red filter blocks light with wavelengths for which absorbance of tested blends is the highest.

5 IMPORTANCE AND IMPLEMENTATION OF PROJECT IN POLAND

Poland's energy depends mostly on coal, in 2002 and 2003 Poland was 7th biggest coal exporter in the world. One day coal resources will end and then Poland will have to find other energy sources. One possibility is to invest in fuel cell technology, very efficient and completely clean power source, which produces electricity and heat same time and can be used in many application replacing traditional combustion engines in power plants and vehicles and batteries in portable applications.

In 1997 the European Commission proposed that the EU should aim to reach a 12% share of renewable energy by 2010. Directives were adopted in the electricity and transport sectors that set national sectoral targets. In 2006 the EU had reached a 7% share. Recently, the Community has agreed targets for 2020. The EU 2020 target is 20%. Considering EU targets, Poland being member of European Union, has to invest in renewable energy to achieve 15% of energy coming from renewable sources and 10% of energy in transport area until 2020 year. Polish green energy policy supports biofuels and bioenergy, by giving bonds, lowering taxes and giving funds for plantations. Biofuels and bioenergy is good solution for energy problems, but only for short period of time. Production of biofuels involve huge area for crop plantation, complicated machinery and processes to produce fuel and is not completely CO₂ free, is rather CO₂ neutral, when world is going to reduce CO₂ emissions.

The way to achieve this level, reduce CO₂ emissions and get green energy sources is fuel cell and hydrogen technology. Fuel cells are still new and developing technology and research to improve them is running all over the world. One of many problems to solve is in materials for fuel cells, how to exclude expensive precious metal – platinum from fuel cells and replace it with new cheap and easy to manufacture materials with same or even better performance, this project can be implemented in Poland, as well as in any other country, no special conditions are needed. Excluding platinum and improving performance of fuel cells has big importance for future, green energy.

Polish energy consumption in the transportation sector depends almost exclusively on imported fossil fuels – oil. The sector is forecast to grow more rapidly than any other up

to 2020 and beyond and the sector is crucial to the functioning of the whole economy. The importance and the vulnerability of the transport sector require to take action rapidly and reduce oil consumption. Reduction in oil consumption is one way, but why not to get rid of oil completely and replace it by clean technology – hydrogen. Getting out oil from beneath the surface is expensive, many countries depend on imported oil, costs of transportation depends on a distance and in many cases are very high, political issues and emissions has to be counted too. To produce hydrogen only water and electricity is needed, water is everywhere around us and electricity can come from renewable sources.

Fuel cells and hydrogen seems to be solution for future energy demand, all automotive companies developed prototype fuel cell vehicles – some of them are already on market. Governments of many countries consider hydrogen as future replacement of gasoline. Research from this paper can have great importance, and can be implemented in Poland as well as in other countries – especially those countries where sun irradiation is high.

6 CONCLUSIONS

Conducting polymer – PEDOT and its blends with PBTh, PTTh and PEG has been tested. 4 point, thickness test and conductivity based on those test, show that PEDOT itself has the highest conductivity. Together with increase in ratio of other polymers added to the blend, conductivity of thin film is decreasing. Lower conductivity of thin film is not the issue, because future electrode can be supported by high conducting material, when PEDOT or its blends will play role of electro-catalyst.

An issue can be low mechanical strength of PEDOT based electrode. Fuel cell or battery environment can be very demanding and material used to build electrode has to meet many requirements, such as high durability, mechanical strength, high conductivity, temperature resistance just to name a few. PEDOT mixed with PBTh and PEG proved higher mechanical strength and durability comparing to PEDOT has been observed during electrode operation, but further improvement may be needed in order to meet all requirements given by harsh fuel cell environment.

PEDOT in presence of light shows increase of performance, this increase is growing with light intensity. Pure PEDOT has long response time on fast light changes, when working in dark conditions and light is introduced PEDOT needs some time to slowly achieve steady-state. However, blends of PEDOT, PBTh and PEG shows very fast, rapid even response to changes in light intensity. Light activation effect is growing with increasing voltage delivered to the electrode. What is very interesting, PEDOT and its blends show light activation even when voltage is not delivered to the electrode, some small amount of current can be drawn from electrode only when light is shining on it (at 0V). This light activation phenomena is higher for blends with higher PBTh/PTTh ratios to PEDOT. PEDOT/PBTh in ratios 1:0.5, 1:1, 1:2, 1:3 and PEG in ratio 2 have been tested, so far PEDOT/PBTh in ratio 1:3 shows the highest performance. Would be good to test other blends with higher PEDOT/PBTh ratios as well. However, there must be a limitation, in higher ratios it is expected that polymers will create heterogeneous thin films, instead of interpenetrating polymer networks.

This research can give a good base for further work and to build working prototype of new kind of hybrid power source, combination of fuel cell and photovoltaic cell in one device. However, further research needs to be done. This research has been performed on

simple electrode design, only to evaluate material properties and this design is not optimal. For further tests or future fuel cell gas diffusion electrode (GDE) has to be build.

Further research would include of better and deeper investigation on PEDOT, PBTh and PEG blends properties. Blends with PTTh instead of PBTh can be worth investigating as well. Would be good to investigate light activation effect itself, why it occurs and how to draw the whole potential out of it. Good idea is to build new and more precise test cell to achieve constant distances between electrodes, solve air/nitrogen bubbling problem and deliver light directly to electrode.

At the end, when answers on all those questions will be given, it is necessary to build prototype model of single fuel cell, test it and build prototype fuel cell stack and test its work for different loads and transients. Challenging will be to design and build fuel cell and fuel cell stack, so that light can be delivered to electrode.

REFERENCES

- [1] Bjorn Winther-Jensen, Orawan Winther-Jensen, Maria Forsyth, Douglas R. MacFarlane (2008) *High Rates of Oxygen Reduction over a Vapor Phase–Polymerized PEDOT Electrode*, Science 321, 671.
- [2] Frank Endres, Douglas MacFarlane, Andrew Abbott, (2008) *Electrodeposition from Ionic Liquids*, Willey-VCH.
- [3] James Larminie, Andrew Dicks (2003) *Fuel cell systems explained, Second Edition*, John Wiley & Sons Ltd.
- [4] Ricardo d'Agostino, Pietro Favia, Christian Oehr, Michael R. Werthmeier (2005) *Plasma Processes and Polymers - 16th International Symposium on Plasma Chemistry*, Wiley-VCH Verlag.
- [5] Crow DR. (1988) *Principles and applications of electrochemistry, Third Edition*, London: Chapman & Hall.
- [6] Fritz. B. Prinz, Ryan O'Hayre, Suk-won Cha (2009) *Fuel Cell Fundamentals*, John Wiley & Sons.
- [7] Cesar Cadena (2009) *Molecular Modeling and Determination of Properties of Ionic Liquids*, VDM Verlag.
- [8] Ryan O'Hayre, Fritz B. Prinz (2004) *The Air/Platinum/Nafion Triple-Phase Boundary: characteristics, Scaling, and Implications for Fuel Cells*, Journal of The Electrochemical Society vol. 151, pp. 756-762.
- [9] Ryan O'Hayre, David M. Barnett, Fritz B. Prinz (2005) *The Triple Phase Boundary – A Mathematical Model and Experimental Investigations for Fuel Cells*, Journal of The Electrochemical Society vol. 152 (2), pp. 439-444.
- [10] Adamson, Kerry-Ann (2007) *Stationary Fuel Cells: An Overview*, Oxford: Elsevier Ltd.
- [11] Bjorn Winther-Jensen (2004) *Towards Micro-patterning of Conducting Polymers – Polymerisation routes and characterization of selected conjugated polymer systems*, Technical University of Denmark, Ph.D. Thesis.
- [12] EG&G Technical Services, Inc. (2004) *Fuel Cell Handbook 7th edition*, U.S. Department of Energy - Office of Fossil Energy, National Energy Technology Laboratory.
- [13] Matthew M. Mench (2008) *Fuel Cell Engines*, John Wiley & Sons, Inc.

- [14] Ryan O'Hayre (2010) *Lecture 2: Intro to Fuel Cells*, Akureyri, Iceland: RES | the School for Renewable Energy Science.
- [15] Supramaniam Srinivasan (2006) *Fuel Cell: From Fundamentals to Applications*, Springer Verlag.
- [16] Carrette, L., Friedrich, K. A., & Stimming, U., (2001) *Fuel Cells - Fundamentals and Applications*, Fuel Cells , 5-39.
- [17] David Dvorak (2010) *Fuel Cell Operation. RES607: Fuel Cell Types and Technologies*, Akureyri, Iceland: RES | the School for Renewable Energy Science / The University of Maine.
- [18] Gregor Hoogers (2003) *Fuel Cell Technology Handbook*, CRC Press LLC.
- [19] Andrzej Wieckowski, Marc Koper (2009) *Fuel Cell Catalysis: A Surface Science Approach*, Wiley.
- [20] Margherita Venturi, Paola Ceroni, Alberto Credi (2010) *Electrochemistry of Functional Supramolecular Systems*, Wiley.
- [21] Elizabeth Santos, Wolfgang Schmickler (2010) *Catalysis in Electrochemistry: From Fundamentals to Strategies for Fuel Cell Development*, Wiley.
- [22] Andrzej Wieckowski, Jens Norskov (2010) *Fuel Cell Science: Theory, Fundamentals, and Biocatalysis*, Wiley.
- [23] Elizabeth Santos, Wolfgang Schmickler (2010) *Catalysis in Electrochemistry: From Fundamentals to Strategies for Fuel Cell Development*, Wiley.
- [24] Milan Paunovic, Mordechai Schlesinger (2006) *Fundamentals of Electrochemical Deposition*, Wiley-VCH.
- [25] Ken Kuang, Keith Easler (2007) *Fuel Cell Electronics Packaging*, Springer Science + Business Media LLC.
- [26] John McMurray (1996) *Organic Chemistry, Fourth Edition*, Brook/Cole Publishing Company.
- [27] Rohit Makharia, Mark F. Mathias, Daniel R. Baker (2005) *Measurement of catalyst layer electrolyte resistance in PEFCs using electrochemical impedance spectroscopy*, J Electrochem Soc 152: A970–A977.
- [28] Sanjeev Mukerjee, Supramaniam Srinivasan (1993) *Enhanced electrocatalysis of oxygen reduction on platinum alloys in proton exchange membrane fuel cells*, J Electroanal Chem 357: 201–224.

- [29] Sanjeev Mukerjee, Supramaniam Srinivasan, Manuel P. Soriaga, James McBreen (1995) *Role of structural and electronic properties of Pt and Pt alloys on electrocatalysis of oxygen reduction*, J Electrochem Soc 142:1409–1422.
- [30] K. C. Neyerlin, Wenbin Gu, Jacob Jorne, Hubert A. Gasteiger (2006) *Determination of catalyst unique parameters for the oxygen reduction reaction in a PEMFC*, J Electrochem Soc 153: A1955–A1963.
- [31] Jens Norskov, Jan Rossmeisl, A. Logadottir, L. Lindqvist, John R. Kitchin, Thomas Bligaard, Hannes Jonsson (2004) *Origin of the overpotential for oxygen reduction at a fuel-cell cathode*, J Phys Chem B 108: 17886.
- [32] Nigel Sammes, Alevtina Smirnova, Oleksandr Vasylyev (2005) *Fuel Cell Technologies: State and Perspectives*, Springer.
- [33] Nigel Sammes (2006) *Fuel Cell Technology - Reaching Towards Commercialization*, Springer-Verlag.
- [34] Alfred B. Anderson, Titus V. Albu (2000) *Catalytic effect of platinum on oxygen reduction. An ab initio model including electrode potential dependence*, J Electrochem Soc 147: 4229–4238.
- [35] L.O. Vasquez (2007) *Fuel Cell Research Trends*, Nova Science Publishers, Inc.
- [36] Bei Gou, Woon Ki Na, Bill Diong (2010) *Fuel Cells – Modeling, Control, and Applications*, CRC Press LLC.
- [37] JiuJun Zhang (2008) *PEM Fuel Cell Electrocatalysts and Catalyst Layer - Fundamentals and Applications*, Springer Verlag.
- [38] Felix N. Buchi, Minoru Inaba, Thomas J. Schmidt (2009) *Polymer Electrolyte Fuel Cell Durability*, Springer.
- [39] Bjorn Winther-Jensen, Maria Forsyth, Keld West, Jens Wenzel Andreasen, Paul Bayley, Steven Pas, Douglas R. MacFarlane (2008) *Order-disorder transitions in poly(3,4-ethylenedioxythiophene)*, Polymer, 49, 481-487.
- [40] Bjorn Winther-Jensen, Keld West (2004) *Vapor-Phase Polymerization of 3,4-Ethylenedioxythiophene: A Route to Highly Conducting Polymer Surface Layers*, Macromolecules 37, 4538-4543.
- [41] Bjorn Winther-Jensen, Frederik C. Krebs (2006) *High Conductivity Large Area Semi-Transparent Electrodes for Polymer Photovoltaics by Silk Screen Printing and Vapour Phase Deposition*, Solar Energy Materials and Solar Cells. Volume 90, Issue 2, 123-132.

- [42] Hirotugu Yasuda (1985) *Plasma Polymerization*, Academic Press Inc.
- [43] Riccardo d'Augustino (1990) *Plasma Deposition, Treatment, and Etching of polymers*, Academic Press Inc. Plasma materials interactions.
- [44] Mitchell Shen (1976) *Plasma Chemistry of Polymers*, Marcel Dekkar Inc.
- [45] Herman V. Boenig (1982) *Plasma Science and Technology*, Cornell University Press.
- [46] Hynek Biederman, Yoshihito Osada (1992) *Plasma Polymerization Processes*, Elsevier publications.
- [47] Richard D. McCullough, Stephanie Tristram-Nagle, Shawn P. Williams, Renae D. Lowe, Manikandan Jayaraman, (1993). "*Self-orienting head-to-tail poly(3-alkylthiophenes): new insights on structure-property relationships in conducting polymers*". Journal of the American Chemical Society 115: 4910. doi:10.1021/ja00064a070 (<http://dx.doi.org/10.1021%2Fja00064a070>).
- [48] M. Mastragostino, L. Soddu, (1990) "*Electrochemical characterization of "n" doped polyheterocyclic conducting polymers—I. Polybithiophene*". Electrochimica Acta 35: 463. doi:10.1016/0013-4686(90)87029-2 (<http://dx.doi.org/10.1016%2F0013-4686%2890%2987029-2>).
- [49] M. Lojonen, T. Taka, J. Laakso, K. Vakiarta, K. Suuronen, P. Valkeinen, J. Osterholm, (1991) "*Doping and dedoping processes in poly (3-alkylthiophenes)*". Synthetic Metals 41: 479. doi:10.1016/0379-6779(91)91111-M (<http://dx.doi.org/10.1016%2F0379-6779%2891%2991111-M>).
- [50] J.J. Bartus, *Macromol. Sci., Chem.* 1991, A28, 917–924.
- [51] X. Qiao, (2001) "*The FeCl₃-doped poly(3-alkylthiophenes) in solid state*". Synthetic Metals 122: 449. doi:10.1016/S0379-6779(00)00587-7 (<http://dx.doi.org/10.1016%2FS0379-6779%2800%2900587-7>).
- [52] F. Garnier, *Field-Effect Transistors Based on Conjugated Materials. In Electronic Materials: The Oligomer Approach* (Eds: Müllen, K.; Wegner, G.), Wiley-VCH, Weinheim, 1998. ISBN 3-527-29438-4
- [53] M. G. Harrison, R. H. Friend, *Optical Applications. In Electronic Materials: The Oligomer Approach* (Eds: Müllen, K.; Wegner, G.), Wiley-VCH, Weinheim, 1998. ISBN 3-527-29438-4.
- [54] V. Martina, K. Ionescu, L. Pigani, F. Terzi, A. Ulrici, C. Zanardi, R. Seeber, *Anal. Bioanal. Chem.* 2007, 387, 2101-2110.

APPENDIX A - LEICA KL 2500 LCD LIGHT SOURCE CALIBRATION

Photovoltaic cell area = 0.16 cm²

Table A.1. Data from solar simulator.

Sun [%]	V _{oc} [V]	Current density [mA/cm ²]
5.8	632	0.699
10.5	654	1.25
14.9	670	1.81
38.5	707	4.59
68	732	8.38
100	747	12.25

Table A.2. Raw current calculation.

Sun [%]	Current [mA]
5.8	0.11184
10.5	0.2
14.9	0.2896
38.5	0.7344
68	1.3408
100	1.96

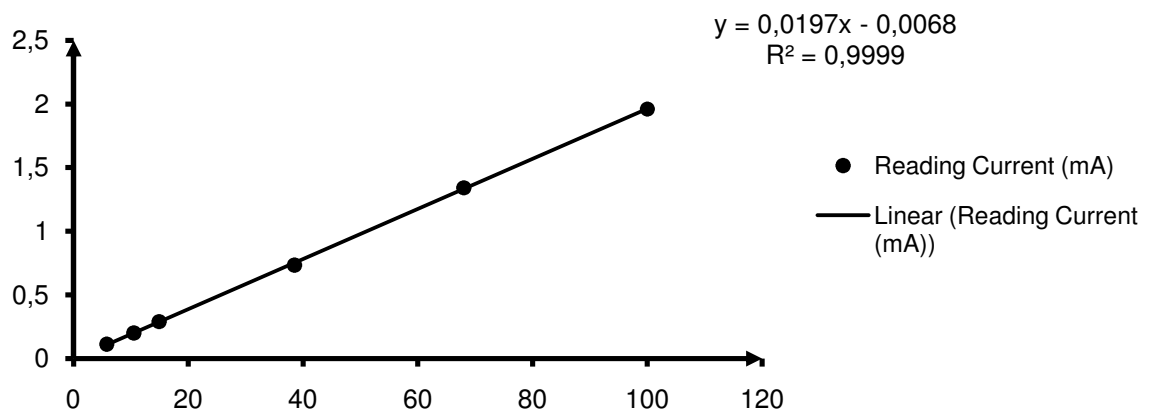


Figure A.1. Sun percentage vs. photovoltaic cell current.

Table A.3. Photovoltaic cell data.

Sun [%]	Reading Current [mA]	Reading Voltage [V]
5.8	0.11184	0.632
10.5	0.2	0.654
14.9	0.2896	0.670
38.5	0.7344	0.707
68	1.3408	0.732
100	1.96	0.747

Table A.4. Leica KL 2500 LED calibration.

Leica lamp light level [-]	Current [mA]	Voltage [V]	Sun [-]	Sun [%]
No. 1	0.87	0.705	0.445076	44.50761
No. 2	1.23	0.72	0.627817	62.78173
No. 3	1.82	0.737	0.92731	92.73096
No. 4	2.5	0.75	1.272487	127.2487
No. 5	4.03	0.769	2.049137	204.9137
No. 6	5.13	0.779	2.607513	260.7513

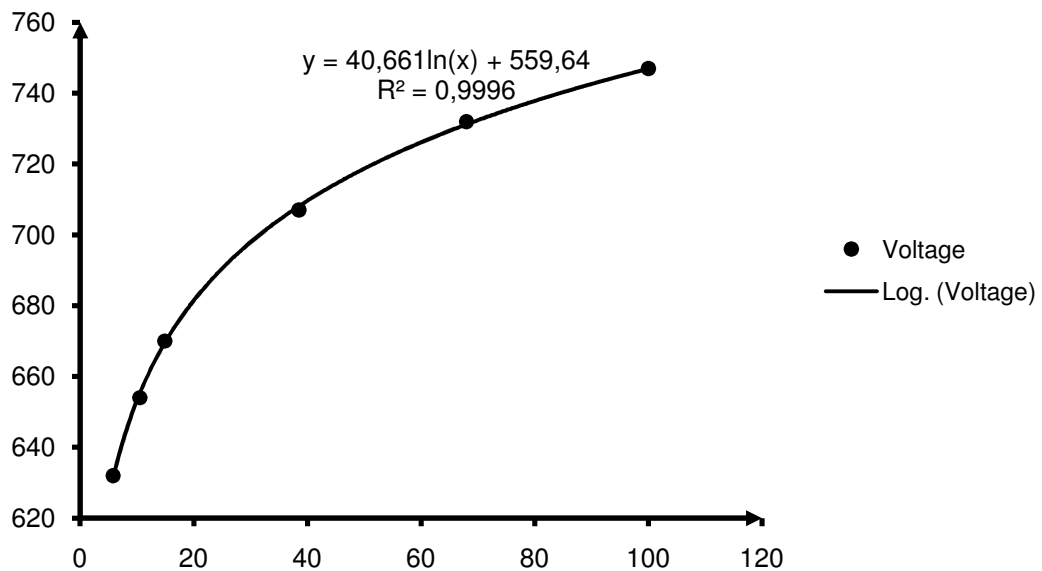


Figure A.2. Sun percentage vs. voltage logarithm.

APPENDIX B – WATER AND HYDROGEN POTENTIALS FOR DIFFERENT PH VALUES

Table B.1. Water and hydrogen potential values for different pH.

pH	Water oxydation	Water reduction	Water oxydation	Water reduction
	vs. NHE	vs. NHE	vs. SCE	vs. SCE
0	1.23	0	0.989	-0.241
1	1.171	-0.059	0.93	-0.3
2	1.112	-0.118	0.871	-0.359
3	1.053	-0.177	0.812	-0.418
4	0.994	-0.236	0.753	-0.477
5	0.935	-0.295	0.694	-0.536
6	0.876	-0.354	0.635	-0.595
7	0.817	-0.413	0.576	-0.654
8	0.758	-0.472	0.517	-0.713
9	0.699	-0.531	0.458	-0.772
10	0.64	-0.59	0.399	-0.831
11	0.581	-0.649	0.34	-0.89
12	0.522	-0.708	0.281	-0.949
13	0.463	-0.767	0.222	-1.008
14	0.404	-0.826	0.163	-1.067

APPENDIX C – RECIPE FOR VARYING THE PEDOT/PBTH RATIO

2 ml Fe(III)PTS in Butanol (40%)

1 ml Butanol

0.047 ml pyridine

33 mg PEG 20000 dissolved in 0.25 ml H₂O (use heating to ~50°C)

EDOT added to cold mixture of the above:

PEDOT to PBTh Ratio

‘1:0.5’ => 0.044 ml EDOT

‘1:1’ => 0.033 ml EDOT

‘1:2’ => 0.022 ml EDOT

‘1:3’ => 0.016 ml EDOT

‘1:4’ => 0.013 ml EDOT

‘1:5’ => 0.011 ml EDOT

‘1:6’ => 0.009 ml EDOT

Coat the mixture on sample surface and put to storage oven at 45°C over the night. Put sample with coated PEDOT/PEG to vapor phase polymerization chamber and next to the oven for 1 hour at 70°C.

When process is done wash the sample twice in ethanol. After washing dry the samples in the oven or air.

APPENDIX D – RECIPE FOR VARYING THE PEDOT/PTTH RATIO

2 ml Fe(III)PTS in Butanol (40%)

1 ml Butanol

0.047 ml pyridine

33 mg PEG 20000 dissolved in 0.25 ml H₂O (use heating to ~50°C)

EDOT added to cold mixture of the above:

PEDOT to PTTh Ratio

‘1:0.5’ => 0.035 ml EDOT

‘1:1’ => 0.024 ml EDOT

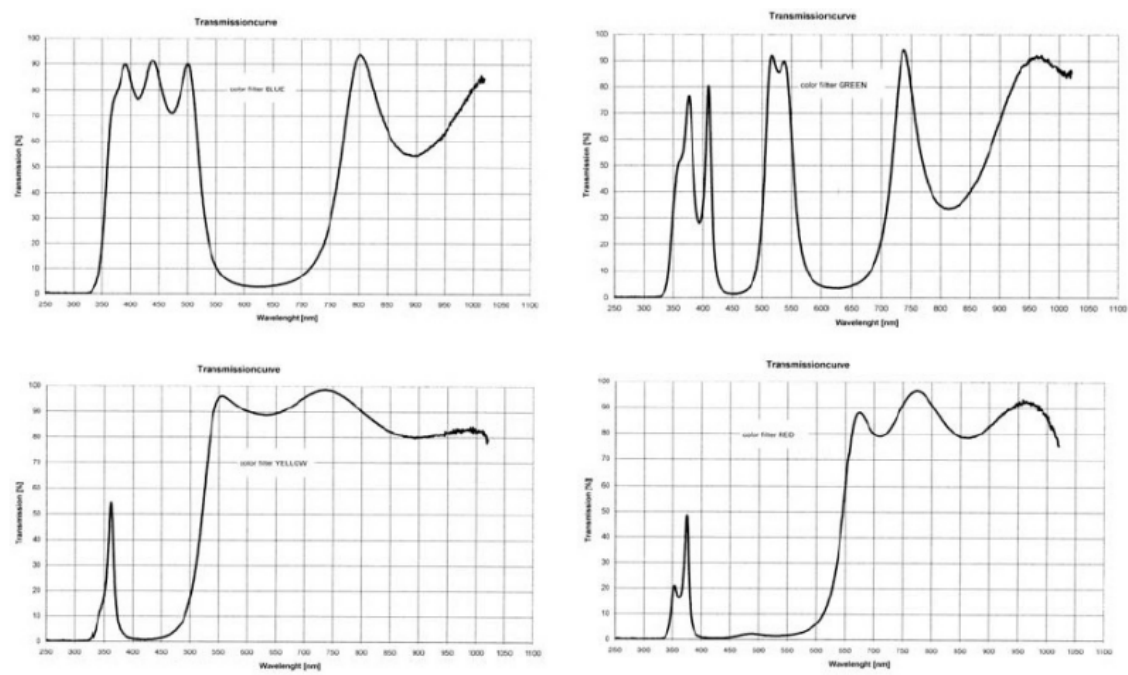
‘1:2’ => 0.015 ml EDOT

‘1:3’ => 0.011 ml EDOT

Coat the mixture on sample surface and put to storage oven at 45°C over the night. Put sample with coated PEDOT/PEG to vapor phase polymerization chamber and next to the oven for 3 hours at 100°C.


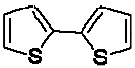

When process is done wash the sample twice in ethanol and then leave it in ethanol for more or less 15 minutes to wash out rest of the impurities. After washing dry the samples in the oven or air.

APPENDIX E – TRANSMISSION CURVES FOR LEICA KL2500 LCD



APPENDIX F – COMPARISON OF THIOPHENE, BITHIOPHENE AND TERTHIOPHENE

Table F-1 Comparison of thiophene, bithiophene and terthiophene properties

	Thiophene (Th)	Bithiophene (BTh)	Terthiophene (TTh)
<i>Empirical Formula</i>	C ₄ H ₄ S	C ₈ H ₆ S ₂	C ₁₂ H ₈ S ₃
<i>Molecular Weight</i>	84.14 g/mol	166.26 g/mol	248.39 g/mol
<i>Boiling Point</i>	84 °C	260 °C	-
<i>Meliting Point</i>	-38 °C	32-33 °C	93-95 °C
<i>Flash Point</i>	-1 °C	110 °C	-
<i>Application</i>	-	Substrate used in a rhodium-catalyzed C-H arylation of heteroarenes with aryl iodides	Monomer precursor for polythiophene. Photosensitizer. Dopant for polycarbonate Natural product occurring in marigold which shows UV-enhanced antibiotic activity.
<i>Chemical Structure</i>			
<i>Price</i>	18.80 USD/5g 22.20 USD/100g 41.40 USD/500g	130.00 USD/10g	138.50 USD/1g

APPENDIX G - DEFENSE QUESTIONS & ANSWERS - ICELAND INNOVATION CENTER, REYKJAVIK, 10.02.2011

1. Why do you use PEG?

PEG is non conducting polymer, but in blends with PEDOT, PEG increases overall conductivity of resulting thin film. PEG improves response time of thin film caused by changes in potential or light intensity. PEG increases ionic conductivity.

2. Why do you use PBTh? Missing in thesis.

PBTh is used to increase light activation effect of thin film. When PBTh is used together with PEDOT, decreases overall conductivity of thin film, but electrocatalytic properties are more or less the same as electrocatalytic properties of pure PEDOT. To increase electrode conductivity any good conductor can be used as a base and thin film consisting of PEDOT, PBTh (PTTh) and PEG deposited onto its surface.

3. Can you compare your polymer electrode to a standard fuel cell electrode?

This research was performed only to characterize material properties, and very simple two dimensional electrode design has been used, which is not optimal design for fuel cells. To compare this electrode with standard fuel cell electrode similar tests have to be performed on electrode with more sophisticated geometry to evaluate which one has better performance.

4. What is your theory on why light intensifies the performance?

Light activation phenomena of PEDOT, PBTh, PEG electrode has to be investigated deeper to give correct answer on this question.

5. What is the most promising composition?

Most promising composition presented in thesis is composition of PEDOT/PBTh ,1:3' PEG ,2', but further research shows that PEDOT/PBTh ,1:4' PEG ,2' has even better performance. However, polymers in thin films made of PEDOT/PBTh ,1:5' PEG ,2' create heterogeneous networks instead of homogeneous, and performance of resulting film is much lower than performance of films with lower PBTh amount.

6. Is the PEDOT good enough as an electrode without illumination?

PEDOT itself is good enough to be used as an electrode, it has been proved by Bjorn Winther-Jensen, Orawan Winther-Jensen, Maria Forsyth, Douglas R. MacFarlane (2008)

High Rates of Oxygen Reduction over a Vapor Phase–Polymerized PEDOT Electrode, Science 321, 671.

7. Explain in your thesis why Gore-Tex is used.

Gore-Tex is used to create breathable electrode, in this research samples on glass and mylar coated with gold substrates has been used, only to characterize material properties. In future, Gore-Tex can be used as a base for real breathable fuel cell electrode.

8. Summary: what is your own contribution to this work?

All the samples and all the tests described in this thesis were performed by me, with prior introduction to devices and processes by laboratory staff.

9. Did you know about light activation from the beginning?

Bjorn Winther-Jensen (my supervisor) expected this properties in this kind of blend, that's why he offered me this topic for deeper investigation.

10. Conductivity calculations, there seems to be a loss of conductivity with PEDOT/PBTh by a factor of 1:5

Yes, that's true. Both, PEDOT and PBTh are conducting polymers, however, between conducting polymers PEDOT is one with the highest conductivity. When mixed with PBTh in blend, conductivity of thin film decreases because PBTh has lower conductivity than PEDOT. What is very surprising PEG, which is non-conducting polymers mixed with PEDOT increases its overall conductivity, that's why other samples have still pretty high conductivity comparing to PEDOT/PBTh , 1:1'.

11. Where is the catalysis happening, is it a surface or bulk property?

Catalysis process takes place only on a surface of electrocatalyst. Catalysis occurs only on where all three phases of three phase boundary meet. That's why it is demanded to increase area of three phase boundary.